RENEWED SIGNIFICANCE OF RAS GTPASES

by

Michael Wey

DISSERTATION

Submitted in partial fulfillment of the requirements
for the degree of Doctor of Philosophy at
The University of Texas at Arlington
August, 2017

Arlington, Texas

Supervising Committee:

Jongyun Heo, Supervising Professor
Kayunta Johnson-Winters
Peter Kroll

Copyright by

Michael Wey

2017

ACKNOWLEDGEMENTS

First and foremost, I would like to thank my advisor, Dr. Jongyun Heo. I have the deepest gratitude to my advisor, Dr. Jongyun Heo for his patience and nurturing. He has provided me with all the necessary guidance to be an independent researcher. Dr. Heo introduced me to the field of enzyme kinetics, financially supported my research and corrected my writing. I am truly fortunate to have had the opportunity to work with him.

I would also like to thank Dr. Inpyo Hong for teaching me all the basic biochemistry lab techniques. I remember asking for his help endlessly as an enthusiastic undergraduate, to which he willingly and most patiently gave me his time. I realize now, that the time he gave to help me in lab is priceless. I am also thankful to Dr. Jinyoung Shin who taught me about mammalian cell culture. I would have not accomplished as much without their assistance.

Next I would like to extend my gratefulness my committee members, Dr. Subhrangsu Mandal and Dr. Kayunta Johnson-Winters for being accommodating and patient with me. Furthermore, I thank Dr. Mandal for instilling in me a deep interest in biochemistry that I hope to carry forward. Thank you, Dr. Peter Kroll, firstly for being a great Graduate Advisor and secondly for our long conversations about anything and everything.

I am grateful to the support staff at the department of Chemistry and Biochemistry – Jill Howard and Debbie Cooke for the numerous “reminder emails” for different duties and Jim Garner and Natalie Croy for enduring my demands while placing orders for the laboratory.

I am lucky to have had many amazing colleagues – those who have left UTA (Dr. Khairul Ansari and Dr. Sahba Kasiri), those still in the program (Hope Umutesi) and those just beginning (Hanh Hoang) – I thank them for their support, feedback and friendship. A very big thanks to Atreyi Dasmahapatra, for her unyielding friendship, that has helped me push through difficult times.

Last, but not the least, I acknowledge my entire family, especially my grandmother who would have been ecstatic about this achievement. Special thanks to my mother and father for their never-ending support and my brother David Wey for providing the much needed “non-work” conversation.

LIST OF FIGURES

Figure 1.1The Ras Superfamily. 3

Figure 1.2 The Classical Ras Cycle 5

Figure 1.3 Superposition of GTP- and GDP-bound HRas. 7

Figure 1.4 Sequence Alignment of Ras Isoforms. 9

Figure 1.5 Downstream Effectors of Ras. 11

Figure 1.6 The Cycling of Ras in the Presence of Redox Agents 16

Figure 2.1 Sequence of wt HRas 29

Figure 2.2 Estimation of the kinetic constants of the intrinsic GTP dissociations from wt and G12S HRas. 43

Figure 2.3 Determination of the kinetic constants for the intrinsic and p120GAP-mediated activities of wt and G12S HRas. 46

Figure 2.4 Determination of the fractions of the HRas-bound GTP in cells. 60

Figure 3.1 Fluorescence Emission Spectra of ERas with Mant-nucleotide 96

Figure 3.2 Estimation of K_d Values Between HRas and Its Effectors 99

Figure 3.3 Estimation of K_d Values Between ERas and its Effectors 101

LIST OF TABLES

Table 2.1 Frequency of HRas Mutations in Costello Syndrome 31

Table 2.2 Kinetic parameters for the intrinsic and GEF-mediated GDP and GTP dissociation from wt HRas and its mutants..... 44

Table 2.3 Kinetic constants for the intrinsic and p120GAP-mediated GTPase activity of wt HRas and its mutants 48

Table 2.4 Theoretically estimated comprehensive $f_{Ras \cdot GTP}$ values of wt HRas and its mutants. 50

Table 3.1 Equilibrium Dissociation Constants of HRas and ERas with Various Effectors 100

LIST OF ABBREVATIONS

2'(3')-O-(N-methylanthraniloyl) 5'-guanylyl-imidodiphosphate ..... mantGppNHp

2'(3')-O-(N-methylanthraniloyl) guanosine diphosphate .....mantGDP

Activator Protein 1 ..... AP-1

CAAX motif.....Cys-aliphatic-aliphatic-X

c-Jun N-terminal kinases ..... JNK

Cullin-3 .....Cul3

E26 transformation-specific..... ETS

Embryonic Ras ..... ERas

emission wavelength ..... λ_{em}

equilibrium dissociation constants .....K_d

excitation wavelength ..... λ_{ex}

extracellular signal-related kinases 1 and 2 .....ERK 1 and 2

Forkhead box ..... FOXO

gastric carcinomas .....GC

GTPase activation proteins .....GAPs

guanine nucleotide exchange..... GNE

guanine nucleotide exchange factors ..... GEFs

Harvey Ras ..... HRas

Hippo.....Hpo

hypervariable region.....HVR

Kirsten Ras..... KRas

lipid post-translational modifications lipid .....PTMs

Mammalian STE20-like protein kinase 1/2 ..... MST1/2

mitogen-activated protein kinases ..... MAPKs

mTOR rictor complex mTORC2

Neuroblastoma Ras..... NRas

Neurofibromin1..... NF1

phosphate-binding loop ..... P-loop

Phosphatidylinositol 3-kinase PI3K

phosphatidylinositol- 4,5-bisphosphate ..... PtdIns(4,5)P2, PIP2

phosphatidylinositol-3,4,5-trisphosphate ..... PtdIns(3,4,5)P3, PIP3

pleckstrin homology domain..... PH domain

post-translational modification..... PTM

Protein kinase B ..... Akt

Pyruvate Dehydrogenase Kinase 1 ..... PDK1

Raf phosphorylates mitogen-activated protein kinases 1 and 2 ..... MEK 1 and 2

RAL guanine nucleotide dissociation stimulator ..... RALGDS

Rapidly Accelerated Fibrosarcoma ..... Raf

Ras ..... Rat Sarcoma

Ras association domain family member ..... Rassf

Ras guanine-nucleotide-release factor ..... RasGRF

Ras guanyl nucleotide-releasing protein ..... RasGRP

Salvador/Rassf/Hippo ..... SARAH

Son of Sevenless ..... SOS

wild type ..... wt

ABSTRACT

Michael Wey, Ph.D.

The University of Texas at Arlington, 2017

Supervising Professor: Jongyun Heo

The Ras superfamily of GTPases act as molecular switches and play a critical role in intracellular signal transduction. These GTPases cycle between an active GTP-bound form and an inactive GDP-bound form to regulate a myriad of cellular processes. However, this classical model of Ras regulation does not accurately project the entire picture of Ras regulation. This work discusses non-classical and newly discovered elements of the Ras signaling network.

While intrinsic kinetic properties of Ras are included in the classical model of Ras regulation, the importance of them is understated. We show that the development Costello Syndrome from somatic Harvey Ras (HRas) mutations, are due to the altered intrinsic kinetic properties of HRas by the mutation. This is counter to the belief, which many believe, that the intrinsic kinetic properties of Ras do not contribute significantly to the overall regulation of Ras.

Recently, the discovery of Embryonic Ras (ERas) has given the Ras subfamily a new and atypical member. While ERas shares significant homology to the other Ras proteins, it has its own unique characteristics such as an extended N-terminus and unusual residues in its G domain. These ERas specific-unusual G domain residues make ERas constitutively active. While not naturally expressed in humans, ERas is found to be expressed in certain human cancers. There have been conflicting reports on the ERas-mediated cell-signaling pathways. My research, equipped with kinetic binding approaches, aims to characterize the ERas-binding interactions with key Ras-effector proteins that delineates the ERas-specific cell-signaling cascades.

TABLE OF CONTENTS

ACKNOWLEDGEMENTS i

LIST OF FIGURES iii

LIST OF TABLES iv

LIST OF ABBREVIATIONS v

ABSTRACT vii

CHAPTER 1: RAS GTPASES: STRUCTURE, REGULATION AND EFFECTORS 1

CHAPTER 2: KINETIC MECHANISMS OF MUTATION-DEPENDENT HARVEY RAS ACTIVATION AND THEIR RELEVANCE FOR THE DEVELOPMENT OF COSTELLO SYNDROME 25

CHAPTER 3: DETERMINATION OF THE EMBRYONIC RAS-SPECIFIC EFFECTOR PROTEINS 87

CHAPTER 1

RAS GTPASES: STRUCTURE, REGULATION, AND EFFECTORS

Introduction

Ras (Rat Sarcoma) GTPases are proteins which are members of the Ras superfamily (Figure 1). Ras GTPases essential to many cellular signaling pathways and are proteins which play an essential role in signal transduction.[1, 2] These signaling pathways include cell growth, apoptosis, motility and cell cycle regulation.[3] Ras proteins bind guanine nucleotides and cycle between their GTP- and GDP-bound states. The cycling between the GTP and GDP states allows for Ras proteins to act as molecular switches. The nucleotide bound to Ras determines whether the protein is in the “on” or “off” state. The having GTP bound to Ras turns the switch “on” while having GDP bound turns the switch “off”. The binding of GTP to the GTPase causes a conformational change which promotes the binding of effectors, thereby turning “on” downstream signaling.[4, 5]

As the name implies, Ras GTPases have the intrinsic capability of hydrolyzing GTP to GDP. This is a form of self-regulation as the Ras GTPase, alone, can potentially terminate downstream signaling once activated. Similarly, Ras GTPases can undergo intrinsic guanine nucleotide exchange (GNE) and exchange the bound GTP/GDP for free GTP/GDP in the cell. While both intrinsic GTP hydrolysis and intrinsic GNE occur with Ras, both intrinsic processes are slow. Various regulator proteins assist Ras in cycling between the GDP- and GTP-bound forms.[6]

GTPase activation proteins (GAPs) drastically increase the intrinsic rate of GTP hydrolysis of Ras GTPases. As the hydrolysis process converts the bound GTP to GDP, it terminates downstream signaling. GAPs are a form of negative regulation to

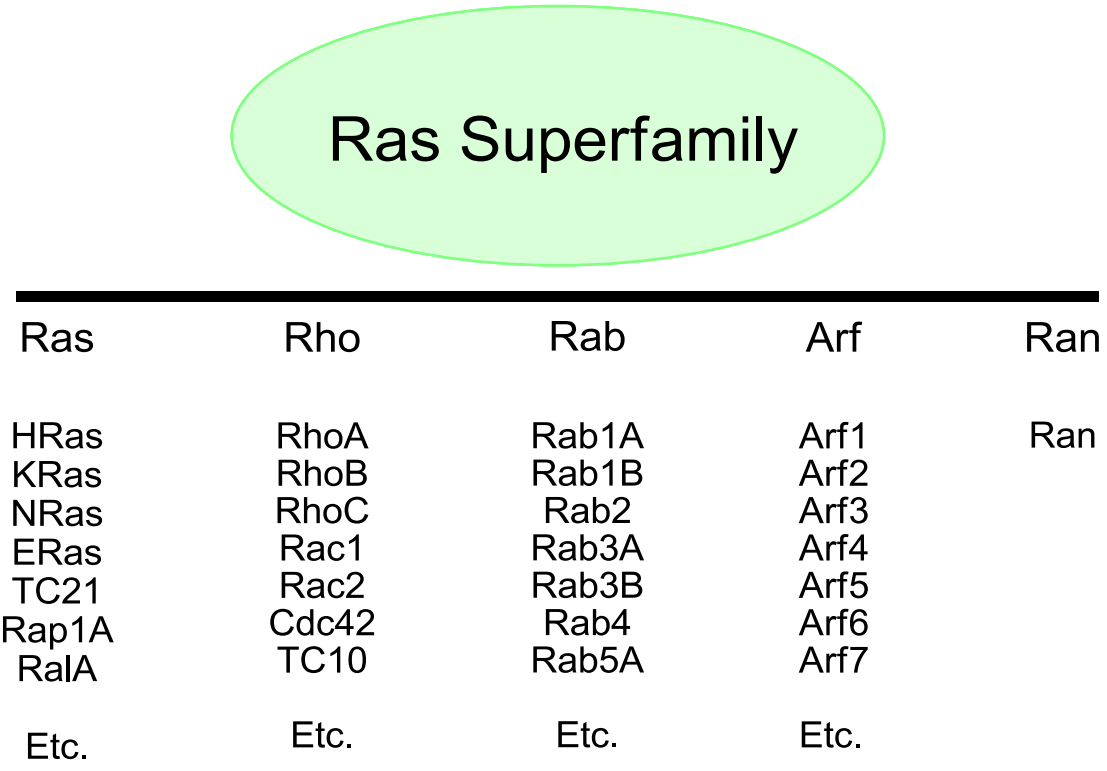

Figure 1. *The Ras Superfamily.*

Under the Ras Superfamily, five major subfamilies can be made based on the homology of their G domains.

Ras GTPases. In contrast, guanine nucleotide exchange factors (GEFs) are a form of positive regulation which populate Ras GTPases into their active GTP-bound states. GEFs populate the active form of Ras GTPases by dislodging the bound guanine nucleotide and allowing another guanine nucleotide to bind. As the cellular concentration of GTP is ~10 fold greater than that of GDP, the binding of GTP is more likely resulting in activation of Ras GTPases. The cycling of Ras GTPases between GTP and GDP forms is summarized in Figure 2. The cycling of GTP- and GDP-bound Ras through GEFs and GAPs can be referred to as the “classical” view of Ras activity regulation.

Structure of Ras GTPases

G Domain

All members of the Ras superfamily of GTPases have a highly conserved set of five guanine nucleotide binding motifs (G1 – G5) which begin at the N-terminus and persist nearly throughout the entire protein. The N-terminal region where the five guanine nucleotide motifs reside is known as the G domain. Catalytic activity and effector binding is determined in the G domain. The G domain of Ras spans from the first residue to residue 166, ~85% of the entire protein. What characterizes and distinguishes the subfamilies in the Ras superfamily is the type of G domain. Within a subfamily, the G domains of different isoforms retain immense sequence identity (nearly identical between some family members). While aligning entire G domains between differing subfamilies may yield varying results, the five guanine nucleotide binding motifs present in the G domain are highly conserved throughout he Ras superfamily.[7]

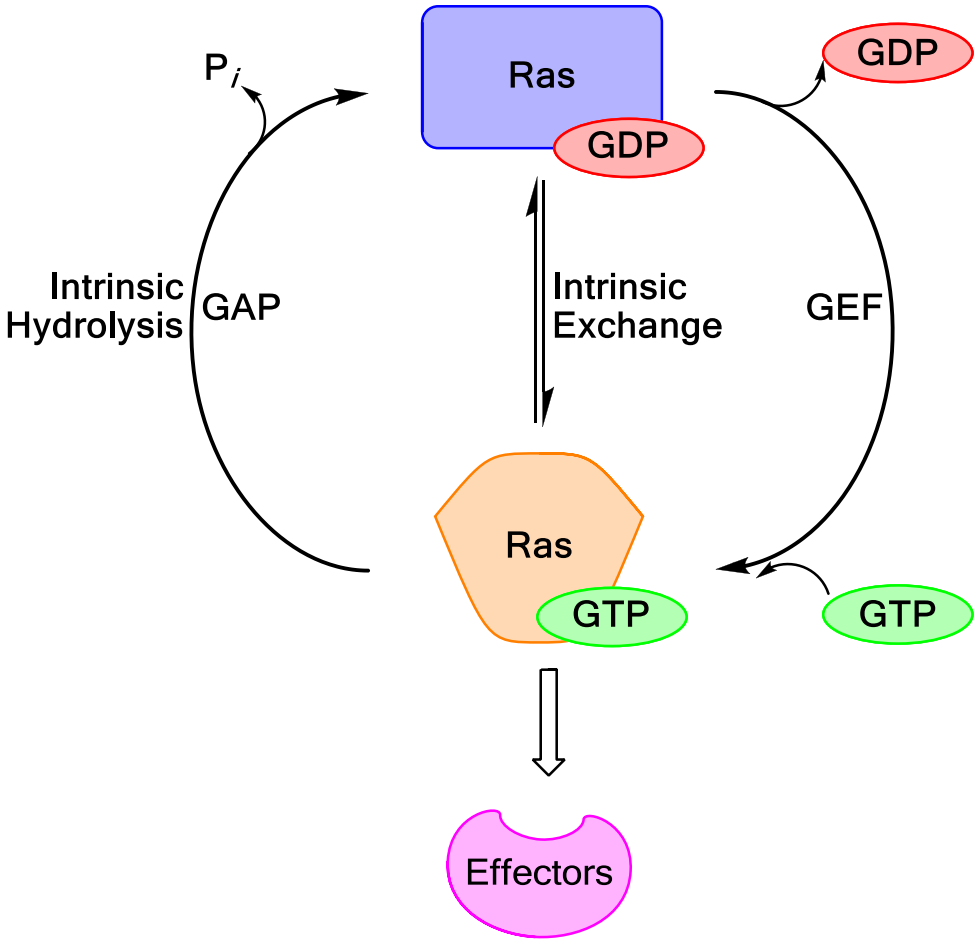

Figure 2. *The Classical Ras Cycle.*

Small GTPases cycle between the active GTP-bound form and the inactive GDP bound form. Small GTPases intrinsically release GDP and bind GTP to activate, but the process is slow. GEFs bind to small GTPases to induce fast nucleotide exchange and active small GTPases. Small GTPases in the active GTP-bound form can bind to downstream effectors. Small GTPases are capable of intrinsically hydrolyzing GTP to GDP very slowly. The binding of GAPs increase the slow hydrolysis rate of small GTPases.

The five guanine nucleotide binding motifs are characteristic motifs of all guanine nucleotide binding proteins. The motifs are localized near the nucleotide binding site as they are essential and assist in the binding of guanine nucleotides. The five conserved motifs are referred to in succession from G1 – G5.[8]

The G1 motif (GXXXXGKS/T), also known as the Walker A motif, is most commonly referred to as the phosphate-binding loop (P-loop). As the name suggests this motif is centered around the phosphates of the guanine nucleotide, particularly theβ- and the γ-phosphate oxygens. The lysine of the P-loop is essential to nucleotide binding as the amine moiety is directly interacting with the β- and the γ-phosphate oxygens. In addition, the hydroxyl group of the serine or the threonine interacts with the magnesium ion, which also present between the β- and the γ-phosphate oxygens for stabilization.

The G2 (a conserved threonine, HRas residue Thr35) and G3 (DXXG, Walker B motif) motifs are in the Switch I (HRas residues 30 – 38) and Switch II (HRas residues 59 – 67) regions, respectively. Switches I and II are the two primary regions of conformational change between the active GTP-bound and the inactive GDP-bound form of GTPases. As seen from Figure 3, Switches I and II have the most pronounced changes in conformation when Ras is cycling between the GTP- and GDP-bound states. The conformation adopted by Switches I and II for the active GTP-bound GTPase result in an increased binding affinity of downstream effector proteins, thereby

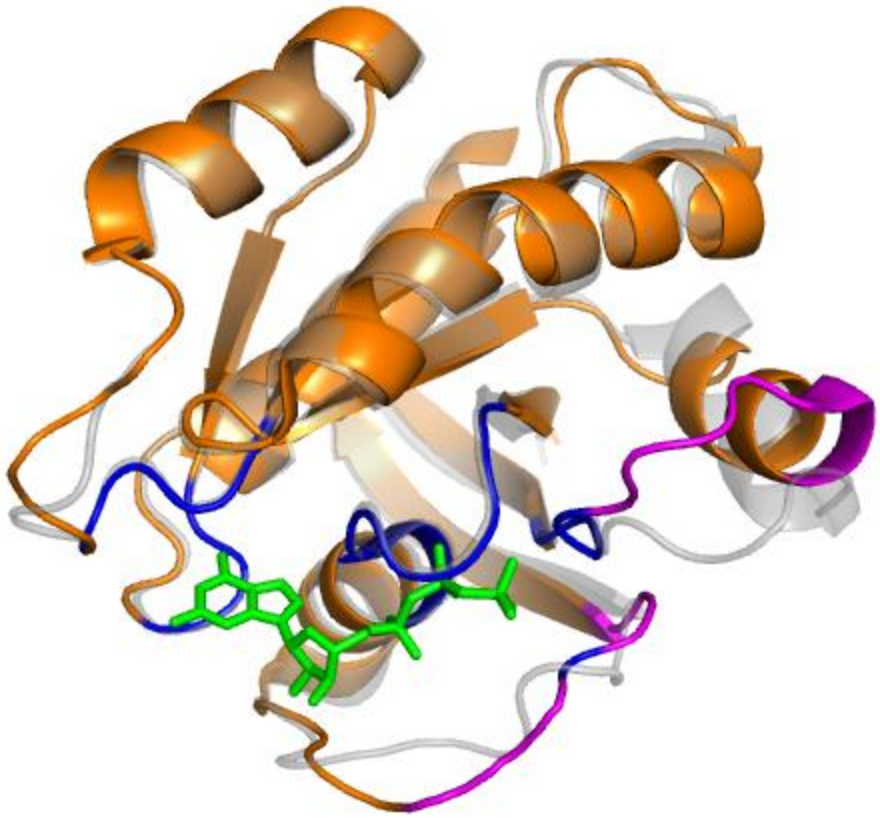

Figure 3. *Superposition of GTP- and GDP-bound HRas.*

The GTP- and GDP-bound forms of HRas are superimposed above. The colored cartoon depicts GTP-bound HRas (PDB 2CE2) while the grey cartoon depicts GDP-bound HRas (PDB 2CL7). The blue areas indicate the five G domains of HRas and the purple areas are Switch I and Switch II. There is a significant movement of the Switches I and II regions between GTP- and GDP-bound forms of HRas. This image was created using PyMOL.

activating signal transduction. Switch I is referred to as the “effector region” as it is primarily involved with the interaction of downstream effectors. The conserved threonine (G2) in Switch I senses the γ-phosphate of GTP, to which Switch I conformationally changes. While the conserved glycine (DXXG motif) in Switch II also interacts/detects the presence of the γ-phosphate, it plays a more crucial role in interactions with regulators (GAPs and GEFs). This localization of conformational change in the Switch regions is a commonality amongst all small GTPases such as Ras proteins.

The asparagine and aspartate of the G4 motif (N/TKXD) directly interact with the oxygen and two nitrogens of the guanine nucleotide base, respectively. The G4 motif is the motif which specifies GTPases to bind guanine nucleotides rather than adenosine nucleotides. The G5 motif (SAK) also plays a role in the selective GTPase-binding interactions with guanine nucleotide. The amine backbone of the alanine residue of G5 motif SAK interacts with the oxygen of the guanine nucleotide base.

Hypervariable Region

In addition to the conserved G domain, Ras superfamily members have a hypervariable region (HVR) at the C-terminus. As the G domains between subfamily isoforms have high sequence identity, the hypervariable region is what mostly differentiates subfamily members from each other (HRas and Neuroblastoma Ras (NRas), for example) (Figure 4). It is in the hypervariable region where lipid post-translational modifications (lipid PTMs) are targeted. Lipid PTMs and upstream membrane-targeting sequences in the HVR control the subcellular localization and membrane targeting of GTPases. Lipid PTMs increase the hydrophobicity of the protein, allowing it to anchor to membranes.

```
                                                  :.*** *****.
KRas        ---------------------------------------MTEYKLVVVGAG    12
NRas        ---------------------------------------MTEYKLVVVGAG    12
HRas        ---------------------------------------MTEYKLVVVGAG    12
ERas        MELPTKPGTFDLGLATWSPSFQGETHRAQARRRDVGRQLPEYKAVVVGAS    50

            *********** :: **:::****:*** *:::.:*.  *:*::******
KRas        GVGKSALTIQLIQNHFVDEYDPTIEDSYRKQVVIDGETCLLDILDTAGQE    62
NRas        GVGKSALTIQLIQNHFVDEYDPTIEDSYRKQVVIDGETCLLDILDTAGQE    62
HRas        GVGKSALTIQLIQNHFVDEYDPTIEDSYRKQVVIDGETCLLDILDTAGQE    62
ERas        GVGKSALTIQLNHQCFVEDHDPTIQDSYWKELTLDSGDCILNVLDTAGQA   100

             : *:*** : . :*.* ***::::..*: :::               *:*
KRas        EYSAMRDQYMRTGEGFLCVFAINNTKSFEDIHHYREQIKRVKDSEDVPMV   112
NRas        EYSAMRDQYMRTGEGFLCVFAINNSKSFADINLYREQIKRVKDSDDVPMV   112
HRas        EYSAMRDQYMRTGEGFLCVFAINNTKSFEDIHQYREQIKRVKDSDDVPMV   112
ERas        IHRALRDQCLAVCDGVLGVFALDDPSSLIQLQQIWATWG---PHPAQPLV   147

            ******** : : :::  *  **:*:*  ::******** **:**  **:
KRas        LVGNKCDLPSRTVDTKQ-AQDLARSYGIPFIETSAKTRQRVEDAFYTLVR   161
NRas        LVGNKCDLPTRTVDTKQ-AHELAKSYGIPFIETSAKTRQGVEDAFYTLVR   161
HRas        LVGNKCDLAARTVESRQ-AQDLARSYGIPYIETSAKTRQGVEDAFYTLVR   161
ERas        LVGNKCDLVTTAGDAHAAAAALAHSWGAHFVETSAKTRQGVEEAFSLLVH   197

            **:       :  : :    .     .     * :
KRas        EIR-------QYRLKKISK-EEKTPGCVKIKKCIIM   189
NRas        EIR-------QYRMKKLNSSDDGTQGCMGLP-CVVM   189
HRas        EIR-------QHKLRKLNPPDESGPGCMSCK-CVLS   189
ERas        EIQRVQEAMAKEPMARSCREKTRHQKATCHCGCSVA   233
```

Figure 4. *Peptide Sequence Alignment of Ras Isoforms.*

The UniProt accession numbers of Kirsten Ras (KRas), NRas, HRas, and Embryonic Ras (ERas) sequences aligned are, respectively, P01116, P01111, P01112 and Q7Z444. This figure was created using Clustal X.

Membrane anchorage and targeting is essential in the proper function of Ras GTPases.[9-11]

Nearly all proteins in the Ras subfamilies have a CAAX motif (Cys-aliphatic-aliphatic-X) at the terminus of their HVRs. The CAAX motif is the classic hallmark of prenylated proteins. The X in the motif determines whether the farnesyl or geranylgeranyl isoprenoid is covalently (thioester) added to the sulfur of the cysteine.[12, 13]

While geranylgeranylation adds sufficient hydrophobicity to anchor a GTPase to a membrane, the hydrophobicity of farnesylation alone cannot. In addition to farnesylation, a second interaction is required for membrane anchorage. The second interaction for Ras proteins is usually a palmitoylation of another cysteine upstream of the CAAX motif or a polybasic region also upstream of the CAAX motif. A polybasic region is a string of basic residues which promote electrostatic interactions with the negatively charged membrane phospholipids. HRas and NRas have palmitoylation sites as the second interaction while KRas contains a polybasic region.[12 11, 14]

Ras Downstream Signaling

When Ras is active, GTP-bound, it is able to bind downstream effectors. The binding of downstream effectors to Ras activates pathways which control but is not limited to, cell proliferation, survival, and transcription. The effectors which bind to the activated Ras indicate the signaling pathways of Ras (Figure 5). The three “classical”

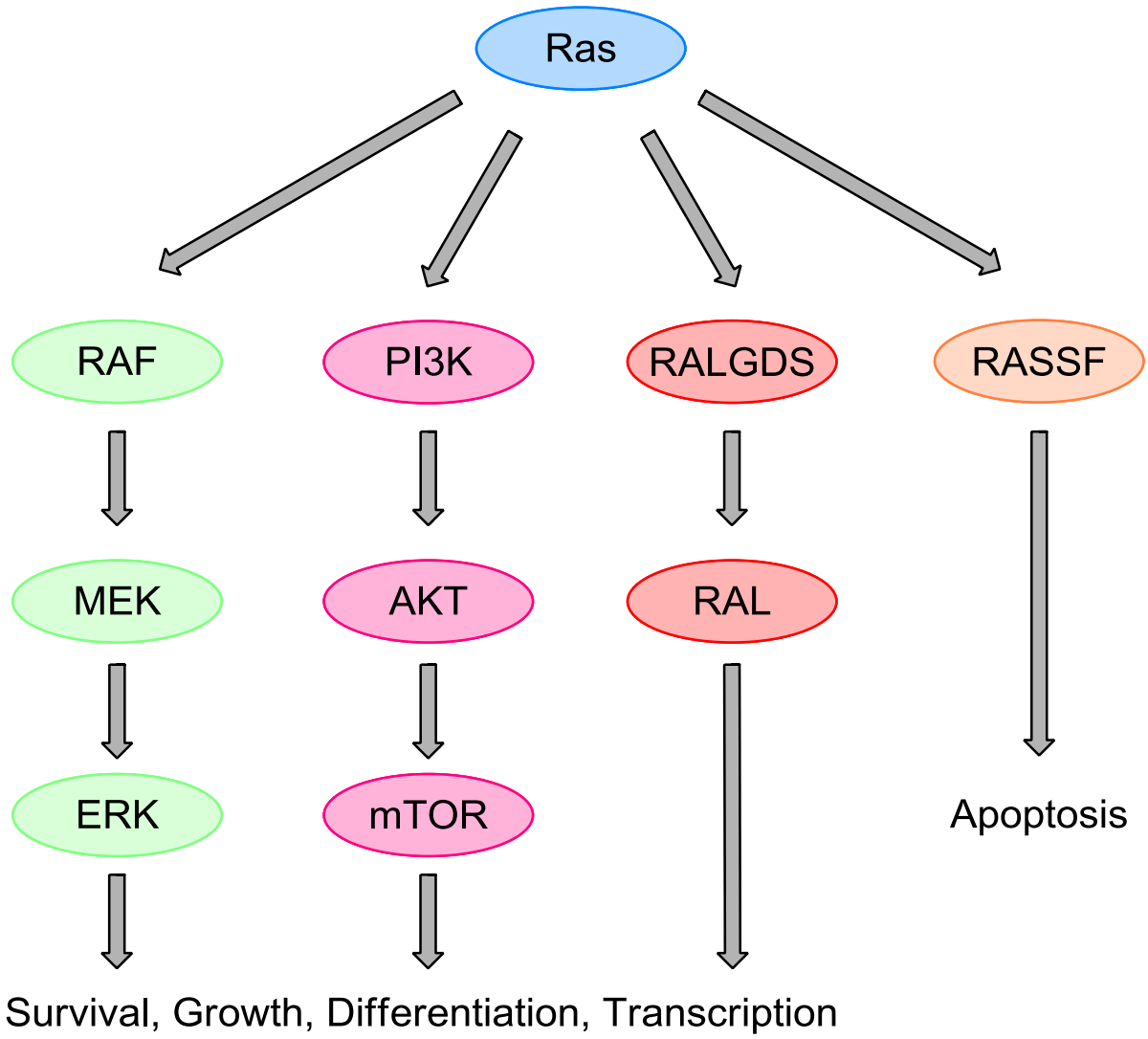

Figure 5. *Downstream Effectors of Ras.*

The downstream effectors of Ras GTPases and their role in cell signaling are shown above. While Rapidly Accelerated Fibrosarcoma (Raf), Phosphatidylinositol 3-kinase (PI3K), and RAL guanine nucleotide dissociation stimulator (RALGDS) are all implicated in cell survival, Ras association domain family member (Rassf) is connected to programed cell death.

effectors of Ras are Raf, PI3K, and RALGDS.[15, 16]

Raf/MEK/ERK pathway

The first effector characterized for Ras was a serine/threonine kinase, Raf. Three common members of the Raf family that have been implicated in binding to Ras are c-Raf1, B-Raf and A-Raf. When a Raf protein binds to Ras, it is recruited to the plasma membrane. The activation of Raf is a result of the relocation of Raf to the plasma membrane. Raf phosphorylates mitogen-activated protein kinases 1 and 2 (MEK 1 and 2). After phosphorylation, MEK 1 and 2 phosphorylates mitogen-activated protein kinases (MAPKs), extracellular signal-related kinases 1 and 2 (ERK 1 and 2). This kinase cascade eventually results in the regulation and expression of transcription factors. ERK phosphorylates c-Jun which leads to the activation of the Activator Protein 1 (AP-1) transcription factor. ERK also directly phosphorylates the E26 transformation-specific (ETS) family of transcription factors, which regulate Fos expression. The regulation and activation of these transcription factors enable the expression of essential cell-cycle regulatory proteins and allows for progression in the cell cycle.[17, 18]

Phosphatidylinositol 3-kinase (PI3K)/AKT/mTOR Pathway

The catalytic subunit of PI3Ks bind to active Ras at the plasma membrane. The localization of PI3K near the plasma membrane, due to binding with active Ras, facilitates the next step of the signal cascade. PI3K phosphorylates phosphatidylinositol-4,5-bisphosphate (PtdIns(4,5)P2, PIP_2) which then produces the second messenger molecule, phosphatidylinositol-3,4,5-trisphosphate (PtdIns(3,4,5)P3, PIP_3). PIP_3 binds a multitude of downstream proteins through its Pleckstrin homology domain (PH domain).

PIP_3 recruits Protein Kinase B (Akt) through the PH domain. Akt activates by duel phosphorylation from Pyruvate Dehydrogenase Kinase 1 (PDK1) and mTOR rictor complex (mTORC2) also recruited by PH domains. Once activated, Akt phosphorylates many other downstream effectors, including mTOR, which promote cell growth and protein synthesis.[19]

RAL guanine nucleotide dissociation stimulator (RALGDS)/RAL

RALGDS is a GEF for the Ral GTPase subfamily of proteins. Active Ras is able to bind RALGDS to activate RALGDS, which in turn facilitates Ral GNE, resulting in activation of Ral GTPases. Ral proteins regulate endocytosis, exocytosis, and actin organization as well as transcription factors such as fos and jun.[20-22] The inhibition of Forkhead box (FOXO) family of transcription factors is a responsibility of the RALGDS and Akt pathways. FOXO transcription factors are control a multitude of processes including apoptosis and cell cycle arrest. The inhibition of FOXO contributes to cell survival.[23]

Renewed Significance of Ras

Ras and its superfamily members have been studied extensively since the discovery of the first Ras protein in 1982.[24] It is through the work of many scientists and 35 years of research that we come to understand what is now what is referred to as the “classical” view of the Ras activity regulation associated with the control of Ras-downstream effectors. It is clear now that the “classical” view of Ras signaling and activity regulation is an immense oversimplification. Many recent discoveries in the field

of Ras proteins indicate that the Ras activity regulation is much more intricate than once thought.

Ubiquitination

Recent studies have uncovered a new post-translational modification (PTM) of Ras, ubiquitination. KRas was shown to be monoubiquitinated at Lys147. The monoubiquitination of KRas populates the active GTP-bound form of KRas, as the monoubiquitinated form of KRas has an impaired ability to GAPs.[25, 26] Another report showed that monoubiquitinated G12V KRas has an increased binding affinity for Ras-downstream effectors, PI3K and Raf.[27] HRas and NRas have been reported to diubiquitinated.[28] The diubiquitination of HRas and NRas cause a significantly different membrane localization profile. Diubiquitinated HRas and NRas localize around cellular enodsomal membranes rather than the plasma membrane or the Golgi.[29]

Intrinsic Kinetic Features of Ras and their Role in Costello Syndrome

The intrinsic Ras-kinetic features that include the intrinsic Ras GNE as well as the intrinsic Ras nucleotide-hydrolysis rate are magnitudes slower than the corresponding processes by Ras regulators. Therefore, it is not surprising that the deregulations of the intrinsic kinetic features of Ras are often overlooked in favor of the corresponding deregulations of the regulator-mediated kinetic processes. However, the research results shown in Chapter 2 suggest that certain somatic mutations of HRas only alter the intrinsic kinetic properties of Ras yet cause to the development of Costello Syndrome. The results call attention to that the deregulations of the intrinsic kinetic features of Ras should not be neglected for the cause of diseases.

Chapter 2 characterizes the somatic mutations of HRas which are responsible for the development of Costello Syndrome. The HRas somatic mutations are known to elevate the levels of active GTP-bound HRas in cells. It is, however, interesting that these cellularly elevated levels of GTP-bound HRas do not reach the levels that are observed in cancer cells. Chapter 2 shows that the cause of Costello Syndrome is a result of the deregulation of two intrinsic kinetic features. (i) The perturbations of the intrinsic kinetic features of Ras: They represent the broad spectrum of the Costello Syndrome mutants which populate the GTP-bound form of HRas. The upper end of this spectrum of HRas mutants, is exemplified by G12S HRas, which can also cause cancer. (ii) The perturbations of the catalytic action of p120GAP on Ras: They cause to a significantly elevated population of the GTP-bound form of HRas that often links to cancer formation. HRas mutant G12V belongs to this case.

Redox Regulation of Ras GTPases

Recently it was shown another entity can control the balance of activity in Ras proteins, redox agents. The superoxide anion ($O_2^{\bullet-}$) and nitrogen dioxide ($^{\bullet}NO_2$) cause GNE in Ras proteins with redox sensitive motifs (Figure 6).[30-34] Certain Ras proteins possess the conserved redox sensitive NK<u>C</u>D motif.[31, 35] The redox sensitive motifs are derivatives of the highly conserved G4 motif (N/TKXD). The cysteine residue in the redox sensitive motif directly interacts with redox reagents. These motifs impart sensitivity towards redox agents to Ras allowing redox agents to play a role in modulating the activity of Ras.

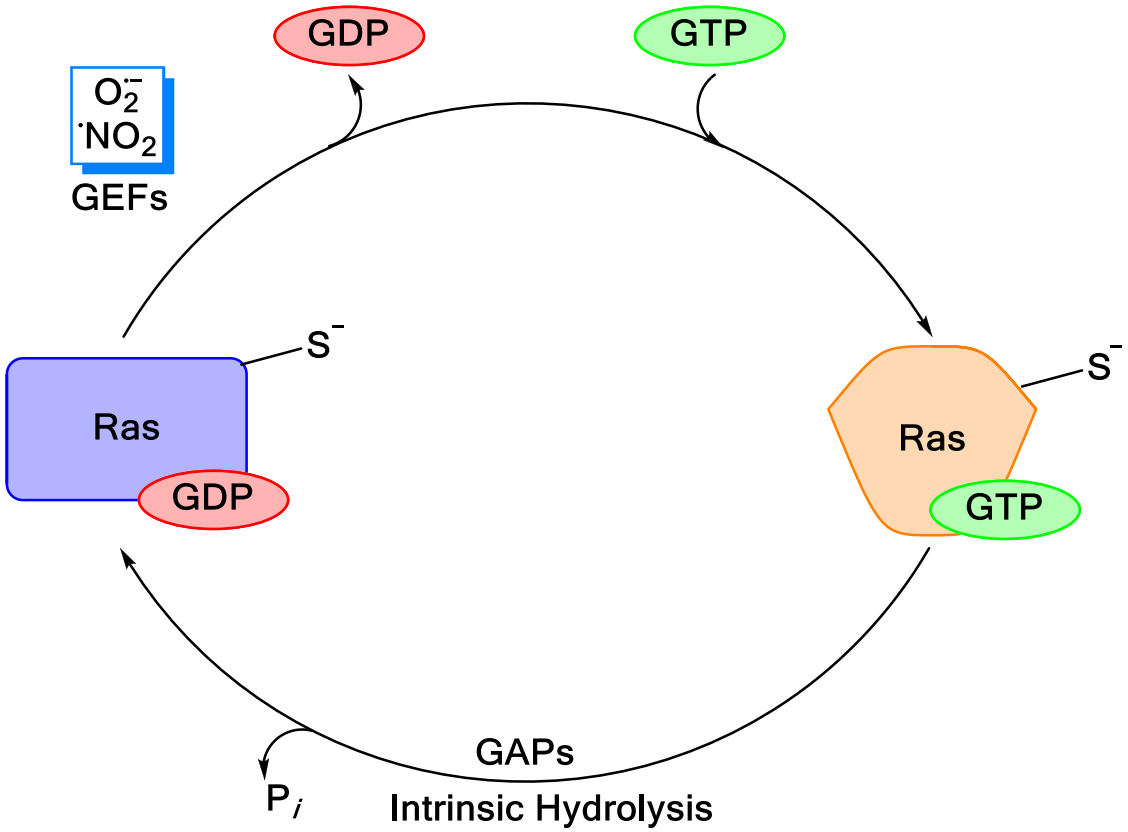

Figure 6. *The Cycling of Ras in the Presence of Redox Agents.*

Inactive Ras GTPase (blue) can be activated by GEFs by Ras GNE: an exchange of GDP for GTP to produce active Ras GTPase (orange). This Ras GNE can also be facilitated by redox agents. The redox-sensitive cysteine in the NKCD motif of Ras is the reaction target of redox agents. The sulfur atom of the redox-sensitive cysteine is predicted to be a thiolate form.

ERas, A New Member of the Ras Family

In 2003, Takahashi et al.[36] identified a distinctly new Ras protein, ERas, in murine embryonic cells. The murine ERas is essential to the proper growth and development of murine embryos. The human orthologue of mERas, human ERas, is epigentically silenced and is considered a psuedogene. While ERas is not expressed in healthy normal human cells, ERas expression has been shown in many human cancer cell-lines counting gastric, colorectal, pancreatic, breast, and neuroblastoma origins.[37-41]

The ERas protein consists of 227 amino acids that shares ~45% sequence homology with the orthodox Ras proteins. However, there are distinct sequential features which make ERas distinct from its other Ras subfamily members. In particular, ERas has a previously unrecognized extended N-terminus (Figure 4). It is unknown what is the function of the extended N-terminus. It has been postulated that it aids in membrane localization.[42] Another feature which distinguishes ERas from other Ras proteins is that ERas is constitutively active.[36] This is because ERas has an intrinsically high GTP-binding affinity and is insensitivity against the GAP action.[43]

While ERas has features which distinguish it from the other members of Ras subfamily, it retains the five highly conserved GTP-binding domains of Ras proteins, including Switch I and Switch II. The regions of Switches I and II change their conformation based on the nucleotide binding and interface with Ras-downstream effectors. ERas as well as others such as HRas, KRas, and NRas have nearly identical Switches I and II sequences, thus ERas may also interact with Ras-downstream effectors that are shown to interact with HRas, KRas, and NRas.

ERas has been reported to interact with primarily with PI3Kα and PI3Kδ.[36, 42, 44] However, there have been no quantitative reports on which PI3K isoforms are the dominant binding partner of ERas:[36, 44-46] It is important to note that these previous studies performed thus far were qualitative analyses by using pulldown assays. Besides, ERas binding interactions with other Ras-downstream effectors, such as RalGDS and Rassf5, have not been investigated. Chapter 3 describes quantitative kinetic-binding studies for ERas with key Ras-downstream effector proteins (Raf1, RalGDS, Rassf5, and PI3K isoforms) that delineate the unclear ERas-specific downstream effectors.

References

1. Klinghoffer, R. A., Duckworth, B., Valius, M., Cantley, L., and Kazlauskas, A. (1996) Platelet-derived growth factor-dependent activation of phosphatidylinositol 3-kinase is regulated by receptor binding of SH2-domain-containing proteins which influence Ras activity, *Mol Cell Biol 16*, 5905-5914.
2. Roberts, P. J., and Der, C. J. (2007) Targeting the Raf-MEK-ERK mitogen-activated protein kinase cascade for the treatment of cancer, *Oncogene 26*, 3291-3310.
3. Wennerberg, K., Rossman, K. L., and Der, C. J. (2005) The Ras superfamily at a glance, *J Cell Sci 118*, 843-846.
4. Vetter, I. R., and Wittinghofer, A. (2001) The guanine nucleotide-binding switch in three dimensions, *Science 294*, 1299-1304.
5. Shields, J. M., Pruitt, K., McFall, A., Shaub, A., and Der, C. J. (2000) Understanding Ras: 'it ain't over 'til it's over', *Trends Cell Biol 10*, 147-154.

6. Lenzen, C., Cool, R. H., and Wittinghofer, A. (1995) Analysis of intrinsic and CDC25-stimulated guanine nucleotide exchange of p21ras-nucleotide complexes by fluorescence measurements, *Methods Enzymol 255*, 95-109.

7. Gideon, P., John, J., Frech, M., Lautwein, A., Clark, R., Scheffler, J. E., and Wittinghofer, A. (1992) Mutational and kinetic analyses of the GTPase-activating protein (GAP)-p21 interaction: the C-terminal domain of GAP is not sufficient for full activity, *Mol Cell Biol 12*, 2050-2056.

8. Wittinghofer, A., and Vetter, I. R. (2011) Structure-function relationships of the G domain, a canonical switch motif, *Annu Rev Biochem 80*, 943-971.

9. Lam, B. D., and Hordijk, P. L. (2013) The Rac1 hypervariable region in targeting and signaling: a tail of many stories, *Small GTPases 4*, 78-89.

10. Welman, A., Burger, M. M., and Hagmann, J. (2000) Structure and function of the C-terminal hypervariable region of K-Ras4B in plasma membrane targetting and transformation, *Oncogene 19*, 4582-4591.

11. Wennerberg, K., and Der, C. J. (2004) Rho-family GTPases: it's not only Rac and Rho (and I like it), *J Cell Sci 117*, 1301-1312.

12. Wright, L. P., and Philips, M. R. (2006) Thematic review series: lipid posttranslational modifications. CAAX modification and membrane targeting of Ras, *J Lipid Res 47*, 883-891.

13. Choy, E., Chiu, V. K., Silletti, J., Feoktistov, M., Morimoto, T., Michaelson, D., Ivanov, I. E., and Philips, M. R. (1999) Endomembrane trafficking of ras: the CAAX motif targets proteins to the ER and Golgi, *Cell 98*, 69-80.

14. Resh, M. D. (2013) Covalent lipid modifications of proteins, *Curr Biol 23*, R431-435.

15. Downward, J. (2003) Targeting RAS signalling pathways in cancer therapy, *Nat Rev Cancer 3*, 11-22.

16. Rajalingam, K., Schreck, R., Rapp, U. R., and Albert, S. (2007) Ras oncogenes and their downstream targets, *Biochim Biophys Acta 1773*, 1177-1195.

17. Chang, F., Steelman, L. S., Shelton, J. G., Lee, J. T., Navolanic, P. M., Blalock, W. L., Franklin, R., and McCubrey, J. A. (2003) Regulation of cell cycle progression and apoptosis by the Ras/Raf/MEK/ERK pathway (Review), *Int J Oncol 22*, 469-480.

18. Zenonos, K., and Kyprianou, K. (2013) RAS signaling pathways, mutations and their role in colorectal cancer, *World J Gastrointest Oncol 5*, 97-101.

19. Alfred Yung, W. K. (2010) Review of the complexities of the PI3K/mTOR pathway presages similar handling of other critical topics, *Neuro Oncol 12*, 763-764.

20. Huang, L., Weng, X., Hofer, F., Martin, G. S., and Kim, S. H. (1997) Three-dimensional structure of the Ras-interacting domain of RalGDS, *Nat Struct Biol 4*, 609-615.

21. Kikuchi, A., Demo, S. D., Ye, Z. H., Chen, Y. W., and Williams, L. T. (1994) ralGDS family members interact with the effector loop of ras p21, *Mol Cell Biol 14*, 7483-7491.

22. Rodriguez-Viciana, P., and McCormick, F. (2005) RalGDS comes of age, *Cancer Cell 7*, 205-206.

23. Carter, M. E., and Brunet, A. (2007) FOXO transcription factors, *Curr Biol 17*, R113-114.

24. Papageorge, A., Lowy, D., and Scolnick, E. M. (1982) Comparative biochemical properties of p21 ras molecules coded for by viral and cellular ras genes, *J Virol 44*, 509-519.

25. Baker, R., Wilkerson, E. M., Sumita, K., Isom, D. G., Sasaki, A. T., Dohlman, H. G., and Campbell, S. L. (2013) Differences in the regulation of K-Ras and H-Ras isoforms by monoubiquitination, *J Biol Chem 288*, 36856-36862.

26. Baker, R., Lewis, S. M., Sasaki, A. T., Wilkerson, E. M., Locasale, J. W., Cantley, L. C., Kuhlman, B., Dohlman, H. G., and Campbell, S. L. (2013) Site-specific monoubiquitination activates Ras by impeding GTPase-activating protein function, *Nat Struct Mol Biol 20*, 46-52.

27. Sasaki, A. T., Carracedo, A., Locasale, J. W., Anastasiou, D., Takeuchi, K., Kahoud, E. R., Haviv, S., Asara, J. M., Pandolfi, P. P., and Cantley, L. C. (2011) Ubiquitination of K-Ras enhances activation and facilitates binding to select downstream effectors, *Sci Signal 4*, ra13.

28. Jura, N., Scotto-Lavino, E., Sobczyk, A., and Bar-Sagi, D. (2006) Differential modification of Ras proteins by ubiquitination, *Mol Cell 21*, 679-687.

29. Jura, N., and Bar-Sagi, D. (2006) Mapping cellular routes of Ras: a ubiquitin trail, *Cell Cycle 5*, 2744-2747.

30. Heo, J., and Campbell, S. L. (2006) Ras regulation by reactive oxygen and nitrogen species, *Biochemistry 45*, 2200-2210.

31. Heo, J., and Campbell, S. L. (2005) Mechanism of redox-mediated guanine nucleotide exchange on redox-active Rho GTPases, *J Biol Chem 280*, 31003-31010.

32. Heo, J., Prutzman, K. C., Mocanu, V., and Campbell, S. L. (2005) Mechanism of free radical nitric oxide-mediated Ras guanine nucleotide dissociation, *J Mol Biol 346*, 1423-1440.

33. Heo, J., and Campbell, S. L. (2005) Superoxide anion radical modulates the activity of Ras and Ras-related GTPases by a radical-based mechanism similar to that of nitric oxide, *J Biol Chem 280*, 12438-12445.

34. Heo, J., and Campbell, S. L. (2004) Mechanism of p21Ras S-nitrosylation and kinetics of nitric oxide-mediated guanine nucleotide exchange, *Biochemistry 43*, 2314-2322.

35. Heo, J., Raines, K. W., Mocanu, V., and Campbell, S. L. (2006) Redox regulation of RhoA, *Biochemistry 45*, 14481-14489.

36. Takahashi, K., Mitsui, K., and Yamanaka, S. (2003) Role of ERas in promoting tumour-like properties in mouse embryonic stem cells, *Nature 423*, 541-545.

37. Iwauchi, T., Tanaka, H., Yamazoe, S., Yashiro, M., Yoshii, M., Kubo, N., Muguruma, K., Sawada, T., Ohira, M., and Hirakawa, K. (2011) Identification of HLA-A*2402-restricted epitope peptide derived from ERas oncogene expressed in human scirrhous gastric cancer, *Cancer Sci 102*, 683-689.

38. Yashiro, M., Yasuda, K., Nishii, T., Kaizaki, R., Sawada, T., Ohira, M., and Hirakawa, K. (2009) Epigenetic regulation of the embryonic oncogene ERas in gastric cancer cells, *Int J Oncol 35*, 997-1003.

39. Kaizaki, R., Yashiro, M., Shinto, O., Yasuda, K., Matsuzaki, T., Sawada, T., and Hirakawa, K. (2009) Expression of ERas oncogene in gastric carcinoma, *Anticancer Res 29*, 2189-2193.

40. Yasuda, K., Yashiro, M., Sawada, T., Ohira, M., and Hirakawa, K. (2007) ERas oncogene expression and epigenetic regulation by histone acetylation in human cancer cells, *Anticancer Res 27*, 4071-4075.

41. Zhang, F., Tang, J. M., Wang, L., Shen, J. Y., Zheng, L., Wu, P. P., Zhang, M., and Yan, Z. W. (2010) Detection of beta-catenin, gastrokine-2 and embryonic stem cell expressed ras in gastric cancers, *Int J Clin Exp Pathol 3*, 782-791.

42. Nakhaei-Rad, S., Nakhaeizadeh, H., Kordes, C., Cirstea, I. C., Schmick, M., Dvorsky, R., Bastiaens, P. I., Haussinger, D., and Ahmadian, M. R. (2015) The Function of Embryonic Stem Cell-expressed RAS (E-RAS), a Unique RAS Family Member, Correlates with Its Additional Motifs and Its Structural Properties, *J Biol Chem 290*, 15892-15903.

43. Wey, M., Lee, J., Kim, H. S., Jeong, S. S., Kim, J., and Heo, J. (2016) Kinetic Mechanism of Formation of Hyperactive Embryonic Ras in Cells, *Biochemistry 55*, 543-559.

44. Nakhaei-Rad, S., Nakhaeizadeh, H., Gotze, S., Kordes, C., Sawitza, I., Hoffmann, M. J., Franke, M., Schulz, W. A., Scheller, J., Piekorz, R. P., Haussinger, D., and Ahmadian, M. R. (2016) The Role of Embryonic Stem Cell-expressed RAS (ERAS) in the Maintenance of Quiescent Hepatic Stellate Cells, *J Biol Chem 291*, 8399-8413.

45. Kubota, E., Kataoka, H., Aoyama, M., Mizoshita, T., Mori, Y., Shimura, T., Tanaka, M., Sasaki, M., Takahashi, S., Asai, K., and Joh, T. (2010) Role of ES cell-expressed Ras (ERas) in tumorigenicity of gastric cancer, *Am J Pathol 177*, 955-963.

46. Yu, Y., Liang, D., Tian, Q., Chen, X., Jiang, B., Chou, B. K., Hu, P., Cheng, L., Gao, P., Li, J., and Wang, G. (2014) Stimulation of somatic cell reprogramming by ERas-Akt-FoxO1 signaling axis, *Stem Cells 32*, 349-363.

CHAPTER 2

KINETIC MECHANISMS OF MUTATION-DEPENDENT HARVEY RAS ACTIVATION AND THEIR RELEVANCE FOR THE DEVELOPMENT OF COSTELLO SYNDROME

KINETIC MECHANISMS OF MUTATION-DEPENDENT HARVEY RAS ACTIVATION AND THEIR RELEVANCE FOR THE DEVELOPMENT OF COSTELLO SYNDROME[1]

Michael Wey, Jungwoon Lee, Soon Seog Jeong, Jungho Kim, and Jongyun Heo

Biochemistry 2013 *52* (47), 8465-8479 DOI: 10.1021/bi400679q

[1]This chapter has been published in Biochemistry and is being used with the permission of the publisher, 2016. My contribution to this article is the creation of Scheme 1 and the derivation of all equations associated with Scheme 1 (Chapter 2 Appendix).

Abstract

Costello syndrome is linked to activating mutations of a residue in the p-loop or the NKCD/SAK motifs of Harvey Ras (HRas). More than 10 HRas mutants that induce Costello syndrome have been identified; G12S HRas is the most prevalent of these. However, certain HRas p-loop mutations also are linked to cancer formation that are exemplified with G12V HRas. Despite these relations, specific links between types of HRas mutations and diseases evade definition because some Costello syndrome HRas p-loop mutations, such as G12S HRas, also often cause cancer. This study established novel kinetic parameter-based equations that estimate the value of the cellular fractions of the GTP-bound active form of HRas mutant proteins. Such calculations differentiate between two basic kinetic mechanisms that populate the GTP-bound form of Ras in cells. (i) The increase in GTP-bound Ras by the HRas mutation-mediated perturbation of the intrinsic kinetic characteristics of Ras. This generates a broad spectrum of the population of the GTP-bound form of HRas that typically causes Costello syndrome. The upper end of this spectrum of HRas mutants, as exemplified by G12S HRas, can also cause cancer. (ii) The increase in GTP-bound Ras because the HRas mutations perturb the p120GAP action on Ras. This causes production of a significantly high population of the only GTP-bound form of HRas linked merely to cancer formation. The HRas mutant G12V belongs to this category.

Introduction

Ras family proteins such as Harvey Ras (HRas), Neuroblastoma Ras (NRas), and Kirsten Ras (KRas) each generate distinct signals despite their interactions with a common set of regulators.[1] These Ras proteins function by cycling between inactive GDP-bound and active GTP-bound states, and various regulators control this GDP/GTP cycling.[2] These regulators include guanine nucleotide exchange factors (GEFs) and GTPase-activating proteins (GAPs).[3] Ras GEFs belong to the positive Ras regulators. Several isoforms of Ras GEFs, including Son of Sevenless (SOS), Ras guanine-nucleotide-release factor (RasGRF), and Ras guanyl nucleotide-releasing protein (RasGRP) have been identified.[4-6] These GEFs contain a common catalytic core domain Cdc25 and facilitate the intrinsically slow rate of guanine nucleotide exchange (GNE) of Ras-bound GDP/GTP with cellular free GDP/GTP.[7] Because the cellular concentration of GTP is ~10-fold higher than the concentration of GDP,[8] GEF-mediated Ras GNE populates Ras in their biologically active GTP-bound states. In turn, activated Ras proteins interact with a variety of downstream effector proteins that modulate numerous cellular signaling processes such as cellular proliferation and gene expression.[9] Ras GAPs are the negative Ras regulators. They consist of p120GAP, neurofibromin1 (NF1), and the GAP1 family.[10] All of these Ras GAPs share a RasGAP catalytic core domain.[11] GAPs increase the intrinsically slow rate of GTP hydrolysis for most Ras family proteins to permit conversion of the bound GTP into GDP, thereby terminating Ras downstream signaling.[12]

Several Ras motifs (Figure 1) — the phosphate-binding loop (P-loop; Gly^{10}-Ser^{17}), Switch I (Gln^{25}-Tyr^{40}), Switch II (Asp^{57}-Tyr^{64}), the nucleotide base-binding NKCD

M[1]TEYKLVVVGA**G[12]G[13]**VGKSALTIQLIQNHFVDEYDPTIEDSYRKQVVIDGET

p-loop

Switch I

- Intrinsic Ras-nucleotide phosphate binding
- Intrinsic Ras GTPase activity
- GAP-mediated Ras GTPase activity

- Ras regulators GEF and GAP binding

C[51]LLDILDTAGQEEYSAMRDQYMRTGEGFLCVFAINNTKSFEDIHQYREQI

Switch II

- Ras regulators GEF and GAP binding

K[101]RVKDSDDVPMVLVGN**K[117]**CDLAARTVESRQAQDLARSYGIPYIETS**A[146]**KTRQ

NKCD motif

SAK motif

- Intrinsic Ras nucleotide

- Intrinsic Ras nucleotide base binding

G[151]VEDAFYTLVREIRQHKLRKLNPPDESGPGCMSCKCVLS

Figure 1. *Sequence of wt HRas.*

The p-loop, Switch I, Switch II, NKCD, and SAK motifs of wt HRas are underlined. The HRas residues that are known to mutate to produce Costello syndrome-relevant HRas mutants are shown in boldface. These include Gly[12] and Gly[13] in the p-loop, Lys[117] in the NKCD, and Ala[146] in the SAK motif. The boxes depict the contributions of these motifs in the binding and/or catalytic function of Ras with nucleotide and/or regulators.

(Asn^{116}-Asp^{119}), and SAK (Ser^{145}-Lys^{147}) motifs (HRas numbering) — are known to be involved in these binding interactions with GDP and GTP. Many of these Ras motif residues are also directly or indirectly involved in the catalytic functions of GEFs and GAPs (Figure 1).[7, 11]

Costello syndrome is a genetic disorder that affects, but is not limited to, the skin and joints; it also often causes heart abnormalities.[13] Other characteristics are postnatal growth delays, mental retardation, and facial dysmorphism.[13] Mutations in the HRAS gene at codons Gly12 and Gly13 in the p-loop as well as at Lys117 and Ala146 in the NKCD and SAK motifs cause the syndrome.[14] The Costello syndrome-relevant HRas mutants for the p-loop Gly^{12} residue include G12A, G12S, G12C, G12D, and G12E (Table 1). Notably, the well-known oncogenic HRas p-loop mutant G12V[15] also causes Costello syndrome (Table 1). Other HRas p-loop mutants that induce Costello syndrome include G13S, G13C, and G13D (Table 1). Symptoms of Costello syndrome also are linked to an unusual HRas NKCD-motif mutant K117R and to the HRas SAK-motif mutants A146T and A146V (Table 1). Of all these HRas mutants, G12S is the most prevalent mutation found in Costello syndrome patients, occurring five times more often than other mutations combined (Table 1). When it occurs in NRas and KRas, the G12S mutation often causes certain cancers.[16-18] Because of its weak oncogenicity,[15, 19] there has been speculation that G12S HRas is present to serve as a partially active form of HRas to upregulate HRas-dependent cellular signaling.[13] The second most prevalent HRas mutant found in Costello Syndrome patients is G12A (Table 1); however, this mutant, unlike G12S, is not commonly found in cancers. Nonetheless, unlike other common HRas p-loop mutants, such as G12V, the

		Aoki *et al.*[20]	Gripp *et al.*[21]	Estep *et al.*[22]	Kerr *et al.*[23]	Sol-Church *et al.*[24]	Zampino *et al.*[25]	Van der Brugt *et al.*[26]	Gripp *et al.*[27]	Burkitt-Wright *et al.*[28]	Niihori *et al.*[29]	Digilio *et al.*[30]	Tidyman *et al.*[31]	Gripp *et al.*[32]	Kuniba *et al.*[33]	Piccione *et al.*[34]	Schulz *et al.*[35]	Denayer *et al.*[36]	Sinico *et al.*[37]
p-loop mutant	G12A	2	2	2	3	2		1			3						3		
	G12C				2						1								
	G12D										1				1				
	G12E				1														
	G12S	7	30	30	30	39	8				16	3	4				23		
	G12V	1						1		4									
	G13C		1	1		1								12		1	1		
	G13D	2										1					1		
	G13S																		1
	G13V[a]																		
NKCD /SAK mutant	K117R				1													1	
	A146T						1												
	A146V								1										
Totals		12	33	33[b]	37	42	9	4[c]	2[c]	4	21	4	4	12	1	1	31[c]	1	1

Table 1. *Frequency of HRas mutations in Costello syndrome*.

Previous reports of the relative occurrence in Costello syndrome of p-loop and NKCD/SAK HRas mutants are summarized.

[a]For comparison with Tables 2, 3, and 4 (see below), G13V HRas also is listed. However, the G13V HRas mutant has been linked to cancer, but not to Costello syndrome.[38] [b]In this study it was noted that 20 of the 33 patients also participated in the investigation done by Gripp *et al*.[21] [c]These studies noted totals of Costello syndrome patients, but only the relevant HRas mutants were specified.

biochemical properties of the listed Costello syndrome-relevant HRas mutants (Table 1) have not been fully investigated either with or without their regulators. Accordingly, no definite link has been established between these HRas mutations and the cellular populations of the GTP-bound form of these HRas mutants. This study used the kinetic parameters of Ras and its regulators to formulate novel equations that allow one to estimate the theoretical populations of the GTP-bound Ras in cells. Equipped with these novel equations, this study estimated the values of the theoretical populations of the GTP-bound form of these HRas mutants. The theoretical values were further evaluated with the directly measured cellular populations of the GTP-bound form of selected HRas mutants. These biochemical approaches reveal the kinetic mechanisms by which these HRas mutations contribute to Costello syndrome.

Materials and Methods

Protein preparations. All protein constructs, including wild type (wt) HRas, p120GAP, and Cdc25, were derived from humans. A full-length wt HRas (1-189) and HRas mutant proteins including G12V, G12A, G12S, G12C, G12D, G12E, G13V, G13S, G13C, G13D, K117R, A146T, and A146V were expressed in and purified from *E. coli,* as described in the previous study.[39]

A full-length p120GAP (1-1047) was overexpressed in insect Sf9 cells by using the pIEx vector (Novagen) and then purified using a sequence of columns, including the Sephadex G-150 gel filtration and FPLC Mono-Q columns, as described in the previous study.[40] However, because of the high cellular expression of p120GAP, the fast-flow S-Sepharose column step was omitted. The Ras SOS1 catalytic core domain Cdc25 (564-1049) was expressed in and purified from *E. coli,* as described in the previous study.[41]

Kinetic assay conditions. All kinetic analyses were performed using proteins more than 95% pure, as judged by SDS-PAGE. The buffer used for all assays consisted of 50 mM NaCl, 10 mM $MgCl_2$, 100 μM diethylenetriaminepentaacetic acid, and 100 mM TrisHCl (pH 7.4).

Estimation of kinetic parameters of Ras GNE in the presence and absence of Cdc25. Kinetic parameters of the intrinsic Ras GTP and GDP binding interactions were determined, respectively, with minor modifications, according to the previously established method.[42] The values of k_{-1} — the intrinsic rate constant of GTP dissociation from Ras protein — were determined by using the nonhydrolyzable radioactive GTP analog [^{35}S]GTPγS (~400 cpm/pmol) paired with GDP. Ras (1 μM)

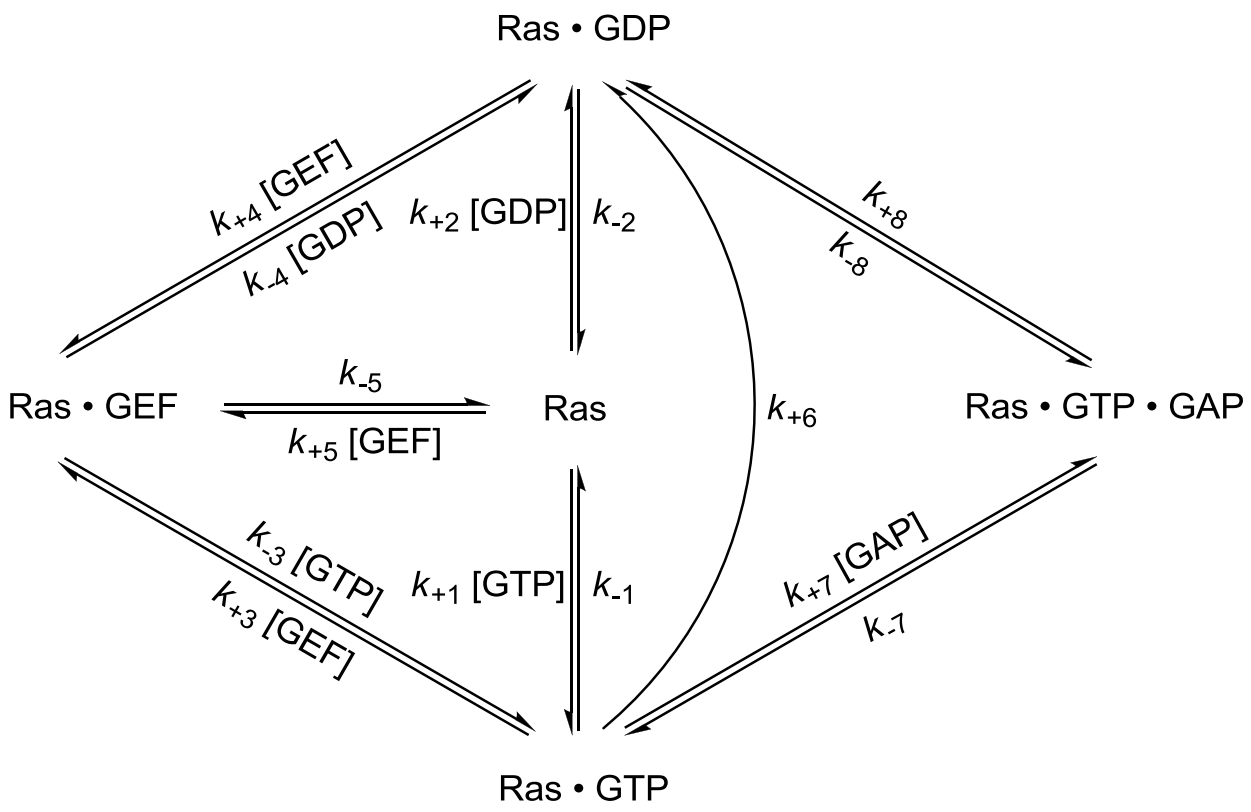

Scheme 1 *Comprehensive Kinetic Scheme of Ras Regulation in Cells*

loaded with [^{35}S]GTPγS was placed in an assay buffer containing GDP (1 μM). Aliquots of the assay mixture were withdrawn at specific intervals over a period of 20,000 s, and spotted onto nitrocellulose filters. The nitrocellulose filters were washed three times with the assay buffer, and the filter-bound radioactivity was measured using a scintillation counter (Beckman LS 6000). These data were fit to single exponential decays that give values of k_{-1}. The values of k_{-2} — the intrinsic rate constant of GDP dissociation from Ras proteins — also were measured as the measurement of k_{-1}, as described above, except that the radioactive [8-^{3}H]GDP (~200 cpm/pmol) paired with GTP were used instead of the [^{35}S]GTPγS paired with GDP.

Kinetic parameters of the Cdc25-mediated Ras-bound GTP and GDP exchange with GDP and GTP were measured, respectively, as described in the previous study.[41] The values of k_{+3} — the exchange rate constant of the Ras-bound GTP with GDP in the presence of Cdc25 — were determined using the 2'(3')-*O*-(*N*-methylanthraniloyl) 5'-guanylyl-imidodiphosphate (mantGppNHp; a nonhydrolyzable GTP analog) paired with GDP. In brief, the reaction was initiated by the addition of the various concentrations of the mantGppNHp-loaded Ras (0-500 μM) into an assay buffer containing GDP (5 mM) and Cdc25 (500 nM). Dissociation of mantGppNHp from Ras was monitored over a period of 20,000 s by using a Fluorescence Spectrometer (LS 55, PerkinElmer). These data were fit to a single exponential decay to determine the apparent dissociation rates of mantGppNHp from Ras in the presence of Cdc25. Once determined, these rates were then replotted against the concentrations of the mantGppNHp-loaded Ras used. These rates were then fit to a hyperbola to determine the maximal velocity (V_{max}) and the Michaelis–Menten constant (K_M) of the Cdc25-mediated dissociation of

mantGppNHp from Ras. According to the Theorell-Chance type mechanism,[43] the dissociation of GTP from Ras couples with the association of GEF, which is then immediately displaced with GDP (if only GDP is present). Hence, the dissociation rate of mantGppNHp from Ras represents the exchange rate of mantGppNHp with GDP. Therefore, from the perspective of the Theorell-Chance type of mechanism, the values of V_{max} of the dissociation of the Ras-bound mantGppNHp from Ras per the total Cdc25 enzyme (E_o) are, respectively, equivalent to k_{+3}. With one exception, the methods and analyses used for the determination of the value of k_{+3} also were applied to determination of the values of k_{+4} — the exchange rate constant of the Ras-bound GDP with GTP in the presence of Cdc25. The exception was the use of the 2'(3')-*O*-(*N*-methylanthraniloyl) guanosine diphosphate (mantGDP) paired with GTP instead of the mantGppNHp paired with GDP.

Estimation of kinetic parameters of Ras GTP hydrolysis in the presence and absence of p120GAP. The intrinsic kinetic parameters of Ras GTPase activity were measured, with minor modifications, as described in the previous study.[44] The values of k_{+6} — the rate constant for the intrinsic Ras GTPase activities — were determined by using [γ-^{32}P]GTP (~500 cpm/pmol). As-purified Ras (1 μM) was added to the assay buffer containing [γ-^{32}P]GTP (50 μM). Aliquots were taken from the assay solution at specific intervals over a period of 20,000 sec and spotted onto nitrocellulose filters. The radioactivity of filtrants that contain only free [γ-^{32}P] was determined by using a scintillation counter (Beckman LS 6000). The values of k_{+6} were then determined by the fit of these data to a function of exponential decay.

It is of interest that, unlike the GEF-mediated enzymatic process, the GAP-mediated enzymatic process does not follow the Theorell-Chance type of mechanism.[43] This is because the formative process of the Ras•GTP•GAP ternary complex intermediate is not so transient.[11] Nonetheless, within this study, the parameters associated with the p120GAP-mediated Ras GTP hydrolysis were calculated based on the values of the K_M and V_{max} of p120GAP for Ras. In brief, the values of k_{+8} — the rate constant for the hydrolysis of GTP of the Ras•GTP•p120GAP ternary complex to produce Ras•GDP — were estimated by dividing the total Ras concentration (E_o) into V_{max}; this yields V_{max}/E_o, which is equivalent to k_{cat}, which is the same as k_{+8}. The values of K_M and k_{cat} of p120GAP for Ras were measured by using radioactive [γ-^{32}P]GTP (~500 cpm/pmol) as described in the previous study.[45] As-purified Ras (1 μM) was added to the assay buffer containing [γ-^{32}P]GTP (50 μM) and various concentrations of p120GAP (0-35 μM). Aliquots of the assay mixture were drawn at specific intervals over a period of 20,000 sec and spotted onto nitrocellulose filters. The radioactivity of only the free [^{32}P]-containing liquid filtrants was determined with a scintillation counter (Beckman LS 6000). The apparent rates of Ras GTPase activity in the presence of p120GAP were then determined by the fit of these data to a function of a single exponential decay. The plots of apparent rates against the concentration of p120GAP that were thus determined were fit to a hyperbola to obtain the values of V_{max} and K_M of p120GAP for Ras GTP hydrolysis.

Comprehensive kinetic scheme of Ras activity regulation in cells. Scheme 1 shows a comprehensive web of kinetic paths that describe the regulation of the binding of Ras with its ligands, GTP and GDP. Scheme 1 comprehensively encompasses all

the known cellular kinetic paths that modulate the Ras binding states with GTP and GDP in the presence and absence of Ras regulators, including GEF and GAP. The kinetic parameters denoted in Scheme 1 stand for the kinetic rate constants associated with the processes of the reactions that occur through the kinetic paths. The kinetic parameters shown in Scheme 1 also represent the steps of the reaction processes that occur through the given kinetic paths. According to Scheme 1, three essential kinetic processes in effect determine the featured state of the Ras binding with GTP and GDP. These three are the intrinsic Ras GNE and GTP hydrolysis, the GEF-mediated Ras GNE, and the GAP-mediated Ras GTP hydrolysis in conjunction with the term of concentrations of GTP and GDP ([GTP] and [GDP], respectively). The kinetic steps of k_{+1}, k_{-1}, k_{+2}, and k_{-2} are involved in the intrinsic Ras GNE. The kinetic steps of k_{+3}, k_{-3}, k_{+4}, k_{-4}, k_{+5}, and k_{-5} in combination with the concentration of GEF ([GEF]) are implicated in the GEF-mediated Ras GNE. The kinetic step of k_{+6} is engaged in the intrinsic Ras GTP hydrolysis. The kinetic steps of k_{+7}, k_{-7}, and k_{+8} in combination with the concentration of GAP ([GAP]) are linked to the process of the GAP-mediated Ras GTP hydrolysis.

Calculation of the theoretical cellular population of the GTP-bound Ras. The result of the regulation of Ras binding interactions with GTP and GDP through these paths (Scheme 1) determines the overall comprehensive cellular fraction of the GTP-bound Ras over the GTP- and GDP-bound Ras (the comprehensive $f_{\text{Ras}\bullet\text{GTP}} = \left(\frac{[\text{Ras}\cdot\text{GTP}]}{[\text{Ras}\cdot\text{GTP}] + [\text{Ras}\cdot\text{GDP}]}\right)$ of Ras. The value of the comprehensive $f_{\text{Ras}\bullet\text{GTP}}$ of Ras is of particular interest because it refers to the overall cellular population of the biologically active form of Ras.

Equation 1 defines the value of the comprehensive $f_{\text{Ras•GTP}}$ of Ras that enables calculation of the theoretical comprehensive cellular population of the GTP-bound form of Ras of interest by using the intrinsic kinetic parameters of Ras as well as the kinetic parameters of GEF and GAP with Ras shown in Scheme 1 (see Appendix for the derivation).

The comprehensive $f_{\text{Ras•GTP}}$ Equation 1

$$= \frac{(k_{-2}+k_{+4}[\text{GEF}])[\text{GTP}]}{(k_{-2}+k_{+4}[\text{GEF}])[\text{GTP}]+(k_{-1}+k_{+3}[\text{GEF}])[\text{GDP}]+\left(\frac{k_{+7}k_{+8}}{k_{-7}+k_{+8}}[\text{GAP}]+k_{+6}\right)([\text{GTP}]+[\text{GDP}])}$$

Equation 2 expresses the intrinsic cellular fraction of the GTP-bound Ras over the GTP- and GDP-bound Ras (the intrinsic $f_{\text{Ras•GTP}}$) of Ras in terms of the kinetic parameters of intrinsic Ras GNE and GTP hydrolysis shown in Scheme 1 (see Appendix for the derivation).

The intrinsic $f_{\text{Ras•GTP}} = \frac{k_{-2}[\text{GTP}]}{k_{-2}[\text{GTP}]+k_{-1}[\text{GDP}]+k_{+6}([\text{GTP}]+[\text{GDP}])}$ Equation 2

Equation 3 denotes the cellular fraction of the GTP-bound Ras over the GTP- and GDP-bound Ras (the GEF-mediated $f_{\text{Ras•GTP}}$) of Ras in the presence of GEF in cells shown in Scheme 1 (see Appendix for the derivation).

The GEF-mediated $f_{\text{Ras•GTP}}$ Equation 3

$$= \frac{(k_{-2}+k_{+4}[\text{GEF}])[\text{GTP}]}{(k_{-2}+k_{+4}[\text{GEF}])[\text{GTP}]+(k_{-1}+k_{+3}[\text{GEF}])[\text{GDP}]+k_{+6}([\text{GTP}]+[\text{GDP}])}$$

Equation 4 expresses the cellular fraction of the GTP-bound Ras over the GTP- and GDP-bound Ras (the GAP-mediated $f_{\text{Ras•GTP}}$) of Ras in the presence of GAP in cells shown in Scheme 1 (see Appendix for the derivation).

$$\text{The GAP-mediated } f_{\text{Ras•GTP}} = \frac{k_{-2}[\text{GTP}]}{k_{-2}[\text{GTP}]+k_{-1}[\text{GDP}]+\left(\frac{k_{+7}k_{+8}}{k_{-7}+k_{+8}}[\text{GAP}]+k_{+6}\right)([\text{GTP}]+[\text{GDP}])} \qquad \text{Equation 4}$$

Quantification of the Ras-bound GTP in cells. Unstimulated NIH 3T3 cells were stably transfected with various HRAS constructs (#1-189) using a mammalian expression vector pCAGGS with FuGene-6-reagent (Roche). Cells were cultured for four days in a complete RPMI 1640 medium, and washed with phosphate-free Eagle's minimum essential medium. Resuspended cells were then incubated for 5 hr with a serum- and phosphate-free RPMI 1640 medium containing ~50 μCi of ^{32}P/mL. Cells were washed twice with ice-cold PBS (Sigma) and then scraped into an ice-cold homogenization buffer containing 500 mM NaCl, 10 mM $MgCl_2$, 5 mM DTT, 1 mM EDTA, 0.1% Triton X-100, 0.005% SDS, protease inhibitors (0.5 mM phenylmethylsulfonyl fluoride, 1 μg/mL peptstain A, 1 μg/mL aproptinin, and 1 μg/mL leupeptin), and 10 mM TrisHCl (pH 7.4). Cells in the ice-cold homogenization buffer were sonificated 4 × 5 sec (40 watts) on ice followed by centrifugation (100,000 × g) at 4 °C for 20 min. The supernatant of the cell lysate extract was nutated with Amine Immobilization Resin (Thermo Scientific) coupled with a pan Ras F132 antibody (Santa Cruz Biotechnology) at 4 °C for 5 hr. Resin was collected by centrifugation (10,000 × g) for 30 min; the proteins bound to the resin were washed with a buffer containing 500 mM NaCl, 10 mM $MgCl_2$, 5 mM DTT, 1 mM EDTA, 0.1% Triton X-100, and 10 mM

TrisHCl (pH 7.4). Nucleotides were eluted from the resin-bound proteins by treatment with a buffer containing 500 mM NaCl, 10 mM $MgCl_2$, 5 mM DTT, 2.5% SDS, and 10 mM TrisHCl (pH 6.8) at 4 °C for 1 hr. The nucleotides were then analyzed by thin-layer chromatography and autoradiographed using a densitometry (Bio-Rad GS-670) as described in the previous study[46] to determine the actual cellular fraction of the GTP-bound HRas proteins in the presence of both GEFs and GAPs (the cellular $f_{Ras \cdot GTP}$).

Results

The course of this study involved preparation of wt HRas and multitudes of p-loop and NKCD/SAK HRas mutants listed in Table 1. Cdc25 and p120GAP were prepared, respectively, as GEF and GAP. The key kinetic parameters (depicted in Scheme 1) of these Ras proteins with and without Cdc25 and/or p120GAP were then determined (Figures 2 and 3). The kinetic values are summarized in Tables 2 and 3. Using Equations 1-4 in conjunction with these values of the kinetic parameters, the intrinsic, GEF- and GAP-mediated and comprehensive values of the $f_{\text{Ras•GTP}}$ of these Ras proteins were assessed (Table 4) and analyzed in detail.

Calculation of the intrinsic $f_{Ras•GTP}$ value of Ras. The value of the intrinsic $f_{\text{Ras•GTP}}$ of Ras denotes the cellular population of the active GTP-bound form of Ras in the absence of any Ras regulators. A number of the intrinsic $f_{\text{Ras•GTP}}$ values of Ras proteins (Table 4) were reached by determination of several kinetic parameters for subsequent calculation in Equation 2. These kinetic parameters include (i) the value of the intrinsic GNE of Ras proteins (k_{-1} and k_{-2}) (Table 2) and (ii) the value of the intrinsic GTP hydrolysis of Ras proteins (k_{+6}) (Table 3). This calculation used the previously reported average values of [GTP] (~300 μM) and [GDP] (~40 μM) in human cells.[8]

Analysis of the intrinsic $f_{Ras•GTP}$ value of wt HRas. The intrinsic $f_{\text{Ras•GTP}}$ value of wt HRas was calculated to be 0.33 (Table 4). The values of k_{-1}, k_{-2}, and k_{+6} of wt HRas (Tables 2 and 3) that determine the intrinsic $f_{\text{Ras•GTP}}$ value of wt HRas did not deviate significantly from those of the previously reported values.[40, 45, 47, 48]

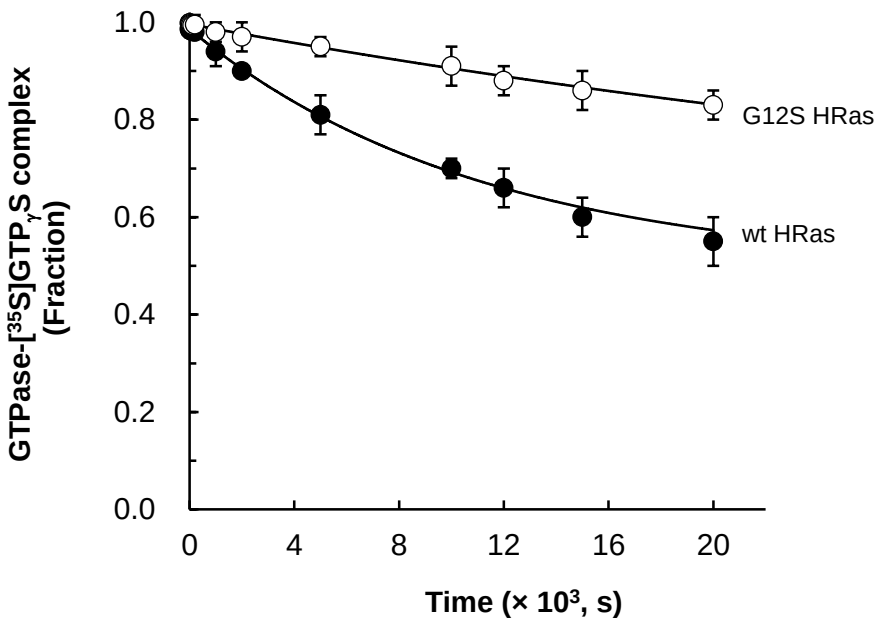

Figure 2. *Estimation of the kinetic constants of the intrinsic GTP dissociations from wt and G12S HRas.*

Measurements of the rate constants for the Ras GTP dissociation using [^{35}S]GTPγS are described in Materials and Methods. Radioactivity values determined for the Ras-bound [^{35}S]GTPγS at various time points were fractionated against the initial radioactivity value of the Ras-bound [^{35}S]GTPγS (time = 0 s); the fractionated radioactivity values were plotted against time. Mean values with the SD of each data point of the plots as derived from three separate independent experiments are shown. Table 2 summarizes the k_{-1} values that were determined by the fit of these plotted values of wt and G12S HRas to a single exponential decay with regression values (r^2) of > 0.9595.

			Intrinsic rate constants for Ras nucleotide dissociation (10^{-4} s^{-1})		Kinetic parameters associated with Cdc25 (10^3 s^{-1} M^{-1})	
			GTP dissociation (k_{-1})	GDP dissociation (k_{-2})	GEF-mediated GTP dissociation (k_{+3})	GEF-mediated GDP dissociation (k_{+4})
HRas	wt HRas		0.9	1.2	7.2	7.8
	p-loop mutants	G12A	0.9	0.5	7.5	7.3
		G12C	0.6	2.2	7.4	8.2
		G12D	9.5 (89[c])	1.6 (1.4[c])	7.6	7.0
		G12E	4.9	1.5	8.0	7.5
		G12S	0.2	4.8	7.0	8.0
		G12V	0.9 (0.78[a])	0.2 (0.38[b])	7.5	7.1
		G13C	0.8	2.5	7.7	8.2
		G13D	6.3	1.6	7.4	7.0
		G13S	0.7 (0.83[d])	3.6 (3.83[d])	8.2	8.8
		G13V	1.2 (5[d])	3.4 (105[d])	7.4	7.9
	NKCD/SAK mutants	K117R	11.1	13.0 (32[e])	8.6	9.0
		A146T	8.1	9.7	8.1	8.2
		A146V	9.3	13.5	8.4	8.8

Table 2. *Kinetic parameters for the intrinsic and GEF-mediated GDP and GTP dissociation from wt HRas and its mutants.*

Table 2. *Kinetic parameters for the intrinsic and GEF-mediated GDP and GTP dissociation from wt HRas and its mutants.*

The kinetic values with standard deviations (SD) of the intrinsic GTP dissociation from wt HRas and G12S were taken from Figure 2. The kinetic values with the SD of intrinsic GTP dissociation from all other listed HRas mutants were obtained as described in Figure 2. In addition, the kinetic values of intrinsic GDP dissociation with the SD from these Ras proteins also were obtained as described in Figure 2, except that [^{3}H]GDP, instead of [γ-^{32}P]GTP, was used. The k_{cat} (V_{max}/E_o) values of the Cdc25-mediated nucleotide dissociation from these Ras proteins were obtained by using a saturation kinetic analysis essentially as described in Materials and Methods. A fixed concentration of Ras (1 μM) loaded with either mantGDP or mantGppNHp and variable concentrations of Cdc25 (0-900 μM) was used in this analysis. The values of K_M also were obtained from this saturation kinetic analysis. However, because all determined K_M values of these HRas mutants were indistinguishable from those of wt HRas (K_M = ~340 μM), a listing of the detailed K_M values of these HRas mutants is omitted. The SD of the estimated values were within 10% of the values shown. The values of "a, b, c, d, and e" were taken from the references "[47], [42], [49], [40], and [36]," respectively.

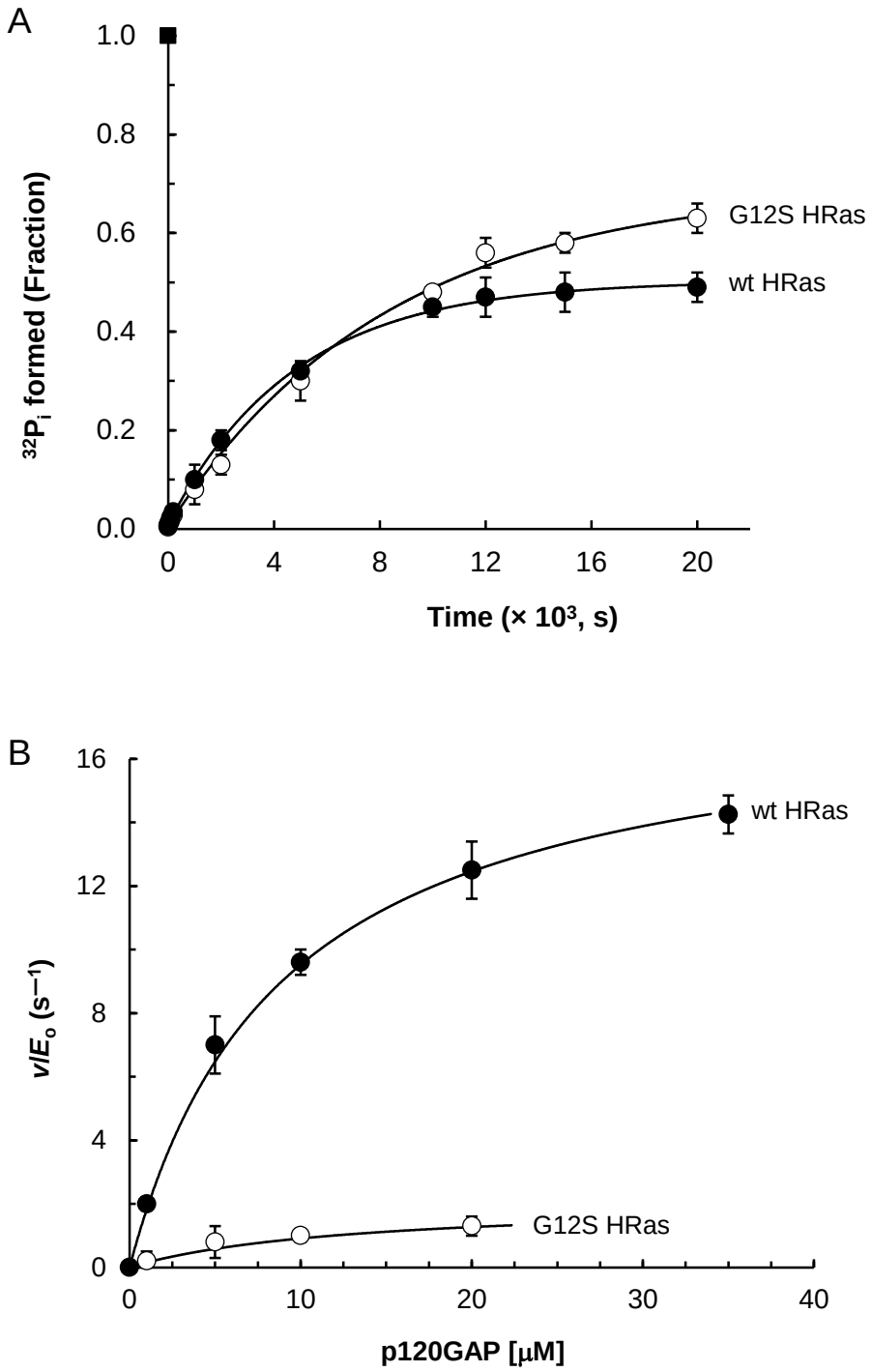

Figure 3. *Determination of the kinetic constants for the intrinsic and p120GAP-mediated activities of wt and G12S HRas.*

Figure 3. *Determination of the kinetic constants for the intrinsic and p120GAP-mediated activities of wt and G12S HRas.*

Kinetic constants of the phosphatase activity of Ras with and without p120GAP were assessed by using [γ-^{32}P]GTP as described in Materials and Methods. **A**. All apparent intrinsic values determined for radioactivity were fractionated against the radioactivity value of [γ-^{32}P]GTP that was initially added to the assay mixture and then plotted against time. All plot values represent mean values with the SD from three separate independent experiments. The estimated values of k_{+6} as determined by the fit of these plot data to a single exponential function with $r^2 > 0.9650$ are summarized in Table 3. **B**. Ras GTPase activity assays in the presence of various concentrations of p120GAP were monitored over a period as described in Materials and Methods. The radioactivity values were plotted against time and fit to a single exponential function with $r^2 > 0.9965$ to determine apparent rates of Ras GTPase activities in the presence of various concentrations of p120GAP. The apparent rates with the SD of Ras GTPase activities were then plotted against the concentration of p120GAP. All apparent values shown are mean values with the SD from three separate independent experiments. The plots were determined to fit to a hyperbola with $r^2 > 0.9695$ to give the V_{max} and K_M values of various Ras proteins coupled with p120GAP for the GTP hydrolysis. The V_{max} values were converted into k_{cat} (V_{max}/E_o) values as described in Materials and Methods. The estimated k_{cat} and K_M values are summarized in Table 3.

			Intrinsic Ras GTP hydrolysis rate (k_{+6}) (10^{-4} s^{-1})	Kinetic parameters associated with p120GAP		
				k_{cat} (k_{+8}) (s^{-1})	K_M (μM)	k_{cat}/K_M ($\times 10^6$ s^{-1} M^{-1})
HRas	wt HRas		2.1	18.0	8.9	2.02
	p-loop mutants	G12A	0.5	0.5	46.8	0.01
		G12C	1.8	3.2	12.3	0.26
		G12D	1.4 (1.7[a])	0.5	4.8	0.10
		G12E	1.6	0.9	4.7	0.20
		G12S	1.2	2.1	15.8	0.13
		G12V	0.05 (< 0.03[a]; 0.33[b])	0.01	< 100	~0
		G13C	1.1	1.9	26.6	0.03
		G13D	1.9	1.3	5.2	0.25
		G13S	3.2 (5.33[d])	1.5 (0.5[d])	19.6 (21.6[d])	0.01 (0.023[d])
		G13V	2.0 (2.17[d])	0.1	87.0	<0.01
	NKCD/SAK mutants	K117R	1.9	16.2	11.9	1.36
		A146T	1.9	12.5	10.7	1.05
		A146V	1.8 (same as wt[e])	10.7	13.8	0.78

Table 3. *Kinetic constants for the intrinsic and p120GAP-mediated GTPase activity of wt HRas and its mutants.*

The kinetic data of the intrinsic and p120GAP-mediated GTPase activities of wt HRas and G12S were taken from Figure 2. Data for other HRas mutants were also collected as described in the legends of Figures 2 and 3. The standard errors of the values were determined to be less than 10% of the values shown. The values of "a, b, c, d, and e" were taken from the references "[50], [47], [51], [40], and [52]", respectively.

Analysis of the intrinsic $f_{Ras\bullet GTP}$ values of HRas mutants. All of the intrinsic $f_{Ras\bullet GTP}$ values of the listed HRas mutants exceeded the intrinsic $f_{Ras\bullet GTP}$ value of wt HRas (Table 4).

The HRas p-loop mutants G12A and G12V both have smaller k_{-2} values than wt HRas but have similar k_{-1} values (Table 2). Although smaller k_{-2} values in Equation 2 would suggest a decrease in intrinsic $f_{Ras\bullet GTP}$ values, an increase in intrinsic $f_{Ras\bullet GTP}$ values (Table 4) is present due to the k_{+6} values in Equation 2 that are much smaller than those of wt HRas (Table 3).

Compared with the values of wt HRas, the values of HRas p-loop mutants G12C, G13S, and G13C have a smaller k_{-1} and a larger k_{-2} (Table 2). Nevertheless, these HRas mutants have slightly decreased k_{+6} values compared with the k_{+6} value of wt HRas (Table 3). These combinations of k values in Equation 2 favor a higher value of intrinsic $f_{Ras\bullet GTP}$ than is found in wt HRas. Another HRas p-loop mutant, G12S, is intriguing, because it has the same trait — a smaller k_{-1} and a larger k_{-2} value than that of wt HRas — but to a larger extent than the HRas mutants G12C, G13S, and G13C (Table 2). G12S HRas also has a slightly increased k_{+6} value compared with the k_{+6} value of wt HRas (Table 3). The combination of these unique k values in Equation 2 is reflected in the intrinsic $f_{Ras\bullet GTP}$ value, because G12S has the largest intrinsic $f_{Ras\bullet GTP}$ value, 0.78, among these mutants (Table 4).

HRas p-loop mutants G12D, G13D, and G12E exhibit much larger k_{-1} values than wt HRas does, but display only marginally increased k_{-2} and marginally decreased k_{+6} values compared with those that wt HRas exhibits for the same elements (Tables 2 and 3). However, the intrinsic $f_{Ras\bullet GTP}$ values of these HRas mutants increased slightly

			$f_{Ras \cdot GTP}$ values (fraction)							
			Intrinsic[a]	GEF-mediated[b]			GAP-mediated[c]	Comprehensive[d]		
				I	II	III		I	II	III
HRas	wt HRas		0.33	0.39	0.89	0.90	0.01	0.01	0.44	0.89
	p-loop mutants	G12A	0.43	0.55	0.89	0.89	0.19	0.28	0.88	0.89
		G12C	0.51	0.55	0.90	0.90	0.07	0.08	0.80	0.90
		G12D	0.37	0.42	0.89	0.90	0.10	0.12	0.84	0.90
		G12E	0.39	0.44	0.88	0.89	0.06	0.07	0.80	0.89
		G12S	0.78	0.79	0.90	0.91	0.23	0.24	0.85	0.91
		G12V	0.55	0.74	0.90	0.90	0.46	0.67	0.89	0.90
		G13S	0.50	0.52	0.89	0.89	0.23	0.25	0.85	0.89
		G13C	0.65	0.68	0.88	0.90	0.21	0.24	0.86	0.90
		G13D	0.36	0.40	0.89	0.90	0.05	0.06	0.78	0.90
		G13V	0.59	0.61	0.89	0.90	0.54	0.57	0.89	0.90
	NKCD/SAK mutants	K117R	0.79	0.79	0.89	0.90	0.08	0.08	0.57	0.89
		A146T	0.76	0.76	0.89	0.90	0.07	0.07	0.58	0.89
		A146V	0.81	0.82	0.90	0.90	0.13	0.07	0.58	0.89

Table 4. *Theoretically estimated comprehensive $f_{Ras \cdot GTP}$ values of wt HRas and its mutants.*

The various $f_{Ras \cdot GTP}$ values of wt HRas and its mutants were estimated by using various kinetic parameters (Tables 2 and 3) and Equations 1-4 as described in the Appendix. The data in this table reflects: (i) the [a]intrinsic $f_{Ras \cdot GTP}$, and the [b]GEF-mediated $f_{Ras \cdot GTP}$ (I, minimally active 5 nM Cdc25; II, highly active 5 nM Cdc25; and III, highly active 0.6 μM Cdc25); (ii) the [c]GAP-mediated $f_{Ras \cdot GTP}$ (10 nM p120GAP), and (iii) the [d]comprehensive $f_{Ras \cdot GTP}$ (I, minimally active 5 nM Cdc25 with 10 nM p120GAP; II, highly active 5 nM Cdc25 with 10 nM p120GAP; and III, highly active 0.6 μM Cdc25 with 10 nM p120GAP).

in comparison with these values of wt HRas. This is the opposite of the decrease that had been expected (Table 4). This demonstrates again that the k_{-1} value contributes little to the denominator in Equation 2 compared with the contribution of k_{-2} and k_{+6}.

The k_{-1} and k_{-2} values of G13V HRas are much higher than these same values of wt HRas (Table 2), but the k_{+6} value of G13V HRas is similar to that of wt HRas (Table 3). The higher k_{-1} and k_{-2} but invariable k_{+6} values indicate the faster Ras GNE. Besides, when the k_{+6} value is unchanged, the higher k_{-1} and k_{-2} values in Equation 2 produce a larger intrinsic $f_{\text{Ras}\bullet\text{GTP}}$ value of Ras. Hence, the larger intrinsic $f_{\text{Ras}\bullet\text{GTP}}$ value of G13V HRas than that of wt HRas (Table 4) reflects that the GNE of G13V HRas is faster than that of wt HRas. This is highlighted again in the case of the NKCD/SAK HRas mutants K117R, A146T, and A146V in which the significant change lies in their increased k_{-1} and k_{-2} values, but not in their k_{+6} value, in comparison with wt HRas (Tables 2 and 3). This causes the intrinsic $f_{\text{Ras}\bullet\text{GTP}}$ values of the NKCD/SAK HRas mutants to be nearly twice that of wt HRas (Table 4).

Calculation of the GEF-mediated $f_{Ras\bullet GTP}$ value of Ras. The cellular effects of the action of the positive Ras regulator GEFs on Ras proteins were assessed by calculation of the theoretical value of the GEF-mediated $f_{\text{Ras}\bullet\text{GTP}}$ of Ras (Equation 3). The value of the GEF-mediated $f_{\text{Ras}\bullet\text{GTP}}$ of Ras represents the cellular populations of the active GTP-bound form of Ras in the presence of GEFs. The factors that determine the GEF-mediated $f_{\text{Ras}\bullet\text{GTP}}$ of Ras are not only GEF-mediated Ras GNE but also intrinsic Ras GNE and GTP hydrolysis. Accordingly, Equation 3 consists of the GEF-relevant kinetic terms in addition to the intrinsic kinetic terms that determine the intrinsic $f_{\text{Ras}\bullet\text{GTP}}$ value.

In Equation 3, the GEF-relevant kinetic terms are defined as k_{+3} and k_{+4} in combination with [GEF] (i.e., k_{+3}·[GEF] and k_{+4}·[GEF]).

[GEF] in Equation 3 stands for the total cellular concentration of GEFs, such as SOS, RasGRF, and RasGRP. The concentration of the dominantly expressed GEF is vastly different from cell to cell. For example, it has been shown that SOS was dominant in HEK-293T cells at a concentration of 5 nM.[53] In Jurkat T cells, however, the SOS concentration was reported as 0.6 μM.[33] For the purposes of this study, these two reported dominant cellular levels of SOS were essentially used as [GEF] in Equation 3. Although these two reported cases of variations in the levels of SOS expression do not necessarily represent its range of concentration in various cells, they certainly cover a cellularly relevant range of its concentrations from the scope of nM to μM.

Within this study, the values of the kinetic terms associated with GEF (i.e., k_{+3}, and k_{+4}) in Equation 3 were determined by using the Cdc25 from SOS. This Cdc25 retains the basal activity of SOS, and thus these estimated unmodified k_{+3} and k_{+4} values of Cdc25 represent the kinetic parameters of the minimally active SOS. SOS activity in cytoplasm is reported to be increased up to 500 times by formation of a complex of SOS with Ras on a plasma membrane.[54] Hence, these values of k_{+3} and k_{+4} multiplied by 500 correspond to the kinetic parameters of the highly active SOS.

Taking into account variations in the levels of cellular expression and activities of SOS permits consideration of three different sets of the values of the GEF-relevant kinetic terms. These are represented by: (I) the minimally active 5 nM SOS (designating the action of 5 nM SOS with the original k_{+3} and k_{+4} values); (II) the highly active 5 nM SOS (representing the action of 5 nM SOS with k_{+3} and k_{+4} values multiplied by 500);

and (III) the highly active 0.6 μM SOS (denoting the action of 0.6 μM SOS with k_{+3} and k_{+4} values multiplied by 500). Note that the case of the minimally active 0.6 μM SOS is unlisted. This is because the values of the case (II) "5 nM SOS with k_{+3} and k_{+4} values multiplied by 500" are equal to the values of the case "0.6 μM SOS with the original k_{+3} and k_{+4} values." Accordingly, we assessed three different values of the GEF-mediated $f_{Ras\bullet GTP}$ of Ras: (i) the GEF-mediated $f_{Ras\bullet GTP}$ of Ras with the minimally active 5 nM SOS (termed the GEF-mediated $f_{Ras\bullet GTP}$ (I) of Ras); (ii) the GEF-mediated $f_{Ras\bullet GTP}$ of Ras with the highly active 5 nM SOS (termed the GEF-mediated $f_{Ras\bullet GTP}$ (II) of Ras); and (iii) the GEF-mediated $f_{Ras\bullet GTP}$ of Ras with the highly active 0.6 μM SOS (termed the GEF-mediated $f_{Ras\bullet GTP}$ (III) of Ras).

Analysis of the GEF-mediated $f_{Ras\bullet GTP}$ values of wt HRas. All of the values of the GEF-mediated $f_{Ras\bullet GTP}$ (I), (II), and (III) of wt HRas, 0.39, 0.89, and 0.90, respectively, were larger than the value of 0.33 of the intrinsic $f_{Ras\bullet GTP}$ of wt HRas (Table 4). This is not too surprising, because the comparison of Equations 2 and 3 predicts that, in general, the presence of the GEF-relevant terms — $k_{+3}\cdot$[GEF] and $k_{+4}\cdot$[GEF] — in Equation 3 produces a GEF-mediated $f_{Ras\bullet GTP}$ (I) of Ras that is at least similar to or larger than the intrinsic $f_{Ras\bullet GTP}$ value of Ras. Also, Equation 3 predicts that a larger value of the GEF-relevant terms produces a larger value of the GEF-mediated $f_{Ras\bullet GTP}$ of wt HRas. Hence, it stands to reason that the GEF-mediated $f_{Ras\bullet GTP}$ (III) of wt HRas has a larger value than the GEF-mediated $f_{Ras\bullet GTP}$ (II) of wt HRas. The same is true for the larger value of the GEF-mediated $f_{Ras\bullet GTP}$ (II) of wt HRas in comparison with the value of the GEF-mediated $f_{Ras\bullet GTP}$ (I) of wt HRas.

Analysis of the GEF-mediated $f_{Ras\bullet GTP}$ values of HRas mutants. Similar to the values associated with wt HRas, the values of the GEF-mediated $f_{Ras\bullet GTP}$ (I) of the listed HRas p-loop mutants were larger than the values of the intrinsic $f_{Ras\bullet GTP}$ of the listed HRas p-loop mutants (Table 4). This is, as with wt Ras, because of the presence of the GEF-relevant terms of these p-loop HRas mutants in Equation 3. Intriguingly, among these listed HRas p-loop mutants, G12A and G12V show the largest increases in the GEF-mediated $f_{Ras\bullet GTP}$ (I) values in comparison with intrinsic $f_{Ras\bullet GTP}$ values (Table 4). Nevertheless, such value increases exceed expectations. One key contributor to such a value increase, in addition to the values of the GEF-relevant terms associated with G12A and G12V HRas, is the particularly small value of the k_{-2} of G12A and G12V HRas (Table 2). The presence of a smaller k_{-2} value in Equation 3 allows for the GEF-relevant terms to weigh more significantly in the determination of the value of the GEF-mediated $f_{Ras\bullet GTP}$ (I) of Ras. The opposite is true of the NKCD/SAK HRas mutants K117R, A146T, and A146V. Because these HRas mutants have a much larger k_{-2} value (Table 2), the GEF-relevant terms in Equation 3 have relatively little effect on the determination of the value of the GEF-mediated $f_{Ras\bullet GTP}$ (I) of Ras (Table 4).

Unlike the case of the GEF-mediated $f_{Ras\bullet GTP}$ (I) of Ras, the values of the GEF-mediated $f_{Ras\bullet GTP}$ (II) and (III) of all of the listed HRas mutants almost uniformly parallel the values of the GEF-mediated $f_{Ras\bullet GTP}$ (II) and (III) of wt HRas. These similarities occur because the values of the GEF-relevant terms of these HRas mutants associated with the highly active 5 nM and 0.6 μM SOS were significantly higher than the values of the combined intrinsic kinetic parameters of these HRas mutants in Equation 3. As a

result, the values of the GEF-mediated $f_{\text{Ras}\bullet\text{GTP}}$ (II) and (III) of these HRas mutants reached their maximum.

Calculation of the GAP-mediated $f_{Ras\bullet GTP}$ value of Ras. The cellular consequences of the actions of the negative Ras regulator GAP on Ras were assessed by calculating the theoretical values of the GAP-mediated $f_{\text{Ras}\bullet\text{GTP}}$ of Ras (Equation 4). The value of the GAP-mediated $f_{\text{Ras}\bullet\text{GTP}}$ of Ras represents the cellular populations of the active GTP-bound Ras in the presence of GAPs.

Equation 4 contains not only the intrinsic kinetic terms that determine the intrinsic $f_{\text{Ras}\bullet\text{GTP}}$ value but also the GAP-relevant kinetic terms; these include k_{+7}, k_{-7}, and k_{+8} in conjunction with [GAP] (i.e., $k_{+7}\cdot k_{+8}/(k_{-7} + k_{+8})\cdot[\text{GAP}]$). Intriguingly, the GAP-relevant kinetic terms, $k_{+7}\cdot k_{+8}/(k_{-7} + k_{+8})$, in the denominator of Equation 4 are equivalent to the catalytic efficiency, $k_{\text{cat}}/K_{\text{M}}$, of GAP on Ras. Hence, with [GAP], the factors that determine the value of the GAP-mediated $f_{\text{Ras}\bullet\text{GTP}}$ of Ras that is of interest are those that govern the catalytic efficiency of GAP on Ras.

[GAP] in Equation 4 signifies the total concentration of the various types of GAPs in cells. Among these GAPs, p120GAP and NF1 are often dominantly and simultaneously expressed in cells.[51] The kinetic values of k_{cat} and K_{M} of GAP for Ras (Table 3) were determined by using p120GAP with Ras. Therefore, the GAP-relevant kinetic values listed in Table 3 can only be used to assess the catalytic action of the p120GAP, but not NF1, on Ras. The concentration of p120GAP across various mammalian cells, including NIH 3T3 cells, was estimated to be ~10 nM.[51] Yet, unlike with GEFs (i.e., 0.6 μM of SOS), the cellular concentration of p120GAP in the range of μM has not been reported. Taking these factors into account, only one value of the

GAP-relevant kinetic terms — the estimated values of k_{cat} and K_M in combination with 10 nM p120GAP — is used within this study for calculation of the values of the GAP-mediated $f_{Ras\bullet GTP}$ of Ras.

Analysis of the GAP-mediated $f_{Ras\bullet GTP}$ value of wt HRas. The estimated GAP-mediated $f_{Ras\bullet GTP}$ value of wt HRas approached 0.01, a value much less than the intrinsic $f_{Ras\bullet GTP}$ value of 0.33 of wt HRas (Table 4). This large difference is due to the magnitude of the value of the GAP-relevant terms — $(k_{+7}\cdot k_{+8}/(k_{-7} + k_{+8})\cdot[GAP]$, which is equivalent to $k_{cat}/K_M\cdot[GAP]$ — added to the denominator in Equation 4.

Analysis of the GAP-mediated $f_{Ras\bullet GTP}$ values of HRas mutants. All of the GAP-mediated $f_{Ras\bullet GTP}$ values of these HRas mutants exceeded the GAP-mediated $f_{Ras\bullet GTP}$ value of wt HRas. HRas mutants G12A, G12C, G12D, G12E, G12S, G13C, G13D, and G13S have GAP-mediated $f_{Ras\bullet GTP}$ values that lie between the two extremes of wt HRas and G12V mutant and also between the two extremes of wt HRas and G13V HRas mutant (see below) (Table 4). Compared with the values of wt HRas, the values of the GAP-relevant kinetic terms of these mutants are smaller, thus closer in value to the intrinsic kinetic terms. The decreased catalytic efficiency of p120GAP on these p-loop HRas mutants allows the intrinsic kinetic terms in Equation 4 to contribute more to the GAP-mediated $f_{Ras\bullet GTP}$ value compared with what occurs with wt HRas. This contribution by the intrinsic kinetic terms is responsible for the partially active states of these p-loop HRas mutants.

Other p-loop HRas mutants such as G12V and G13V have the largest GAP-mediated $f_{Ras\bullet GTP}$ values. They also have GAP-mediated $f_{Ras\bullet GTP}$ values that changed

the least from their intrinsic $f_{Ras \cdot GTP}$ value. This is because of the miniscule catalytic efficiency of p120GAP on these HRas mutants (Table 3).

Unlike what happens with the p-loop HRas mutants, the catalytic efficiency of p120GAP on the NKCD/SAK HRas mutants K117R, A146T, and A146V does not significantly differ from wt HRas (Table 3). However the GAP-mediated $f_{Ras \cdot GTP}$ values of these NKCD/SAK HRas mutants are significantly higher than in wt HRas (Table 4). The increase in the GAP-mediated $f_{Ras \cdot GTP}$ value is because of the sufficiently large intrinsic kinetic values of these NKCD/SAK HRas mutants that counteract the values of the GAP-relevant kinetic terms in Equation 4 that are associated with these NKCD/SAK HRas mutants.

Calculation of the comprehensive $f_{Ras \cdot GTP}$ value of Ras. The effects of the simultaneous actions of both GEF and GAP on Ras were analyzed by calculation of the theoretical value of the comprehensive $f_{Ras \cdot GTP}$ of Ras (Equation 1). The comprehensive $f_{Ras \cdot GTP}$ of Ras represents the populations of the active GTP-bound Ras in the presence of both GEF and GAP in cells.

Within this study, three different values of the GEF-relevant kinetic terms were used to calculate the GEF-mediated $f_{Ras \cdot GTP}$ values of Ras (see above). For calculation of the GAP-mediated $f_{Ras \cdot GTP}$ values of Ras, only one value of the GAP-relevant kinetic terms was used (see above). Three distinct combinational value sets of the GEF/GAP-relevant kinetic terms are possible. These are represented by: (I) the minimally active 5 nM SOS/10 nM p120GAP; (II) the highly active 5 nM SOS/10 nM p120GAP; and (III) the highly active 0.6 μM SOS/10 nM p120GAP. Accordingly, three different sets of the comprehensive $f_{Ras \cdot GTP}$ values of Ras were calculated: the comprehensive $f_{Ras \cdot GTP}$ of

Ras with the minimally active 5 nM SOS/10 nM p120GAP (termed the comprehensive $f_{Ras\bullet GTP}$ (I) of Ras); the comprehensive $f_{Ras\bullet GTP}$ of Ras with the highly active 5 nM SOS/10 nM p120GAP (termed the comprehensive $f_{Ras\bullet GTP}$ (II) of Ras); and the comprehensive $f_{Ras\bullet GTP}$ of Ras with the highly active 0.6 μM SOS/10 nM p120GAP (termed the comprehensive $f_{Ras\bullet GTP}$ (III) of Ras). These values of the comprehensive $f_{Ras\bullet GTP}$ (I), (II), and (III) of the Ras of interest, including wt, G12V, and G12S HRas, were further used to analyze the corresponding actual values of the fraction of the GTP-bound form (the cellular $f_{Ras\bullet GTP}$) of Ras measured in NIH 3T3 cells.

Analysis of the comprehensive $f_{Ras\bullet GTP}$ values of wt HRas. The values of the comprehensive $f_{Ras\bullet GTP}$ (I), (II), and (III) of wt HRas are, respectively, 0.01, 0.44, and 0.89 (Table 4). The results suggest that the comprehensive $f_{Ras\bullet GTP}$ value of wt HRas depends largely on the combinational actions of SOS with p120GAP.

The cellular $f_{Ras\bullet GTP}$ value of the transfected wt HRas in unstimulated NIH 3T3 cells was estimated to be 0.12 (Figure 4). Notably, a previously measured cellular $f_{Ras\bullet GTP}$ value of the transfected wt HRas in unstimulated NIH 3T3 cells was reported to be 0.025.[55] One possible reason for such different values would be the different quantification methods used for the GTP- and GDP-bound Ras isolated from cells. The difference in cell culture conditions may also affect the ratio of the GTP-bound Ras over the GDP-bound Ras. Regardless of the value differences, those of the estimated cellular $f_{Ras\bullet GTP}$ values of the transfected and endogenous wt HRas in unstimulated NIH 3T3 cells fall between the values of the comprehensive $f_{Ras\bullet GTP}$ (I) and (II) of wt HRas (Table 4). This is not unexpected because the cellular expression and activity of GEFs and GAPs in unstimulated NIH 3T3 cells would not duplicate the value sets in Equation

1 for the calculations of any of these comprehensive $f_{Ras\bullet GTP}$ (I), (II), and (III) values of wt HRas. By setting the values of the GEF- and GAP-relevant kinetic terms for the calculation of the comprehensive $f_{Ras\bullet GTP}$ (I), (II), and (III) values of wt HRas as default values, a comparison of these comprehensive $f_{Ras\bullet GTP}$ values of wt HRas with the cellular $f_{Ras\bullet GTP}$ values of wt HRas in unstimulated NIH 3T3 cells may predict the status of SOS in unstimulated NIH 3T3 cells. For example, the estimated value of the cellular $f_{Ras\bullet GTP}$ of the transfected wt HRas in unstimulated NIH 3T3 cells (Figure 4) can be obtained by a value combination of ~80% of the minimally active 5 nM SOS with ~20% of the highly active 5 nM SOS plus 10 nM p120GAP in Equation 1. Nevertheless, direct measurements of the cellular expression levels and activities of GEFs and GAPs are necessary. Such measurements increase the likelihood of obtaining meaningful estimated percentages for the cellular expression levels and activities of SOS and p120GAP associated with the comprehensive $f_{Ras\bullet GTP}$ value of wt HRas.

Note that the previous study also showed that the fraction of the cellular $f_{Ras\bullet GTP}$ value of the transfected wt HRas in unstimulated NIH 3T3 cells does not significantly differ from the cellular $f_{Ras\bullet GTP}$ value of the endogenous wt HRas in unstimulated NIH 3T3 cells.[55] This lack of a significant difference was found despite the expression level of the transfected wt HRas being much higher than that of the endogenous wt HRas in unstimulated NIH 3T3 cells. Hence, the feature analysis of the cellular $f_{Ras\bullet GTP}$ value of the transfected wt HRas in unstimulated NIH 3T3 cells that was performed by using the comprehensive $f_{Ras\bullet GTP}$ (I), (II), and (III) values of wt HRas (see above) may reflect the cellular traits of the endogenous wt HRas. This endogenous wt HRas is associated with.

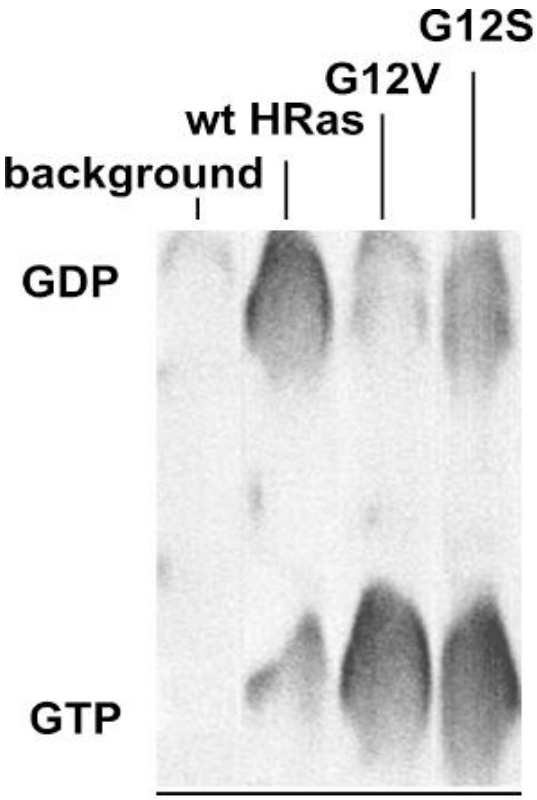

Figure 4. *Determination of the fractions of the HRas-bound GTP in cells.*

GTP fractions bound to various Ras expressed in unstimulated NIH 3T3 cells were determined as described in Materials and Methods. Western blot analysis showed that all transfected Ras proteins were evenly expressed. The fraction values of the Ras-bound GTP ($\frac{[\text{Ras}\cdot\text{GTP}]}{[\text{Ras}\cdot\text{GTP}] + [\text{Ras}\cdot\text{GDP}]}$) using densitometry estimation of GTP and GDP concentrations were calculated to be: background (transfection of the mammalian expression vector without *ras* gene), not determined; wt HRas, 0.12; G12V HRas, 0.81; and G12S HRas, 0.62. The presented values are the averages of the values of the independent triplicate measurements using separate cell culture samples, and the SD are less than 10% of the GTP fraction values that were indicated.

the cellular expressions and activities of SOS and p120GAP in unstimulated NIH 3T3 cells

Analysis of the comprehensive $f_{Ras\bullet GTP}$ values of HRas mutants. To one degree or another, all of the values of the comprehensive $f_{Ras\bullet GTP}$ (I) of these HRas mutants exceeded the values of the comprehensive $f_{Ras\bullet GTP}$ (I) of wt HRas.

According to the main kinetic factor that changes the value of the comprehensive $f_{Ras\bullet GTP}$ (I) of Ras, the values of the comprehensive $f_{Ras\bullet GTP}$ (I) of the p-loop and NKCD/SAK HRas mutants can be divided into two types for purposes of comparison with the values of the comprehensive $f_{Ras\bullet GTP}$ (I) of wt HRas. First, the values of the GAP-relevant kinetic terms of HRas mutants in Equation 1 are almost 0; as a consequence, the outcome of the value of the comprehensive $f_{Ras\bullet GTP}$ (I) of HRas mutants is significantly large. Mechanically, such small values of the GAP-relevant kinetic terms of HRas mutants are rooted in the almost total impairment of the catalytic action of p120GAP on HRas mutants. The two p-loop HRas mutants G12V and G13V possess this kinetic characteristic. Second, the higher values of the intrinsic kinetic terms of HRas mutants and/or the lower values of the GAP-relevant kinetic terms for HRas mutants, when compared with the values associated with wt HRas in Equation 1, yield larger values of the comprehensive $f_{Ras\bullet GTP}$ (I) of HRas mutants than the value of the comprehensive $f_{Ras\bullet GTP}$ (I) of wt HRas. In all of these cases, these altered values are because of the perturbed intrinsic kinetic processes of HRas mutants and/or GAP catalytic efficiencies on HRas mutants. With the exceptions of G12V and G13V HRas, all of the examined HRas mutants have this kinetic trait.

Similar to the case of the comprehensive $f_{Ras\bullet GTP}$ (I) of these HRas mutants, all of the values of the comprehensive $f_{Ras\bullet GTP}$ (II) of HRas mutants were higher under the same conditions than the values of the comprehensive $f_{Ras\bullet GTP}$ of wt HRas (Table 4). Based upon the main kinetic factor that contributes to altering the value of the comprehensive $f_{Ras\bullet GTP}$ (II) of Ras, the values of the comprehensive $f_{Ras\bullet GTP}$ (II) of the p-loop and NKCD/SAK HRas mutants fall into two categories when compared with the value of the comprehensive $f_{Ras\bullet GTP}$ (II) of wt HRas. First, the higher values of the intrinsic kinetic terms of these HRas mutants — in conjunction with the comparatively lower values of the catalytic efficiencies of p120GAP on these HRas mutants than those of wt HRas — mainly contribute to give higher values for the comprehensive $f_{Ras\bullet GTP}$ (II) of HRas mutants than for the comprehensive $f_{Ras\bullet GTP}$ (II) of wt HRas. The perturbed intrinsic processes of HRas mutants and GAP catalytic efficiencies on HRas mutants are, respectively, responsible for such value changes in the intrinsic kinetic terms and/or the GAP-relevant kinetic terms of HRas mutants. All p-loop HRas mutants, but not these NKCD/SAK HRas mutants, have this kinetic trait. Second, only a significantly high value of the intrinsic kinetic terms of HRas mutants, compared with those of wt HRas, contributes to the generation of higher values of the comprehensive $f_{Ras\bullet GTP}$ (II) of HRas mutants than of the comparative values of wt HRas. The significantly higher values of the intrinsic kinetic terms of HRas mutants, compared with those of wt HRas, is because of the perturbed intrinsic processes of HRas mutants. In this case, no causation can be attributed to the change in the values of the catalytic efficiencies of p120GAP of HRas mutants. The NKCD/SAK HRas mutants, including K117R, A146T, and A146V HRas, have this kinetic feature.

All values of the comprehensive $f_{Ras\bullet GTP}$ (III) of these HRas mutants are almost uniformly similar to the value of the comprehensive $f_{Ras\bullet GTP}$ (III) of wt HRas, which is extremely high (i.e., ≥ 0.87) (Table 4). This similarity is because the value of the GEF-relevant kinetic terms (the value associated with the highly active 0.6 μM SOS) overwhelms all other kinetic parameters associated with the value of the GAP-relevant kinetic terms (the value associated with 10 nM p120GAP) and the intrinsic kinetic parameter values of Ras in Equation 1. In addition, as discussed elsewhere, this highly active 0.6 μM SOS/10 nM p120GAP condition can also generate an extremely high value for the comprehensive $f_{Ras\bullet GTP}$ of wt HRas. The highly active 0.6 μM SOS/10 nM p120GAP generates significantly higher values for the comprehensive $f_{Ras\bullet GTP}$ (III) of Ras than it does for any examined HRas proteins. Because of these high values, it is certain that a cellular condition with the highly active 0.6 μM SOS/10 nM p120GAP is sufficient to produce uncontrolled Ras-dependent cellular signaling events without regard to the values of any other examined HRas mutants or wt HRas.

G12S HRas is one of the most predominant forms found in Costello syndrome (Table 1).[56] Hence, the value of the cellular $f_{Ras\bullet GTP}$ of G12S HRas in unstimulated NIH 3T3 cells was determined as a way to use various combinations of activities and expression levels of SOS with p120GAP to evaluate the various comprehensive $f_{Ras\bullet GTP}$ values of G12S HRas. Because of the important role of G12V HRas in cancer formation, the cellular $f_{Ras\bullet GTP}$ value of G12V HRas in unstimulated NIH 3T3 cells also was determined to be a way to use various combinations of activities and expression levels of SOS with p120GAP to evaluate these various comprehensive $f_{Ras\bullet GTP}$ (I), (II), (III) values of G12V HRas. The cellular $f_{Ras\bullet GTP}$ value of G12V HRas in unstimulated

NIH 3T3 cells also serves as a positive control for the analysis of the cellular $f_{Ras \cdot GTP}$ value of G12S HRas in unstimulated NIH 3T3 cells. The value of the cellular $f_{Ras \cdot GTP}$ of wt HRas in unstimulated NIH 3T3 cells serves as a negative control for this analysis. This cellular $f_{Ras \cdot GTP}$ value of G12V and G12S HRas in unstimulated NIH 3T3 cells was determined to be 0.80 and 0.63, respectively, which is ~8.0- and 6.3-fold higher than the cellular $f_{Ras \cdot GTP}$ value of wt HRas in unstimulated NIH 3T3 cells (Figure 4).

Discussion

This study established novel kinetic parameter-based calculations of the values of intrinsic, GEF- and GAP-mediated, and comprehensive $f_{Ras\bullet GTP}$ of Ras proteins that represent the cellular content of the GTP-bound form of Ras in the presence and absence of GEF and/or GAP. The kinetic characterizations linked with the calculations of the population of the GTP-bound form of Ras first provide an overall picture of the inherited causality between Ras mutations and changes in the cellular population of the GTP-bound Ras. These linkages explain the biochemical roles of these HRas mutants in various diseases. These roles include diseases such as Costello syndrome and certain cancers.

Depending on the cellular activity and expression of GEFs in combination with GAPs, three sets of values of the comprehensive $f_{Ras\bullet GTP}$ of Ras — the comprehensive $f_{Ras\bullet GTP}$ (I), (II), and (III) of these HRas — were calculated. Comparison of these calculated values with the values of the cellular $f_{Ras\bullet GTP}$ of selected HRas proteins in the unstimulated NIH 3T3 cells suggests that the comprehensive $f_{Ras\bullet GTP}$ (I) values of HRas mainly represents the actual cellular f Ras•GTP values of HRas in the unstimulated NIH 3T3 cells. This recognition takes into account the component of the comprehensive $f_{Ras\bullet GTP}$ (II) of HRas. Intriguingly, although there are no clear-cut dividing lines, the spectrum of the calculated values of the comprehensive $f_{Ras\bullet GTP}$ (I) of HRas mutants can be classified into three groups. The first group encompasses the values of 0.57-0.67 and is associated with G12V and G13V HRas mutants. The G12V and G13V HRas mutations are the only ones linked specifically and exclusively to cancer formation. The second group spans 0.24-0.28 and is linked to G12A, G12S, G13S, and G13C HRas

mutations. These HRas mutations are mainly linked to development of Costello syndrome, but they are also often linked to cancers. Finally, the third group has a range of 0.06-0.12 and is associated with all other listed HRas mutants. This group includes G12C, G12D, G12E, G13D, K117R, A146T, and A146V HRas mutations that are only linked to development of Costello syndrome. These groups and their links to cancer and/or Costello syndrome suggest that the high end of the spectrum of values of the comprehensive $f_{\text{Ras}\bullet\text{GTP}}$ (I) of HRas mutants is certainly linked to cancer formation, but the low end of this spectrum is only associated with the development of Costello syndrome. Values in the midrange of this spectrum are linked with the development of both of Costello syndrome and cancer. Accordingly, it is possible to postulate that the values of the comprehensive $f_{\text{Ras}\bullet\text{GTP}}$ (I) of HRas mutants can be used to gauge whether Ras mutants cause development of diseases such as cancers and/or Costello syndrome. For example, if a comprehensive $f_{\text{Ras}\bullet\text{GTP}}$ (I) value of a certain HRas mutant is 0.25, this HRas mutation is likely to cause development of Costello syndrome and/or cancers. However, if the same value of a certain HRas mutant is 0.10, this HRas mutation is likely to lead only to development of Costello syndrome. The cellular $f_{\text{Ras}\bullet\text{GTP}}$ values of HRas proteins from unstimulated NIH 3T3 cells were used as references for the analyses of the comprehensive $f_{\text{Ras}\bullet\text{GTP}}$ (I) values of HRas proteins. Therefore, the analytical results discussed above cannot be applied immediately to diseases associated with Ras mutations in other cells. Use of our results to gauge other diseases must await further evaluation of the comprehensive $f_{\text{Ras}\bullet\text{GTP}}$ (I) of HRas by using the cellular $f_{\text{Ras}\bullet\text{GTP}}$ values of HRas from various other cells.

As was discussed in the Results section, the reason for such a high spectrum of values for the comprehensive $f_{Ras \cdot GTP}$ (I) of HRas mutants — G12V and G13V HRas — is because the catalytic action of p120GAP on these HRas mutants is impaired. However, the middle and the lower end of this spectrum — which includes all of the HRas mutants of this study except G12V and G13V HRas —reflects the perturbation of the intrinsic kinetic parameters of HRas mutants in combination with the partial perturbation of these mutants by the catalytic action of p120GAP. Accounting for the linkages between certain groups of the comprehensive $f_{Ras \cdot GTP}$ (I) values of these HRas mutants and certain types of diseases (see above), the features of the mechanical perturbation of these HRas mutants can be further linked to the type of the diseases that they are associated with. The severe impairment of the catalytic action of p120GAP on HRas mutants results in the high-end values of the comprehensive $f_{Ras \cdot GTP}$ (I) of Ras. These values at the upper end of the spectrum cause development of cancers. The perturbation of the intrinsic kinetic parameters of HRas mutants in combination with the partial perturbation of HRas mutants by the catalytic action of p120GAP leads to values in the middle or low ranges of the spectrum. Values in these ranges are sufficient for development of cancers and/or the Costello syndrome.

Earlier, the main factor in increases in the cellular population of the GTP-bound Ras was thought to be caused by the impaired catalytic action of GAP on HRas, with HRas mutations as the culprits in the impairment. This outlook remains consistent with the values at the upper end of the spectrum of values of the comprehensive $f_{Ras \cdot GTP}$ (I) of the tumorigenic G12V and G13V HRas mutants. However, this study is the first to show that perturbation that these HRas mutations cause in the intrinsic kinetic

properties of Ras also plays a key role in increases in the cellular population of the GTP-bound HRas. This notion is supported by the middle and low end spectrum of values of the comprehensive $f_{Ras \cdot GTP}$ (I) of HRas proteins. Values in these ranges of the spectrum include all of the listed HRas mutants, except G12V and G13V HRas. One of the best examples of this is the value of the comprehensive $f_{Ras \cdot GTP}$ (I) of the G12S HRas mutation. This occurrence is intriguing because G12S HRas is the most prevalent form of HRas mutant found in patients with Costello syndrome.

The value of the comprehensive $f_{Ras \cdot GTP}$ (III) of Ras represents a case in which the population of the GTP-bound form of Ras exists under conditions of extreme SOS expression and activity in cells. Regardless of the features of the HRas mutants, the values of the comprehensive $f_{Ras \cdot GTP}$ (III) of these HRas mutants are significantly high. Intriguingly, the development of at least one case of Noonan syndrome has been linked to high cellular $f_{Ras \cdot GTP}$ values of wt KRas and wt NRas.[13] The high values encountered in this case are suspected to be the result of upregulation of SOS that was caused by mutations of the *sos1* gene.[13] This SOS upregulation-dependent development of Noonan syndrome can be explained by an incident in the calculation of the value of the comprehensive $f_{Ras \cdot GTP}$ value (III) of wt HRas that dovetails with high SOS activity and expression.

Because other GAPs, such as NF1, have not been included in these analyses, an assessment of the effect of p120GAP on the cellular population of the GTP-bound Ras through the action of these HRas mutations should not be overinterpreted. Moreover, no exploration has been undertaken of the possibility of a change in the p120GAP expression-dependent cellular population of the GTP-bound form of Ras that

is associated with these HRas mutations. This limitation reflects the lack of evidence of higher or lower cellular expression of p120GAP other than as 10 nM p120GAP. Future studies are expected to examine the possibility that the various cellular expressions of p120GAP as well as NF1 modulate the cellular population of these HRas mutations in the GTP-bound form of Ras.

References

1. Oxford, G., and Theodorescu, D. (2003) Ras superfamily monomeric G proteins in carcinoma cell motility, *Cancer Lett 189*, 117-128.
2. Marshall, C. B., Meiri, D., Smith, M. J., Mazhab-Jafari, M. T., Gasmi-Seabrook, G. M. C., Rottapel, R., Stambolic, V., and Ikura, M. (2012) Probing the GTPase cycle with real-time NMR: GAP and GEF activities in cell extracts, *Methods 57*, 473-485.
3. Geyer, M., and Wittinghofer, A. (1997) GEFs, GAPs, GDIs and effectors: taking a closer (3D) look at the regulation of Ras-related GTP-binding proteins, *Curr Opin Struct Biol 7*, 786-792.
4. Bonfini, L., Karlovich, C. A., Dasgupta, C., and Banerjee, U. (1992) The Son of sevenless gene product: a putative activator of Ras, *Science 255*, 603-606.
5. Ebinu, J. O., Bottorff, D. A., Chan, E. Y., Stang, S. L., Dunn, R. J., and Stone, J. C. (1998) RasGRP, a Ras guanyl nucleotide- releasing protein with calcium- and diacylglycerol-binding motifs, *Science 280*, 1082-1086.
6. Bottorff, D., Ebinu, J., and Stone, J. C. (1999) RasGRP, a Ras activator: mouse and human cDNA sequences and chromosomal positions, *Mamm Genome 10*, 358-361.
7. Boriack-Sjodin, P. A., Margarit, S. M., Bar-Sagi, D., and Kuriyan, J. (1998) The structural basis of the activation of Ras by Sos, *Nature 394*, 337-343.
8. Traut, T. W. (1994) Physiological concentrations of purines and pyrimidines, *Mol Cell Biochem 140*, 1-22.

9. Sprang, S. (2001) GEFs: master regulators of G-protein activation, *Trends Biochem Sci 26*, 266-267.

10. Grewal, T., Koese, M., Tebar, F., and Enrich, C. (2011) Differential Regulation of RasGAPs in Cancer, *Genes Cancer 2*, 288-297.

11. Scheffzek, K., Ahmadian, M. R., Kabsch, W., Wiesmuller, L., Lautwein, A., Schmitz, F., and Wittinghofer, A. (1997) The Ras-RasGAP complex: structural basis for GTPase activation and its loss in oncogenic Ras mutants, *Science 277*, 333-338.

12. Boguski, M. S., and McCormick, F. (1993) Proteins regulating Ras and its relatives, *Nature 366*, 643-654.

13. Schubbert, S., Shannon, K., and Bollag, G. (2007) Hyperactive Ras in developmental disorders and cancer, *Nat Rev Cancer 7*, 295-308.

14. Roberts, P. J., and Der, C. J. (2007) Targeting the Raf-MEK-ERK mitogen-activated protein kinase cascade for the treatment of cancer, *Oncogene 26*, 3291-3310.

15. Fasano, O., Aldrich, T., Tamanoi, F., Taparowsky, E., Furth, M., and Wigler, M. (1984) Analysis of the transforming potential of the human H-ras gene by random mutagenesis, *Proc Natl Acad Sci U S A 81*, 4008-4012.

16. Matsuda, K., Shimada, A., Yoshida, N., Ogawa, A., Watanabe, A., Yajima, S., Iizuka, S., Koike, K., Yanai, F., Kawasaki, K., Yanagimachi, M., Kikuchi, A., Ohtsuka, Y., Hidaka, E., Yamauchi, K., Tanaka, M., Yanagisawa, R., Nakazawa, Y., Shiohara, M., Manabe, A., and Kojima, S. (2007) Spontaneous improvement

of hematologic abnormalities in patients having juvenile myelomonocytic leukemia with specific RAS mutations, *Blood 109*, 5477-5480.

17. Jakubauskas, A., and Griskevicius, L. (2010) KRas and BRaf mutational status analysis from formalin-fixed, paraffin-embedded tissues using multiplex polymerase chain reaction-based assay, *Arch Pathol Lab Med 134*, 620-624.

18. Sahu, R. P., Batra, S., Kandala, P. K., Brown, T. L., and Srivastava, S. K. (2011) The role of K-ras gene mutation in TRAIL-induced apoptosis in pancreatic and lung cancer cell lines, *Cancer Chemother Pharmacol 67*, 481-487.

19. Seeburg, P. H., Colby, W. W., Capon, D. J., Goeddel, D. V., and Levinson, A. D. (1984) Biological properties of human c-Ha-ras1 genes mutated at codon 12, *Nature 312*, 71-75.

20. Aoki, Y., Niihori, T., Kawame, H., Kurosawa, K., Ohashi, H., Tanaka, Y., Filocamo, M., Kato, K., Suzuki, Y., Kure, S., and Matsubara, Y. (2005) Germline mutations in HRAS proto-oncogene cause Costello syndrome, *Nat Genet 37*, 1038-1040.

21. Gripp, K. W., Lin, A. E., Stabley, D. L., Nicholson, L., Scott, C. I., Jr., Doyle, D., Aoki, Y., Matsubara, Y., Zackai, E. H., Lapunzina, P., Gonzalez-Meneses, A., Holbrook, J., Agresta, C. A., Gonzalez, I. L., and Sol-Church, K. (2006) HRAS mutation analysis in Costello syndrome: genotype and phenotype correlation, *Am J Med Genet A 140*, 1-7.

22. Estep, A. L., Tidyman, W. E., Teitell, M. A., Cotter, P. D., and Rauen, K. A. (2006) HRAS mutations in Costello syndrome: detection of constitutional

activating mutations in codon 12 and 13 and loss of wild-type allele in malignancy, *Am J Med Genet A 140*, 8-16.

23. Kerr, B., Delrue, M. A., Sigaudy, S., Perveen, R., Marche, M., Burgelin, I., Stef, M., Tang, B., Eden, O. B., O'Sullivan, J., De Sandre-Giovannoli, A., Reardon, W., Brewer, C., Bennett, C., Quarell, O., M'Cann, E., Donnai, D., Stewart, F., Hennekam, R., Cave, H., Verloes, A., Philip, N., Lacombe, D., Levy, N., Arveiler, B., and Black, G. (2006) Genotype-phenotype correlation in Costello syndrome: HRAS mutation analysis in 43 cases, *J Med Genet 43*, 401-405.

24. Sol-Church, K., Stabley, D. L., Nicholson, L., Gonzalez, I. L., and Gripp, K. W. (2006) Paternal bias in parental origin of HRAS mutations in Costello syndrome, *Hum Mutat 27*, 736-741.

25. Zampino, G., Pantaleoni, F., Carta, C., Cobellis, G., Vasta, I., Neri, C., Pogna, E. A., De Feo, E., Delogu, A., Sarkozy, A., Atzeri, F., Selicorni, A., Rauen, K. A., Cytrynbaum, C. S., Weksberg, R., Dallapiccola, B., Ballabio, A., Gelb, B. D., Neri, G., and Tartaglia, M. (2007) Diversity, parental germline origin, and phenotypic spectrum of de novo HRAS missense changes in Costello syndrome, *Hum Mutat 28*, 265-272.

26. van der Burgt, I., Kupsky, W., Stassou, S., Nadroo, A., Barroso, C., Diem, A., Kratz, C. P., Dvorsky, R., Ahmadian, M. R., and Zenker, M. (2007) Myopathy caused by HRAS germline mutations: implications for disturbed myogenic differentiation in the presence of constitutive HRas activation, *J Med Genet 44*, 459-462.

27. Gripp, K. W., Innes, A. M., Axelrad, M. E., Gillan, T. L., Parboosingh, J. S., Davies, C., Leonard, N. J., Lapointe, M., Doyle, D., Catalano, S., Nicholson, L., Stabley, D. L., and Sol-Church, K. (2008) Costello syndrome associated with novel germline HRAS mutations: an attenuated phenotype?, *Am J Med Genet A 146A*, 683-690.

28. Burkitt-Wright, E. M., Bradley, L., Shorto, J., McConnell, V. P., Gannon, C., Firth, H. V., Park, S. M., D'Amore, A., Munyard, P. F., Turnpenny, P. D., Charlton, A., Wilson, M., and Kerr, B. (2012) Neonatal lethal Costello syndrome and unusual dinucleotide deletion/insertion mutations in HRAS predicting p.Gly12Val, *Am J Med Genet A 158A*, 1102-1110.

29. Niihori, T., Aoki, Y., Okamoto, N., Kurosawa, K., Ohashi, H., Mizuno, S., Kawame, H., Inazawa, J., Ohura, T., Arai, H., Nabatame, S., Kikuchi, K., Kuroki, Y., Miura, M., Tanaka, T., Ohtake, A., Omori, I., Ihara, K., Mabe, H., Watanabe, K., Niijima, S., Okano, E., Numabe, H., and Matsubara, Y. (2011) HRAS mutants identified in Costello syndrome patients can induce cellular senescence: possible implications for the pathogenesis of Costello syndrome, *J Hum Genet 56*, 707-715.

30. Digilio, M. C., Lepri, F., Baban, A., Dentici, M. L., Versacci, P., Capolino, R., Ferese, R., De Luca, A., Tartaglia, M., Marino, B., and Dallapiccola, B. (2011) RASopathies: Clinical Diagnosis in the First Year of Life, *Mol Syndromol 1*, 282-289.

31. Tidyman, W. E., Lee, H. S., and Rauen, K. A. (2011) Skeletal muscle pathology in Costello and cardio-facio-cutaneous syndromes: developmental consequences

of germline Ras/MAPK activation on myogenesis, *Am J Med Genet C Semin Med Genet 157*, 104-114.

32. Gripp, K. W., Hopkins, E., Sol-Church, K., Stabley, D. L., Axelrad, M. E., Doyle, D., Dobyns, W. B., Hudson, C., Johnson, J., Tenconi, R., Graham, G. E., Sousa, A. B., Heller, R., Piccione, M., Corsello, G., Herman, G. E., Tartaglia, M., and Lin, A. E. (2011) Phenotypic Analysis of Individuals With Costello Syndrome due to HRAS p.G13C, *Am J Med Genet A 155A*, 706-716.

33. Kuniba, H., Pooh, R. K., Sasaki, K., Shimokawa, O., Harada, N., Kondoh, T., Egashira, M., Moriuchi, H., Yoshiura, K., and Niikawa, N. (2009) Prenatal diagnosis of Costello syndrome using 3D ultrasonography amniocentesis confirmation of the rare HRAS mutation G12D, *Am J Med Genet A 149A*, 785-787.

34. Piccione, M., Piro, E., Pomponi, M. G., Matina, F., Pietrobono, R., Candela, E., Gabriele, B., Neri, G., and Corsello, G. (2009) A Premature Infant With Costello Syndrome Due to a Rare G13C HRAS Mutation, *Am J Med Genet A 149A*, 487-489.

35. Schulz, A. L., Albrecht, B., Arici, C., van der Burgt, I., Buske, A., Gillessen-Kaesbach, G., Heller, R., Horn, D., Hubner, C. A., Korenke, G. C., Konig, R., Kress, W., Kruger, G., Meinecke, P., Mucke, J., Plecko, B., Rossier, E., Schinzel, A., Schulze, A., Seemanova, E., Seidel, H., Spranger, S., Tuysuz, B., Uhrig, S., Wieczorek, D., Kutsche, K., and Zenker, M. (2008) Mutation and phenotypic spectrum in patients with cardio-facio-cutaneous and Costello syndrome, *Clin Genet 73*, 62-70.

36. Denayer, E., Parret, A., Chmara, M., Schubbert, S., Vogels, A., Devriendt, K., Frijns, J. P., Rybin, V., de Ravel, T. J., Shannon, K., Cools, J., Scheffzek, K., and Legius, E. (2008) Mutation analysis in Costello syndrome: functional and structural characterization of the HRAS p.Lys117Arg mutation, *Hum Mutat 29*, 232-239.

37. Sinico, M., Bassez, G., Touboul, C., Cave, H., Vergnaud, A., Zirah, C., Fleury-Feith, J., Gettler, S., Vojtek, A. M., Chevalier, N., Amram, D., Alsamad, I. A., Haddad, B., and Encha-Razavi, F. (2011) Excess of neuromuscular spindles in a fetus with Costello syndrome: a clinicopathological report, *Pediatr Dev Pathol 14*, 218-223.

38. Piispanen, A. E., Bonnefoi, O., Carden, S., Deveau, A., Bassilana, M., and Hogan, D. A. (2011) Roles of Ras1 membrane localization during Candida albicans hyphal growth and farnesol response, *Eukaryot Cell 10*, 1473-1484.

39. Hall, A., and Self, A. J. (1986) The effect of Mg2+ on the guanine nucleotide exchange rate of p21N-ras, *J Biol Chem 261*, 10963-10965.

40. Gideon, P., John, J., Frech, M., Lautwein, A., Clark, R., Scheffler, J. E., and Wittinghofer, A. (1992) Mutational and kinetic analyses of the GTPase-activating protein (GAP)-p21 interaction: the C-terminal domain of GAP is not sufficient for full activity, *Mol Cell Biol 12*, 2050-2056.

41. Lenzen, C., Cool, R. H., Prinz, H., Kuhlmann, J., and Wittinghofer, A. (1998) Kinetic analysis by fluorescence of the interaction between Ras and the catalytic domain of the guanine nucleotide exchange factor $Cdc25^{Mm}$, *Biochemistry 37*, 7420-7430.

42. Cotton, F. A., and Wilkinson, G. (1988) *Advanced Inorganic Chemistry*, 5th ed., John Wiley & Sons, New York.

43. Heo, J., and Campbell, S. L. (2005) Superoxide Anion Radical Modulates the Activity of Ras and Ras-related GTPases by a Radical-based Mechanism Similar to that of Nitric Oxide, *J Biol Chem 280*, 12438-12445.

44. Leupold, C. M., Goody, R. S., and Wittinghofer, A. (1983) Stereochemistry of the elongation factor Tu X GTP complex, *Eur J Biochem 135*, 237-241.

45. Eccleston, J. F., Moore, K. J., Morgan, L., Skinner, R. H., and Lowe, P. N. (1993) Kinetics of interaction between normal and proline 12 Ras and the GTPase-activating proteins, p120-GAP and neurofibromin. The significance of the intrinsic GTPase rate in determining the transforming ability of ras, *J Biol Chem 268*, 27012-27019.

46. Downward, J., Graves, J. D., Warne, P. H., Rayter, S., and Cantrell, D. A. (1990) Stimulation of p21ras upon T-cell activation, *Nature 346*, 719-723.

47. Krengel, U., Schlichting, I., Scherer, A., Schumann, R., Frech, M., John, J., Kabsch, W., Pai, E. F., and Wittinghofer, A. (1990) Three-dimensional structures of H-ras p21 mutants: molecular basis for their inability to function as signal switch molecules, *Cell 62*, 539-548.

48. John, J., Frech, M., and Wittinghofer, A. (1988) Biochemical properties of Ha-ras encoded p21 mutants and mechanism of the autophosphorylation reaction, *J Biol Chem 263*, 11792-11799.

49. Franken, S. M., Scheidig, A. J., Krengel, U., Rensland, H., Lautwein, A., Geyer, M., Scheffzek, K., Goody, R. S., Kalbitzer, H. R., Pai, E. F., and et al. (1993)

Three-dimensional structures and properties of a transforming and a nontransforming glycine-12 mutant of p21H-ras, *Biochemistry 32*, 8411-8420.

50. Gibbs, J. B., Schaber, M. D., Allard, W. J., Sigal, I. S., and Scolnick, E. M. (1988) Purification of ras GTPase activating protein from bovine brain, *Proc Nat Acad Sci U S A 85*, 5026-5030.

51. Bollag, G., and McCormick, F. (1991) Differential regulation of rasGAP and neurofibromatosis gene product activities, *Nature 351*, 576-579.

52. Feig, L. A., and Cooper, G. M. (1988) Relationship among guanine nucleotide exchange, GTP hydrolysis, and transforming potential of mutated ras proteins, *Mol Cell Biol 8*, 2472-2478.

53. Maurer, T., Garrenton, L. S., Oh, A., Pitts, K., Anderson, D. J., Skelton, N. J., Fauber, B. P., Pan, B., Malek, S., Stokoe, D., Ludlam, M. J., Bowman, K. K., Wu, J., Giannetti, A. M., Starovasnik, M. A., Mellman, I., Jackson, P. K., Rudolph, J., Wang, W., and Fang, G. (2012) Small-molecule ligands bind to a distinct pocket in Ras and inhibit SOS-mediated nucleotide exchange activity, *Proc Natl Acad Sci U S A 109*, 5299-5304.

54. Gureasko, J., Galush, W. J., Boykevisch, S., Sondermann, H., Bar-Sagi, D., Groves, J. T., and Kuriyan, J. (2008) Membrane-dependent signal integration by the Ras activator Son of sevenless, *Nat Struct Mol Biol 15*, 452-461.

55. Scheele, J. S., Rhee, J. M., and Boss, G. R. (1995) Determination of absolute amounts of GDP and GTP bound to Ras in mammalian cells: comparison of parental and Ras-overproducing NIH 3T3 fibroblasts, *Proc Natl Acad Sci U S A 92*, 1097-1100.

56. Gelb, B. D., and Tartaglia, M. (2006) Noonan syndrome and related disorders: dysregulated RAS-mitogen activated protein kinase signal transduction, *Hum Mol Genet 15 Spec No 2*, R220-226.

CHAPTER 2 APPENDIX

Derivation of the expression of the fraction of the GTP-bound form of Ras in terms of the kinetic parameters of the intrinsic Ras GNE and GTP hydrolysis and of GEF and GAP with Ras.

Scheme 1

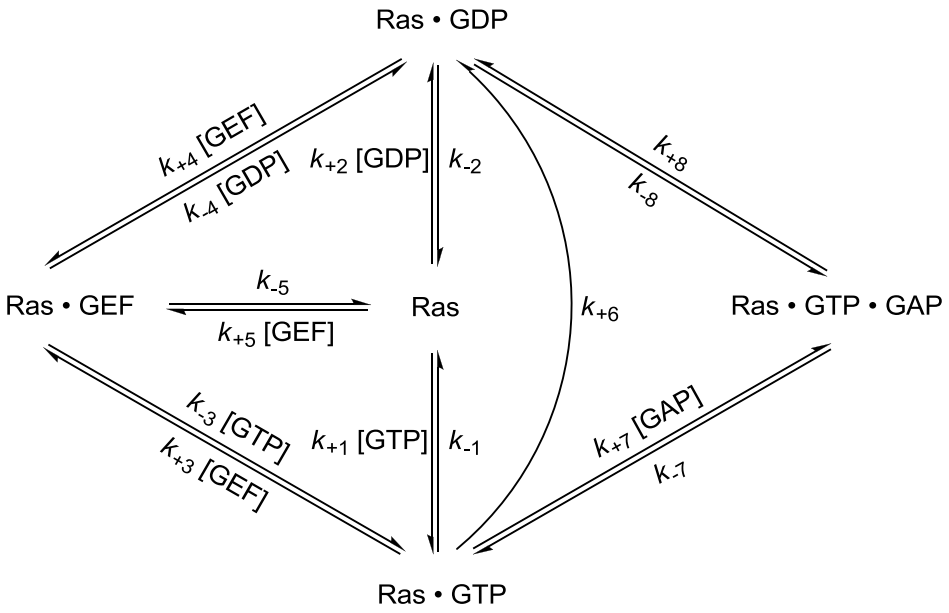

As shown in Scheme 1, Ras has a variety of forms that can be referred to as nodes. Each node will be assigned a corresponding letter for simplicity.

Ras → A

Ras • GTP → B

Ras • GDP → C

Ras • GEF → D

Ras • GTP • GAP → E

The notation of an intermediate form/node enclosed in parentheses equals the sum of all arrows leading away from the node. Each arrow is represented by a notation of two letters in parentheses in which the first letter is the origin and the second the destination.

$$(\mathrm{A}) = (\mathrm{AB}) + (\mathrm{AC}) + (\mathrm{AD}) = k_{+1}[\mathrm{GTP}] + k_{+2}[\mathrm{GDP}] + k_{+5}[\mathrm{GEF}]$$

$$(\mathrm{B}) = (\mathrm{BA}) + (\mathrm{BC}) + (\mathrm{BD}) + (\mathrm{BE}) = k_{-1} + k_{+6} + k_{+3}[\mathrm{GEF}] + k_{+7}[\mathrm{GAP}]$$

$$(\mathrm{C}) = (\mathrm{CA}) + (\mathrm{CD}) = k_{-2} + k_{+4}[\mathrm{GEF}]$$

$$(\mathrm{D}) = (\mathrm{DA}) + (\mathrm{DB}) + (\mathrm{DC}) = k_{-5} + k_{-3}[\mathrm{GTP}] + k_{-4}[\mathrm{GDP}]$$

$$(\mathrm{E}) = (\mathrm{EB}) + (\mathrm{EC}) = k_{-7} + k_{+8}$$

Using the "one-branch" approach [1], the determinant of any enzyme species is the summation of the products of the nearest paths leading toward the node and all other remaining nodes.

$$[\mathrm{Ras} \bullet \mathrm{GTP}] = (\mathrm{AB})(\mathrm{C})(\mathrm{D})(\mathrm{E}) + (\mathrm{DB})(\mathrm{A})(\mathrm{C})(\mathrm{E}) + (\mathrm{EB})(\mathrm{A})(\mathrm{C})(\mathrm{D})$$

Applying the "consecutive branch" approach [2], the (EB) term is canceled because no path connects the remaining nodes to (EB).

$$[\mathrm{Ras} \bullet \mathrm{GTP}] = (\mathrm{AB})(\mathrm{C})(\mathrm{D})(\mathrm{E}) + (\mathrm{DB})(\mathrm{A})(\mathrm{C})(\mathrm{E})$$

Ras•GDP has been chosen as the common node for simplicity in the resulting equation. The "consecutive branch" approach is continued further until C is the origin of all paths.

$$[\mathrm{Ras} \bullet \mathrm{GTP}] = (\mathrm{AB})[(\mathrm{CA})(\mathrm{D})(\mathrm{E}) + (\mathrm{CD})(\mathrm{DA})(\mathrm{E})] + (\mathrm{DB})[(\mathrm{CD})(\mathrm{A})(\mathrm{E}) + (\mathrm{CA})(\mathrm{AD})(\mathrm{E})]$$

The (E) term is then factored out.

$$[\text{Ras} \bullet \text{GTP}] = (\text{E})\big((\text{AB})[(\text{CA})(\text{D}) + (\text{CD})(\text{DA})] + (\text{DB})[(\text{CD})(\text{A}) + (\text{CA})(\text{AD})]\big)$$

The rate constants are now substituted into the equation.

$$\begin{aligned}[\text{Ras} \bullet \text{GTP}] = (k_{-7} \\ &+ k_{+8})\Big(k_{+1}[\text{GTP}]\big(k_{-2}(k_{-5} + k_{-3}[\text{GTP}] + k_{-4}[\text{GDP}]) + (k_{+4}[\text{GEF}])(k_{-5})\big) \\ &+ k_{-3}[\text{GTP}]\big(k_{+4}[\text{GEF}](k_{+1}[\text{GTP}] + k_{+2}[\text{GDP}] + k_{+5}[\text{GEF}]) \\ &+ (k_{-2})(k_{+5}[\text{GEF}])\big)\Big)\end{aligned}$$

We assume that k_{+1} and k_{+2} are equivalent and that k_{-3} and k_{-4} are equivalent because Ras and Ras•GEF have almost equal affinities for GTP and GDP.

if $k_{+1} = k_{+2} = k'$ and $k_{-3} = k_{-4} = k''$

$$\begin{aligned}[\text{Ras} \bullet \text{GTP}] = (k_{-7} + k_{+8})\big(k'[\text{GTP}](k_{-2}(k_{-5} + k''[\text{GTP}] + k''[\text{GDP}]) + k_{+4}k_{-5}[\text{GEF}]) \\ + k''[\text{GTP}](k_{+4}[\text{GEF}](k'[\text{GTP}] + k'[\text{GDP}] + k_{+5}[\text{GEF}]) + k_{-2}k_{+5}[\text{GEF}])\big)\end{aligned}$$

[GTP] is factored out, and the remaining terms are distributed.

$$\begin{aligned}[\text{Ras} \bullet \text{GTP}] = (k_{-7} + k_{+8})[\text{GTP}](k'k_{-2}k_{-5} + k'k''k_{-2}([\text{GTP}] + [\text{GDP}]) + k'k_{+4}k_{-5}[\text{GEF}] \\ + k'k''k_{+4}[\text{GEF}]([\text{GTP}] + [\text{GDP}]) + k''k_{+4}k_{+5}[\text{GEF}]^2 + k''k_{-2}k_{+5}[\text{GEF}])\end{aligned}$$

The term ($k_{-2} + k_{+4}$[GEF]) is then factored out of the equation.

$$\begin{aligned}[\text{Ras} \bullet \text{GTP}] = (k_{-7} + k_{+8})[\text{GTP}]\big(k'k_{-5}(k_{-2} + k_{+4}[\text{GEF}]) \\ + k'k''([\text{GTP}] + [\text{GDP}])(k_{-2} + k_{+4}[\text{GEF}]) + k''k_{+5}[\text{GEF}](k_{-2} + k_{+4}[\text{GEF}])\big)\end{aligned}$$

$$= (k_{-7} + k_8)(k_{-2} + k_{+4}[\text{GEF}])[\text{GTP}]\big(k'k_{-5} + k''k_{+5}[\text{GEF}] + k'k''([\text{GTP}] + [\text{GDP}])\big)$$

The same approach is applied to Ras•GDP, but with B used as the common node.

$$[\text{Ras} \bullet \text{GDP}] = (\text{AC})(\text{B})(\text{D})(\text{E}) + (\text{DC})(\text{A})(\text{B})(\text{E}) + (\text{EC})(\text{A})(\text{B})(\text{D}) + (\text{BC})(\text{A})(\text{D})(\text{E})$$

$$= (\text{AC})[(\text{BA})(\text{D})(\text{E}) + (\text{BD})(\text{DA})(\text{E})] + (\text{DC})[(\text{BD})(\text{A})(\text{E}) + (\text{BA})(\text{AD})(\text{E})]$$

$$+ (\text{EC})(\text{BE})(\text{A})(\text{D}) + (\text{BC})(\text{A})(\text{D})(\text{E})$$

$$= (\text{E})\big((\text{AC})[(\text{BA})(\text{D}) + (\text{BD})(\text{DA})] + (\text{DC})[(\text{BD})(\text{A}) + (\text{BA})(\text{AD})]\big) + (\text{A})(\text{D})[(\text{EC})(\text{BE})$$

$$+ (\text{BC})(\text{E})]$$

$$= (k_{-7} + k_{+8})\Big(k_{+2}[\text{GDP}]\big(k_{-1}(k_{-5} + k_{-3}[\text{GTP}] + k_{-4}[\text{GDP}]) + (k_{+3}[\text{GEF}])(k_{-5})\big)$$

$$+ k_{-4}[\text{GDP}]\big(k_{+3}[\text{GEF}](k_{+1}[\text{GTP}] + k_{+2}[\text{GDP}] + k_{+5}[\text{GEF}])$$

$$+ (k_{-1})(k_{+5}[\text{GEF}])\big)\Big)$$

$$+ (k_{+1}[\text{GTP}] + k_{+2}[\text{GDP}] + k_{+5}[\text{GEF}])(k_{-5} + k_{-3}[\text{GTP}]$$

$$+ k_{-4}[\text{GDP}])\big((k_{+8})(k_{+7}[\text{GAP}]) + (k_{+6})(k_{-7} + k_{+8})\big)$$

Once again the assumption that Ras and Ras • GEF have almost equal affinities for GTP and GDP is applied.

if $k_{+1} = k_{+2} = k'$ and $k_{-3} = k_{-4} = k''$

$$[\text{Ras} \bullet \text{GDP}] = (k_{-7} + k_{+8})\Big(k'[\text{GDP}]\big(k_{-1}(k_{-5} + k''[\text{GTP}] + k''[\text{GDP}]) + (k_{+3}[\text{GEF}])(k_{-5})\big)$$

$$+ k''[\text{GDP}]\big(k_{+3}[\text{GEF}](k'[\text{GTP}] + k'[\text{GDP}] + k_{+5}[\text{GEF}]) + (k_{-1})(k_{+5}[\text{GEF}])\big)\Big)$$

$$+ (k'[GTP] + k'[GDP] + k_{+5}[GEF])(k_{-5} + k''[GTP]$$

$$+ k''[GDP])\big((k_{+8})(k_{+7}[GAP]) + (k_{+6})(k_{-7} + k_{+8})\big)$$

[GDP] is factored out, and the remaining terms are distributed.

$$[\text{Ras} \bullet \text{GDP}] = (k_{-7} + k_{+8})[\text{GDP}](k'k_{-1}k_{-5} + k'k''k_{-1}([\text{GTP}] + [\text{GDP}]) + k'k_{+3}k_{-5}[\text{GEF}]$$
$$+ k'k''k_{+3}[\text{GEF}]([\text{GTP}] + [\text{GDP}]) + k''k_{+3}k_{+5}[\text{GEF}]^2 + k''k_{-1}k_{+5}[\text{GEF}])$$
$$+ (k'([\text{GTP}] + [\text{GDP}]) + k_{+5}[\text{GEF}])\big(k_{-5} + k''([\text{GTP}] + [\text{GDP}])\big)\big(k_{+7}k_{+8}[\text{GAP}]$$
$$+ k_{+6}(k_{-7} + k_{+8})\big)$$

After distributing the $k_{+5}k_{-5}$[GEF] term is removed because it is a cyclic term.

$$[\text{Ras} \bullet \text{GDP}] = (k_{-7} + k_{+8})[\text{GDP}]\big(k'k_{-5}(k_{-1} + k_{+3}[\text{GEF}])$$
$$+ k'k''(k_{-1} + k_{+3}[\text{GEF}])([\text{GTP}] + [\text{GDP}]) + k''k_{+5}[\text{GEF}](k_{-1} + k_{+3})\big)$$
$$+ \big(k'k_{-5}([\text{GTP}] + [\text{GDP}]) + k'k''([\text{GTP}] + [\text{GDP}])^2$$
$$+ k''k_{+5}[\text{GEF}]([\text{GTP}] + [\text{GDP}])\big)\big(k_{+7}k_{+8}[\text{GAP}] + k_{+6}(k_{-7} + k_{+8})\big)$$

The term (k_{-1} + k_{+3}[GEF]) is then factored out of the equation.

$$[\text{Ras} \bullet \text{GDP}] = (k_{-7} + k_{+8})(k_{-1} + k_{+3}[\text{GEF}])[\text{GDP}](k'k_{-5} + k'k''([\text{GTP}] + [\text{GDP}])$$
$$+ k''k_{+5}[\text{GEF}])$$
$$+ (k'k_{-5} + k'k''([\text{GTP}] + [\text{GDP}]) + k''k_{+5}[\text{GEF}])\big(k_{+7}k_{+8}[\text{GAP}]$$
$$+ k_{+6}(k_{-7} + k_{+8})\big)([\text{GTP}] + [\text{GDP}])$$

The term $(k'k_{-5} + k'k''([\text{GTP}] + [\text{GDP}]) + k''k_{+5}[\text{GEF}])$ is then factored out of the equation.

$$[\text{Ras} \bullet \text{GDP}] = \Big((k_{-7} + k_{+8})(k_{-1} + k_{+3}[\text{GEF}])[\text{GDP}]$$
$$+ \big(k_{+7}k_{+8}[\text{GAP}] + k_{+6}(k_{-7} + k_{+8})\big)([\text{GTP}] + [\text{GDP}])\Big)(k'k_{-5}$$
$$+ k'k''([\text{GTP}] + [\text{GDP}]) + k''k_{+5}[\text{GEF}])$$

The fraction of GTP-bound Ras can be defined as,

$$= \frac{[\text{Ras} \bullet \text{GTP}]}{[\text{Ras} \bullet \text{GTP}] + [\text{Ras} \bullet \text{GDP}]}$$

After substituting the values of Ras•GTP and Ras•GDP, the fraction of GTP-bound Ras is

$$= \frac{(k_{-7} + k_8)(k_{-2} + k_{+4}[\text{GEF}])[\text{GTP}]\big(k'k_{-5} + k''k_{+5}[\text{GEF}] + k'k''([\text{GTP}] + [\text{GDP}])\big)}{\Big((k_{-7} + k_{+8})(k_{-1} + k_{+3}[\text{GEF}])[\text{GDP}] + \big(k_{+7}k_{+8}[\text{GAP}] + k_{+6}(k_{-7} + k_{+8})\big)([\text{GTP}] + [\text{GDP}])\Big)\,(k'k_{-5} + k'k''([\text{GTP}] + [\text{GDP}]) + k''k_{+5}[\text{GEF}])}$$

Divide by the terms $(k_{-7} + k_{+8})(k'k_{-5} + k'k''([\text{GTP}] + [\text{GDP}]) + k''k_{+5}[\text{GEF}])$, and the resulting Equation 1 defines the comprehensive fraction of the GTP-bound Ras (the comprehensive $f_{\text{Ras•GTP}}$).

$$= \frac{(k_{-2} + k_{+4}[\text{GEF}])[\text{GTP}]}{(k_{-2} + k_{+4}[\text{GEF}])[\text{GTP}] + (k_{-1} + k_{+3}[\text{GEF}])[\text{GDP}] + \left(\frac{k_{+7}k_{+8}}{k_{-7} + k_{+8}}[\text{GAP}] + k_{+6}\right)([\text{GTP}] + [\text{GDP}])} \qquad \text{Equation 1}$$

To account for only the intrinsic turnover of GTP to GDP by Ras, all terms relating to GEF and GAP can be canceled to yield Equation 2 for the intrinsic fraction of the GTP-bound Ras (the intrinsic $f_{\text{Ras•GTP}}$).

$$= \frac{k_{-2}[\text{GTP}]}{k_{-2}[\text{GTP}] + k_{-1}[\text{GDP}] + k_{+6}([\text{GTP}] + [\text{GDP}])} \qquad \text{Equation 2}$$

The same principle can be applied to GEF- and/or GAP-only situations, thus resulting in equations for the fraction of GTP-bound Ras as follows. In a case in which only GEF is

active, Equation 3 for the GEF-mediated fraction of the GTP-bound Ras (the GEF-mediated $f_{\text{Ras•GTP}}$) is

$$= \frac{(k_{-2} + k_{+4}[\text{GEF}])[\text{GTP}]}{(k_{-2} + k_{+4}[\text{GEF}])[\text{GTP}] + (k_{-1} + k_{+3}[\text{GEF}])[\text{GDP}] + k_{+6}([\text{GTP}] + [\text{G}}$$ Equation 3

Similarly, if only GAP is active, Equation 4 for the GAP-mediated fraction of the GTP-bound Ras (the GAP-mediated $f_{\text{Ras•GTP}}$) is

$$= \frac{k_{-2}[\text{GTP}]}{k_{-2}[\text{GTP}] + k_{-1}[\text{GDP}] + \left(\frac{k_{+7}k_{+8}}{k_{-7} + k_{+8}}[\text{GAP}] + k_{+6}\right)([\text{GTP}] + [\text{GDP}])}$$ Equation 4

References

1. Fromm, H. J. (1970) A simplified schematic method for deriving steady-state rate equations using a modification of the "theory of graphs" procedure, *Biochem Biophys Res Commun 40*, 692-697.
2. Huang, C. Y. (1979) [4] Derivation of initial velocity and isotope exchange rate equations, In *Methods Enzymol*, pp 54-84, Academic Press.

CHAPTER 3

DETERMINATION OF THE EMBRYONIC RAS-SPECIFIC EFFECTOR PROTEINS

DETERMINATION OF THE EMBRYONIC RAS-SPECIFIC EFFECTOR PROTEINS

Michael Wey and Jongyun Heo

Abstract

ERas is the newest member of the Ras subfamily. Unlike other members of the Ras subfamily, ERas is constitutively active and not normally expressed in humans. The expression of ERas in humans is correlated to human cancers. It was proposed that ERas enhances tumorigenicity through PI3K/Akt pathway. However, another work found ERas directly activating JNK directly without PI3K/Akt involvement.

All previous work was qualitative and did not recognize the differences in binding affinity of amongst several key Ras-downstream effector proteins. Through kinetic binding approaches, my research results elucidate and refine the ERas-specific effector proteins. I uncover that ERas shows a high affinity for PI3Kα and PI3Kδ. This finding is significant because as it delineates the exact interaction counterparts of ERas with the PI3K/Akt pathway, thus suggesting a clearer target for possible drug design to cure or alleviate ERas-mediated human cancer.

Additionally, I also discover that ERas has a sufficient affinity for the tumor suppressor protein Rassf5. I propose that the binding interaction between ERas and Rassf5 leads to a direct JNK activation that explains the previous reports. The clarification of the ERas-mediated JNK activation is important because it aids in the explanation of the reprogramming ability of ERas in mice.

Introduction

The Ras subfamily of small GTPases are one of the most studied signaling proteins in humans. The major family members of the Ras subfamily include HRas, KRas, and NRas. These Ras isoforms have closely related.[1] Ras proteins function as molecular switches through the binding and release of GTP and GDP. The cycling of Ras proteins between the active GTP- and the inactive GDP-bound form functions as molecular switch that controls various cellular signaling cascades.[2, 3] When in the active GTP-bound form, Ras proteins are able to bind to their downstream effectors and stimulate various cellular processes.[4, 5] Ras-downstream effectors encompass Raf1, RalGDS, Rassf5, and PI3Ks.[6]

ERas was first reported in 2003 in murine embryonic cells, and its functions are tied with the growth and development of murine embryos.[7] Unlike murine ERas, human version of ERas is epigentically silenced.[8] ERas is not normally expressed in human cells and when expressed cause cancers.[8-12] Unlike with other Ras proteins, ERas has an extended N-terminus as well as unique Switch I and Switch II regions. The role of the ERas N-terminus in ERas function is unclear. A recent study shows the N-terminus could affect the subcellular localization of ERas.[13] N-terminal truncated ERas was observed to slightly diminish the population of ERas localized to the plasma membrane, however it is noted that the changes were marginal.

The ERas-specific Switches I and II render ERas to have an intrinsically high GTP-binding affinity and to block ERas GAP-binding interaction, populating the GTP-bound active form of ERas in cells.[14] The constitutively active feature of ERas engenders its tumorigenic and reprogramming ability.[15]

It is notable that the expression of ERas in humans cause various types of cancers.[8-12] A clinical study on gastric carcinomas (GC) found 44% of biopsied tumors expressed ERas, compared to only 10% expressing KRas mutations.[10] Later Liu et al. proved that ERas enhances the ability of GC to proliferate and metastasize.[16] In addition, Liu showed that ERas expression is common in GC and is a key protein to the development of GC. ERas was also found to be expressed in various human cancer cell lines such as gastric, brain, breast, and pancreatic cancer cells lines.[17] When ERas was overexpressed in neuroblastoma cells, it was shown to increase in transforming activity as well as confer resistance to chemotherapeutic drugs, promoting tumorigenicity.[18, 19]

ERas has been shown to interact with primarily with PI3Kα and PI3Kδ.[7, 13, 20] The original Takahashi et al. study,[7] as well as ones which followed,[15, 17, 20] showed that ERas mainly functions to activate the PI3K/Akt pathway in cells. Another research reports that, regardless of the Akt activity, ERas directly activates JNK.[21] It is important to note that these studies are reliant on qualitative pull-down assays and give conflicting information. To delineate the conflict and to gain insight into the ERas functions in cells, quantitative binding studies were performed for ERas with key Ras-downstream effector proteins that include Raf1, RalGDS, PI3Kα, PI3Kγ, PI3Kδ and Rassf5. For these kinetic studies, I have produced a full-length native ERas protein by using a baculovirus in Sf9 insect cells. Previously, functional ERas has only been obtained from ERas expression in mammalian cells. Based upon the comparative analyses of the binding study results, I propose a role of ERas in cells and an answer for the reason of the previous conflicting results.

Materials and Methods

Expression and purification of human ERas. Full-length human ERas was provided by Dr. Jungho Kim and expressed with the Invitrogen Bac-to-Bac™ Baculovirus system. The full-length ERas gene was cloned into the pFastBac/NT-TOPO vector. After successful cloning, the pFastbac vector containing the ERas gene was transformed into DH10Bac to create a recombinant bacmid. The recombinant bacmid was isolated from the transformed DH10Bac using an endotoxin free purification kit. The isolated recombined bacmid was transfected into healthy (>95% viability) Sf9 cells with Cellfectin® II following the manufacturer's protocols. The Sf9 cells were grown as a monolayer in SF-900™ III media at 27 °C in absence CO_2. Four days after transfection, the culture was centrifuged to remove cell debris and the supernatant kept as a viral stock.

For expression of full length ERas, Sf9 cells were grown in a suspension culture in a non-humidified shaker incubator at 27 °C and 150 rpm. Sf9 cells were grown until ~1.5×10^6 cells/mL then inoculated with viral stock at a MOI of 5. After ~48 hrs the Sf9 cells were collected by centrifugation. Cells were lysed by a combination of freeze-thawing and a detergent buffer containing 100 mM NaCl, 1% NP-40, 0.5% sodium deoxycholate, and 50 mM Tris-HCl (pH 7.4). The lysate was centrifuged for 10 min at $10000 \times g$ to clear the cell debris and the supernatant was collected. To purify ERas from the supernatant collected, a column of Ni-NTA agarose affinity resin (Qiagen) was used.

Western blot. The western blot performed for ERas proteins purified from Sf9 insect cells were done as previously described in a previous study.[22] The ERas antibody was purchased from Sigma-Aldrich and has a monoclonal epitope for the unique N-terminal region.

Expression and purification of HRas and downstream effectors. All the downstream effector protein constructs and HRas were of human origin. Full-length HRas (#1-189) and the Ras Binding Domains (RBD) of Raf1 (#56-131), PI3Kα (#187-289), PI3Kγ (#217-309), and PI3Kδ (#187-278) were cloned into the maltose binding fusion protein vector, pMal-c2e. The Ras-associating domains of RalGDS (#798-885) and Rassf5 (#203-364) were also cloned into the pMalc2e vector for expression. The downstream effector proteins were then expressed and purified from the BL21 strain of *E. coli* as followed.

A single colony was inoculated into Lysogeny broth at 37 °C and incubated until the optical density at 600 nm was greater than 0.4. At this time, Isopropyl β-D-1-thiogalactopyranoside (IPTG) was added to a final concentration of 0.5 mM and the temperature as adjusted to 25 °C. After IPTG induction, the culture was incubated an additional 6-8 hrs. The cells were then centrifuged and sonicated. The recombinantly expressed downstream effector proteins were affinity purified using amylose resin. The proteins purified from the amylose resin were then subject to dialysis to remove excess salt and maltose from the buffer.

Determination of dissociation constants of ERas and HRas with Ras-downstream effectors. The dissociation constants (K_d) of ERas and HRas with selected Ras-downstream effector proteins were estimated by a fluorescence-based titration (LS 55,

PerkinElmer). Fluorescence intensity increases upon the binding of an effector to a Ras protein loaded with a fluorescent nucleotide.[23] This fluorescence intensity increase can be used to monitor the fraction of Ras bound to the effector. The estimation of K_d values of the GTP-bound ERas and HRas with effector proteins was performed by using 2'(3')-O-(N-methylanthraniloyl) 5'-guanylyl-imidodiphosphate (mant-GppNHp) as a fluorescent non-hydrolyzable analog of GTP. The K_d value determinations of the GDP-bound ERas and HRas was conducted by using 2'(3')-O-(N-methylanthraniloyl) guanosine diphosphate (mant-GDP), a fluorescent analog of GDP.

Ras loaded with mant-GDP (Ras•mant-GDP) and Ras loaded with mant-GppNHp (Ras•mant-GppNHp) were prepared by loading Ras proteins with a 5-fold molar excess of the fluorescent nucleotide in the presence of 200 mM ammonium sulfate and 10 mM EDTA. Unbound nucleotide and salts were separated from nucleotide-bound Ras by gel filtration with Sephadex G-10 resin (GE Healthcare).

For the fluorescence titrations, 1 μM of Ras•mant-GDP or Ras•mant-GppNHp, was titrated with a single RBD/RA of a predicted downstream effector until saturation. An excitation wavelength (λ_{ex}) of 355 nm was used, and fluorescence intensity was measured at an emission wavelength (λ_{em}) of 448 nm. For each addition of the downstream effector to the loaded Ras, ~600 sec were given for equilibration. All fluorescence assays were performed using proteins more than 95% pure, as judged by SDS-PAGE. The buffer used for all assays consisted of 50 mM NaCl, 5 mM $MgCl_2$, and 100 mM TrisHCl (pH 7.4). All assays were performed at room temperature. The program GraphPad Prism was used for all fitting.

Results

Recombinant Sf9 cells expression of native human ERas. Previously ERas expression has been solely achieved through overexpression in human cancer cell lines.[13, 14, 20] Expression of ERas through human cancer cells is labor intense and do not easily allow for bulk purification. Our lab has attempted to express ERas through bacterial expression systems, but none were successful. I was able to express ERas in a baculoviral insect expression system (see details in the Materials and Methods section). Briefly, full-length ERas gene was cloned into the Invitrogen pFastbac vector and transformed into DH10Bac for recombination. The plasmids were then transfected into Sf9 insect cells and a baculoviral stock was made. Fresh Sf9 cells were infected with the baculovius and harvested after 48 hrs. The ERas protein was purified using a Ni-NTA column.

A Western blot analysis by using ERas antibody confirmed that the purified protein by using the baculoviral insect expression system is ERas (not shown). The purified ERas protein was loaded with mant-GDP as described in the Materials and Method section. Figure 1 shows that the ERas protein expressed and purified from Sf9 cells is in a native form as it is capable of binding mant-guanine nucleotide.

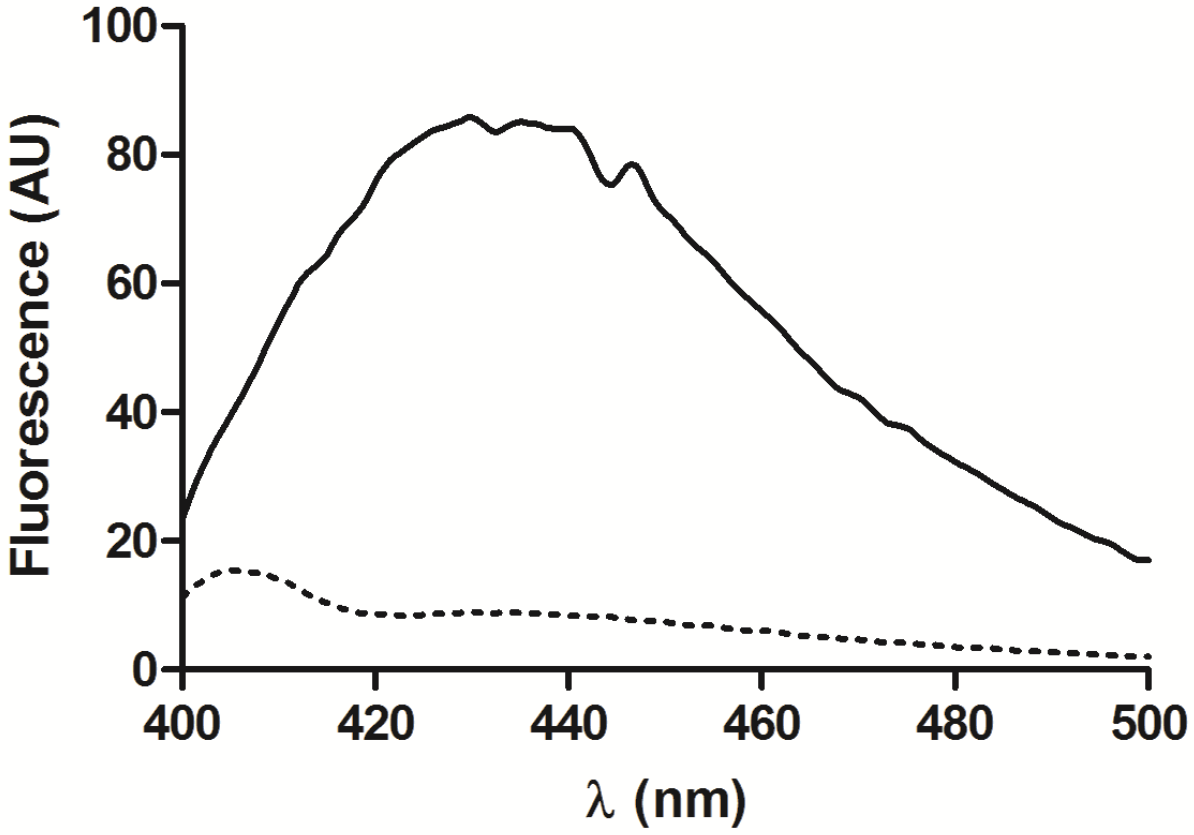

Figure 1. *Fluorescence Emission Spectra of ERas with Mant-nucleotide.*

Free mant-GDP (1 μM, dashed line) and ERas-bound mant-GDP (1 μM, solid line) were excited at 355 nm, and their fluorescence emissions were monitored from 400-500 nm. The binding of mant-GDP to ERas results in a significant change in mant fluorescence emission at 440 nm.

Fluorescence titrations with mant-GppNHp and mant-GDP loaded HRas. K_d values of GTP-bound HRas with Ras-downstream effectors (Table 1) were determined by the titration of HRas•mant-GppNHp with Ras-downstream effectors (Figure 2). HRas•mant-GppNHp shows moderate affinity for the RBD's of PI3Kα, PI3Kδ, PI3Kγ, and the RA of RalGDS with a K_d values between 1-5 μM. These results are similar to those of previous studies.[24] The binding affinity of HRas•mant-GppNHp with the RBD of Raf1 is by far the greatest among the downstream effectors titrated within this study. HRas•mant-GppNHp has a K_d value of 0.27 ± 0.06 μM with Raf-1 RBD; an order of magnitude smaller compared to the other downstream effectors titrated. Rassf5 RA does not show meaningful binding affinity to HRas•mant-GppNHp (K_d = 50 ± 20 μM).

Estimation of K_d values for GDP-bound HRas with Ras downstream effectors were performed by using HRas•mant-GDP (Table 1). Except for the Raf-1 RBD, HRas•mant-GDP does not show any significant binding affinity for the selected downstream effector proteins. The K_d values of HRas•mant-GDP with RA of Rassf5 and RalGDS were not determined because there was no noticeable change in mant fluorescence upon the titrations. The estimated K_d values of HRas•mant-GDP with Ras downstream effectors PI3Kα, PI3Kγ, and PI3Kδ are all greater than 270 μM, indicating that HRas•GDP has only a little affinity with these effector proteins.

While other downstream effectors showed little to no affinity for HRas•mant-GDP, the Raf-1-RBD had a K_d value of 2.8 ± 0.5 μM. This affinity is comparable to the affinity of active GTP-bound HRas with downstream effectors.[24]

Fluorescence titrations with mant-GppNHp and mant-GDP loaded human ERas. Qualitative binding studies have been conducted to determine the downstream effectors of ERas. A fluorescent titration of ERas•mant-GppNHp with various downstream effectors (Figure 3A) allows one to estimate the K_d values of GTP-bound ERas with various downstream effectors (Table 1). The results indicate that ERas has a high affinity with PI3Kα, PI3Kδ, and Rassf5, consistent with the previous studies that used pull down assays.[13, 20] ERas•mant-GppNHp shows strong affinity for PI3Kα RBD on the nanomolar scale (K_d = 0.5 ± 0.2 μM). Such a binding affinity is comparable to that of HRas•mant-GppNHp to Raf1 RBD (K_d = 0.27 ± 0.06 μM). The K_d values of ERas•mant-GppNHp with PI3Kδ RBD and Rassf5 RA are ~10-fold greater compared to that with PI3Kα-RBD. The ERas•mant-GppNHp binding affinity with PI3Kγ-RBD is significantly low because the K_d value of ERas•mant-GppNHp with PI3Kγ-RBD was greater than 20 μM.

Similar to the cases with HRas, titrations of ERas•mant-GDP with PI3Kα RBD, PI3Kδ RBD, and Rassf5 RA yield K_d values orders of magnitude greater than the K_d values of ERas•mant-GppNHp with the corresponding effector proteins (Figure 3B and Table 1). It is notable that the K_d value of ERas•mant-GppNHp with PI3Kα RBD is not significantly deviated from that of ERas•mant-GDP with PI3Kα RBD. The relative constant binding affinity of Ras with its effector proteins regardless of Ras•GTP or Ras•GDP form also is observed in HRas with Raf1. Raf1 RBD and RalGDS RA showed no affinity for either ERas•mant-GppNHp or ERas•mant-GDP. Therefore, no K_d values were determined for these combinations.

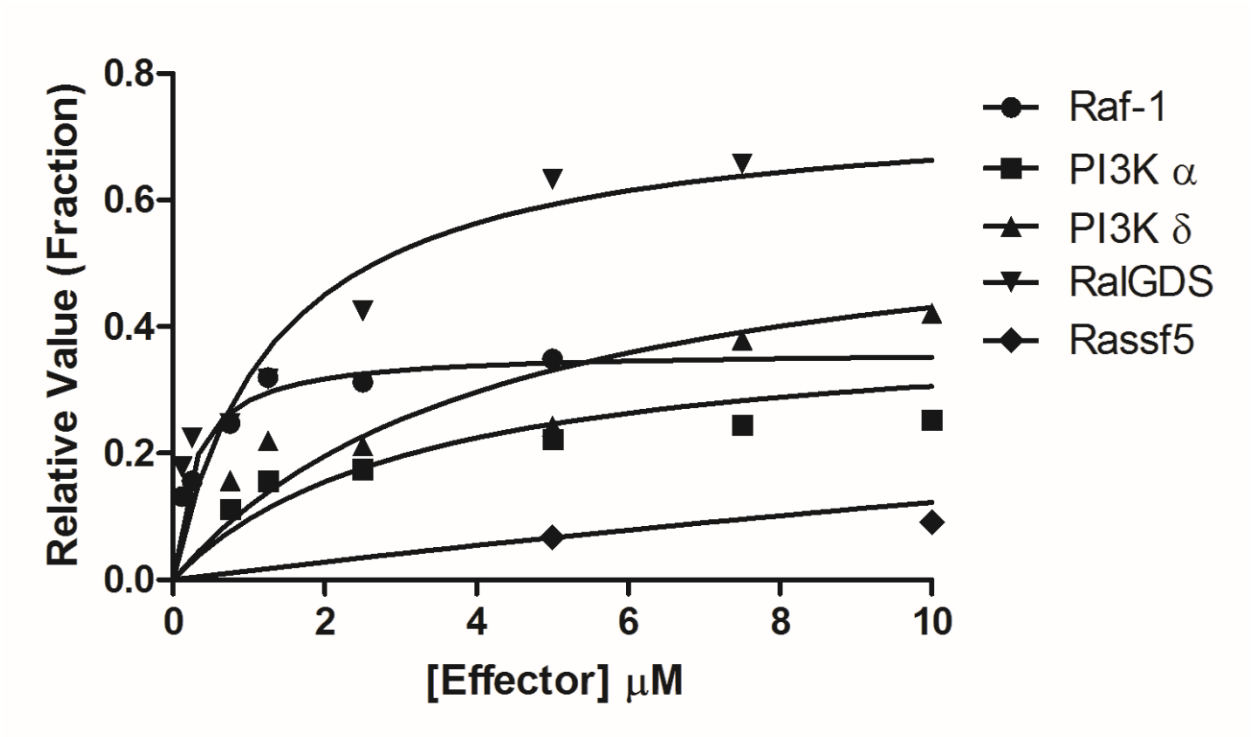

Figure 2. *Estimation of K_d Values Between HRas and Its Effectors.*

The measurements of K_d between HRas and selected downstream effectors are described in the Materials and Methods section. Equilibrium titrations were performed with HRas•mant-GppNHp (1 μM) with various concentrations of effectors. Each sample was given 300 sec to equilibrate before continuing the titration. All fluorescence values were normalized against the highest fluorescence value obtained. The estimation of K_d values are shown in Table 1.

	K_d (μM)			
	HRas		**ERas**	
Effector	**Mant-GDP**	**Mant-GppNHp**	**Mant-GDP**	**Mant-GppNHp**
Raf1 RBD	2.8 ± 0.5	0.27 ± 0.06	ND	ND
RalGDS RA	ND	1.1 ± 0.7	ND	ND
PI3Kα RBD	~270	3 ± 1	13 ± 2	0.5 ± 0.2
PI3Kγ RBD	~338	5 ± 2	~120	20 ± 5
PI3Kδ RBD	~300	4 ± 2	~146	4.9 ± 0.7
Rassf5 RA	ND	~50	~40	3.4 ± 0.5

Table 1. Equilibrium Dissociation Constants of HRas and ERas with Various Effectors.

The determined K_d values of HRas and ERas were taken from fits in Figures 2 and 3. Error shown is the fit error at a 95% confidence interval. All fitting was done using GraphPad Prism. For effectors where K_d was not determined, ND was used.

A

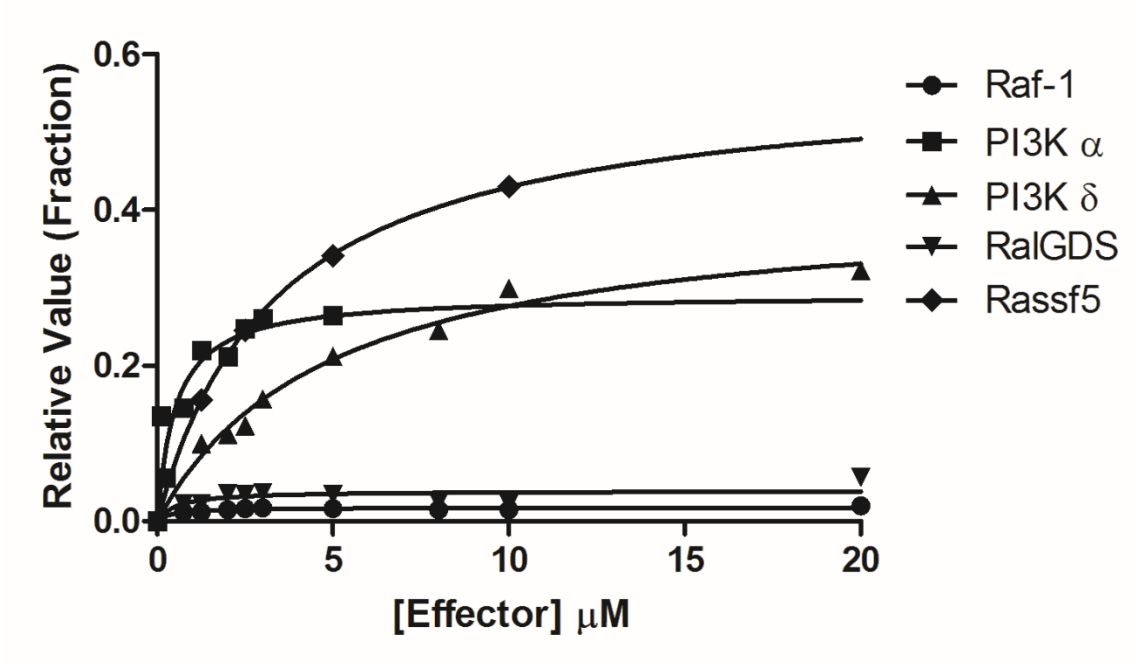
Relative Value (Fraction)
0.6
0.4
0.2
0.0
0
5
10
15
20
[Effector] μM
Raf-1
PI3K α
PI3K δ
RalGDS
Rassf5

B

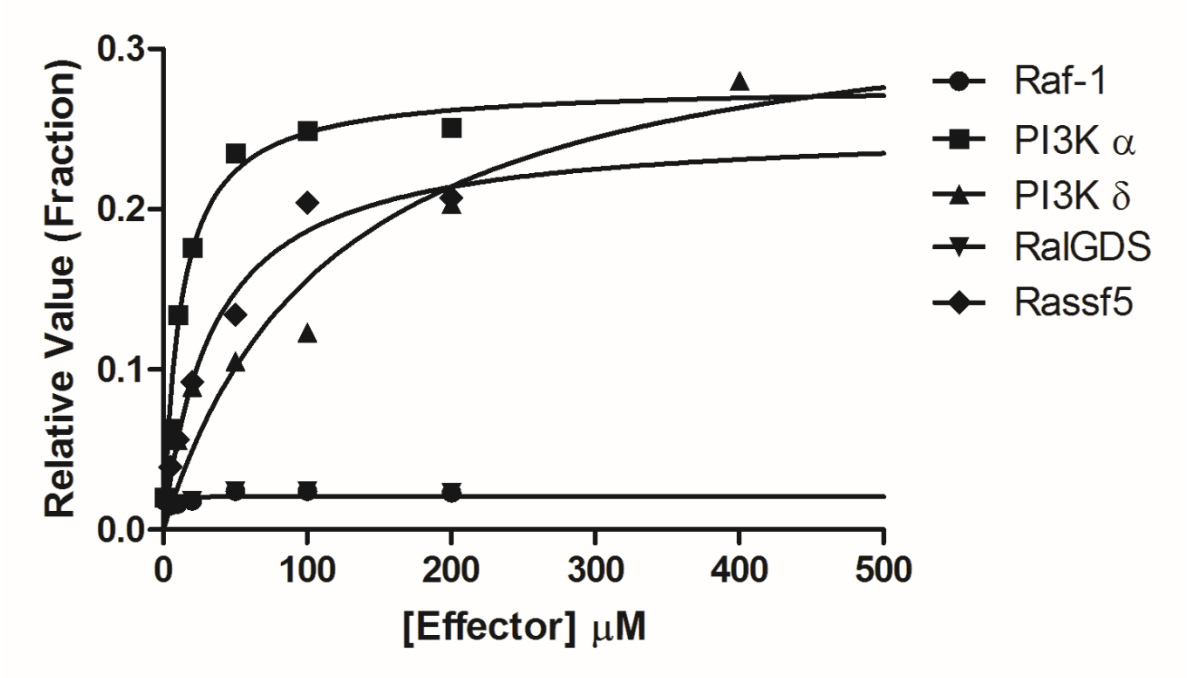
Relative Value (Fraction)
0.3
0.2
0.1
0.0
0
100
200
300
400
500
[Effector] μM
Raf-1
PI3K α
PI3K δ
RalGDS
Rassf5

Figure 3. *Estimation of K_d Values Between ERas and its Effectors.*

The measurements of K_d between ERas and selected downstream effectors are described in the Materials and Methods section. Equilibrium titrations were performed with **A.** ERas•mant-GppNHp (1 μM) and **B.** ERas•mant-GDP (1 μM). Each sample was given 300 s to equilibrate prior to continuation of the titration. All fluorescence values were normalized against the highest fluorescence value obtained. The estimation of K_d values are shown in Table 1.

Discussion and Conclusion

PI3Kα is the primary downstream effector of human ERas. In this study, I quantified the binding interacting between ERas and common Ras downstream effector proteins including Raf, RalGDS, PI3Kα, PI3Kγ, PI3Kδ and Rassf5. Because PI3Kβ is shown to interact with a different set of small GTPases, Rho proteins, but not Ras GTPases,[25] PI3Kβ is not listed within this study. It also is notable that ERas exerts its cellular function through Akt pathway through the binding and activation of PI3K.[17, 18]

I have found that the tightest binding effector of ERas, among the ones I examined, was RBD of PI3Kα (Table 1). The estimated K_d value of ERas with PI3Kα RBD was in the nanomolar range (Table 1). ERas showed a weaker affinity with PI3Kδ, whose K_d value was approximately 10-fold greater than that of (Table 1). ERas showed limited affinity with Raf1 and PI3Kγ (Table 1). Given these K_d values in combination with the previous reports.[7, 17, 20] it is evident that certain PI3Ks such as PI3Kα and PI3Kδ (see below) are immediate downstream effectors of ERas. Therefore, I propose that ERas functions through the PI3K-directed Akt pathway.

PI3Kα is a ubiquitously expressed protein in humans.[26] Thus ERas, regardless of the origin of expression in humans, can transmit its downstream signaling through its binding interaction with the ubiquitously expressed PI3Kα. The expression of PI3Kδ is skewed toward the hemopoietic system.[27] However, outside the hemopoietic system, PI3Kδ is most commonly expressed in cells that are originating from breast[28, 29] and embryonic tissues.[30] In addition, certain colorectal cancer cell lines showed slight expression of PI3Kδ mRNA.[31] ERas has been found in various cancers and cancer cell lines.[11] MDA-MB-231 is a triple negative breast cancer cell line, known to be particularly

metastatic and aggressive. MDA-MB-231 was found to express ERas mRNA[11] and greater than normal amounts of PI3Kδ.[32] It is possible that ERas could play a tumorigenic role in MDA-MB-231 cells through the activation of PI3Kα and PI3Kδ. Elucidating the means by which ERas activates the PI3K/Akt pathway allows one to have a clearer drug-target design for the ERas-mediated cancers.

Human ERas binds Rassf5 RA domain. Takahashi et al. showed that ERas mediated its oncogenic transformation of NIH3T3 cells through PI3K/Akt pathway.[7] Other researchers have also supported the initial finding that ERas-mediated oncogenic transformation of cells is due to the activation of PI3K/Akt pathway.[13, 15, 17, 20] However, a recent study in 2015 by Kwon et al. reported that the reprogramming efficiency of murine induced pluripotent stem cells, which expressed ERas, did not change when an Akt inhibitor was used.[21] Instead, the study proposed that ERas directly activated JNK which enhanced the phosphorylation and activation of the SP1 transcription factor. This activation of the JNK-SP1 signaling pathway resulted in facilitation of cell cycle progression, thus improving the efficiency of reprogramming fibroblast cells. The result suggests that the PI3K/Akt pathway is not the only means by which ERas has an influence over cellular functions. The suggestion is sound, because Nakhaei-Rad et al.[20] show that ERas has an affinity to a tumor suppressor protein Rassf5.

Rassf5 belongs to a family of tumor suppressor proteins which link Ras to the pro-apoptotic Hippo pathway.[33-36] The Hippo pathway regulates tissue homeostasis, proliferation and organ size.[37 38 39] The original description of the Hippo pathway was described in *Drosophila*. The pathway is named after the serine/threonine kinase Hippo (Hpo), which is one of the core proteins of *Drosophila* Hippo signaling.[40] This pathway is

conserved from *Drosophila* to mammals. The mammalian homologue of Hpo is mammalian STE20-like protein kinase 1/2 (MST1/2).[41]

Active KRas and HRas are able to bind Rassf5 and alleviate its autoinhibited state.[24, 36, 42, 43] Rassf5 is then able heterodimerize with MST1/2 through their respective Salvador/Rassf/Hippo (SARAH) domains and activate MST1/2.[36, 44-47] The activation of MST1/2 leads to stimulation of the Hippo pathway.[36] My results show that the binding affinity between HRas and Rassf5 is limited (Table 1). This is not unexpected, because the previous pulldown studies have shown that HRas is unable to bind with the RA domain of Rassf5 alone.[33] However, the results in Table 1 indicate that the RA domain of Rassf5 *per se* can bind to active ERas without the presence of the adjacent SARAH domain. The ERas-binding feature with Rassf5 suggests that ERas can also play a role in the pro-apoptotic Hippo pathway.

The binding interaction between ERas and the Rassf5 RA domain (Table 1) also explains the previously observed yet uncharacterized feature of the direct ERas-mediated activation of the JNK-SP1 signaling cascade.[21] MST1/2 was shown to couple with the JNK pathway.[48-50] Given that ERas can bind the Rassf5 RA domain and thus activate Rassf5, which in turn further activates MST1/2, I propose that the ERas binding interaction with the Rassf5 RA domain leads to activation of JNK pathway.

Several previous studies propose that ERas increases reprogramming efficiency that are likely attributed to the PI3K/Akt pathway.[7, 13, 15, 17] However, as mentioned above, Kwon et al. showed that ERas increased reprogramming efficiency from JNK signaling but not PI3K/Akt signaling.[21] I believe both cases are true. It has been reported that the Hippo pathway also assists in reprogramming of cells and

regeneration of several damaged mice organs.[51] Also induced pluripotent-stem cells were stimulated to reprogram by the activation of the Hippo pathway.[52]

My research results in combination with these previous results can be summarized as following: (i) ERas increased reprogramming efficiency through the JNK pathway[21]; (ii) the Hippo pathway activates the JNK pathway[48-50]; (iii) Hippo pathway is shown to assist in reprogramming[51]; and (iv) ERas is capable of binding Rassf5, which is linked to the Hippo pathway (Table 1)[33-36]. Accordingly, I propose that ERas can also induce reprogramming of cells through the Hippo/JNK pathways.

In *Drosophila*, it was shown that the constitutively active Ras (e.g., G12V Ras) can alter JNK function from pro-apoptotic signaling to anti-apoptotic signaling through the Hippo signal cascade.[53] ERas is constitutively active.[7] Thus, even if ERas binds Rassf5 that is an initiator of the pro-apoptotic Hippo pathway, by the counteraction of the ERas-mediated JNK function, the ERas-binding interaction with Rassf5 may not be a sufficient pro-apoptotic signal as reported by the previous study.

Regulation of ERas through effectors not regulators. ERas is shown to be constitutively active.[7] GAPs are incapable of facilitating ERas GTPase activity and the intrinsic ERas GTPase activity also is stunted.[14] In typical cell signaling-transduction events, cells must have the ability to quench its signaling cascade once it has been activated. A study shows that ERas can be epigenetically silenced as a form of regulation.[20] However, when ERas is cellularly expressed, the ERas signaling is likely to be controlled by its effectors rather than regulators. ERas is shown to interact with PI3Ks such as PI3Kα and PI3Kδ to promote cell proliferation[15, 17, 20] and with Rassf5 (Table 1), which has been implicated to promote apoptosis[33-36]. It is interesting that Rassf5 is a part of the

Hippo pathway that functions against the PI3K/Akt pathway.[54] The JNK pathway that also implicated with ERas is shown to involve in both anti- and pro-tumorigenic courses of cells.[53] There is a potential binding-interaction balance between ERas with these effectors of PI3Kα/δ and Rassf5 by competing for the effector-binding region in ERas. On the basis of the kinetic study results within this research, I propose that the pro-tumorigenic properties are more dominant, as the binding affinity of ERas for PI3Kα and PI3Kδ is a magnitude higher than that for Rassf5. ERas is not normally expressed in human cells. It is possible that an erroneous cellular expression of ERas without a balance of ERas effector expressions causes to produce the pro-tumorigenic cellular features of ERas-relevant cancer cell lines.[8, 10, 11, 17] Further researches would have to follow to explore this mechanism.

Human ERas expressed from Sf9 cells. In this study, all ERas proteins used in the fluorescence titrations were expressed using the Sf9 cell line. Post-translation modifications could occur on ERas proteins expressed in Sf9 cells, because the Sf9 cell line is derived from an eukaryotic organism, an insect. It is possible that a non-native protein expressed in an insect cell has atypical post-translational modifications in comparison to the protein expressed in a human cell line.[55] The ERas construct used for expression originated from humans. Therefore, it is possible that atypical post-translational modifications on ERas due to its expression in the Sf9 cell line affect the binding interactions between ERas and other proteins. Insect cell-expressed ERas has never been used for such kinetic analyses performed within Chapter 3, thus further studies are necessary to compare the K_d values of ERas expressed from insect cells with those of ERas expressed from mammalian cells.

References

1. Wennerberg, K., Rossman, K. L., and Der, C. J. (2005) The Ras superfamily at a glance, *J Cell Sci 118*, 843-846.

2. Klinghoffer, R. A., Duckworth, B., Valius, M., Cantley, L., and Kazlauskas, A. (1996) Platelet-derived growth factor-dependent activation of phosphatidylinositol 3-kinase is regulated by receptor binding of SH2-domain-containing proteins which influence Ras activity, *Mol Cell Biol 16*, 5905-5914.

3. Roberts, P. J., and Der, C. J. (2007) Targeting the Raf-MEK-ERK mitogen-activated protein kinase cascade for the treatment of cancer, *Oncogene 26*, 3291-3310.

4. Vetter, I. R., and Wittinghofer, A. (2001) The guanine nucleotide-binding switch in three dimensions, *Science 294*, 1299-1304.

5. Shields, J. M., Pruitt, K., McFall, A., Shaub, A., and Der, C. J. (2000) Understanding Ras: 'it ain't over 'til it's over', *Trends Cell Biol 10*, 147-154.

6. Simanshu, D. K., Nissley, D. V., and McCormick, F. (2017) RAS Proteins and Their Regulators in Human Disease, *Cell 170*, 17-33.

7. Takahashi, K., Mitsui, K., and Yamanaka, S. (2003) Role of ERas in promoting tumour-like properties in mouse embryonic stem cells, *Nature 423*, 541-545.

8. Yashiro, M., Yasuda, K., Nishii, T., Kaizaki, R., Sawada, T., Ohira, M., and Hirakawa, K. (2009) Epigenetic regulation of the embryonic oncogene ERas in gastric cancer cells, *Int J Oncol 35*, 997-1003.

9. Iwauchi, T., Tanaka, H., Yamazoe, S., Yashiro, M., Yoshii, M., Kubo, N., Muguruma, K., Sawada, T., Ohira, M., and Hirakawa, K. (2011) Identification of

HLA-A*2402-restricted epitope peptide derived from ERas oncogene expressed in human scirrhous gastric cancer, *Cancer Sci 102*, 683-689.

10. Kaizaki, R., Yashiro, M., Shinto, O., Yasuda, K., Matsuzaki, T., Sawada, T., and Hirakawa, K. (2009) Expression of ERas oncogene in gastric carcinoma, *Anticancer Res 29*, 2189-2193.
11. Yasuda, K., Yashiro, M., Sawada, T., Ohira, M., and Hirakawa, K. (2007) ERas oncogene expression and epigenetic regulation by histone acetylation in human cancer cells, *Anticancer Res 27*, 4071-4075.
12. Zhang, F., Tang, J. M., Wang, L., Shen, J. Y., Zheng, L., Wu, P. P., Zhang, M., and Yan, Z. W. (2010) Detection of beta-catenin, gastrokine-2 and embryonic stem cell expressed ras in gastric cancers, *Int J Clin Exp Pathol 3*, 782-791.
13. Nakhaei-Rad, S., Nakhaeizadeh, H., Kordes, C., Cirstea, I. C., Schmick, M., Dvorsky, R., Bastiaens, P. I., Haussinger, D., and Ahmadian, M. R. (2015) The Function of Embryonic Stem Cell-expressed RAS (E-RAS), a Unique RAS Family Member, Correlates with Its Additional Motifs and Its Structural Properties, *J Biol Chem 290*, 15892-15903.
14. Wey, M., Lee, J., Kim, H. S., Jeong, S. S., Kim, J., and Heo, J. (2016) Kinetic Mechanism of Formation of Hyperactive Embryonic Ras in Cells, *Biochemistry 55*, 543-559.
15. Yu, Y., Liang, D., Tian, Q., Chen, X., Jiang, B., Chou, B. K., Hu, P., Cheng, L., Gao, P., Li, J., and Wang, G. (2014) Stimulation of somatic cell reprogramming by ERas-Akt-FoxO1 signaling axis, *Stem Cells 32*, 349-363.

16. Liu, Y., Wang, Z., Li, H., Wu, Z., Wei, F., and Wang, H. (2013) Role of the ERas gene in gastric cancer cells, *Oncol Rep 30*, 50-56.

17. Kubota, E., Kataoka, H., Aoyama, M., Mizoshita, T., Mori, Y., Shimura, T., Tanaka, M., Sasaki, M., Takahashi, S., Asai, K., and Joh, T. (2010) Role of ES cell-expressed Ras (ERas) in tumorigenicity of gastric cancer, *Am J Pathol 177*, 955-963.

18. Aoyama, M., Kataoka, H., Kubota, E., Tada, T., and Asai, K. (2010) Resistance to chemotherapeutic agents and promotion of transforming activity mediated by embryonic stem cell-expressed Ras (ERas) signal in neuroblastoma cells, *Int J Oncol 37*, 1011-1016.

19. Kubota, E., Kataoka, H., Tanaka, M., Okamoto, Y., Ebi, M., Hirata, Y., Murakami, K., Mizoshita, T., Shimura, T., Mori, Y., Tanida, S., Kamiya, T., Aoyama, M., Asai, K., and Joh, T. (2011) ERas enhances resistance to CPT-11 in gastric cancer, *Anticancer Res 31*, 3353-3360.

20. Nakhaei-Rad, S., Nakhaeizadeh, H., Gotze, S., Kordes, C., Sawitza, I., Hoffmann, M. J., Franke, M., Schulz, W. A., Scheller, J., Piekorz, R. P., Haussinger, D., and Ahmadian, M. R. (2016) The Role of Embryonic Stem Cell-expressed RAS (ERAS) in the Maintenance of Quiescent Hepatic Stellate Cells, *J Biol Chem 291*, 8399-8413.

21. Kwon, Y. W., Jang, S., Paek, J. S., Lee, J. W., Cho, H. J., Yang, H. M., and Kim, H. S. (2015) E-Ras improves the efficiency of reprogramming by facilitating cell cycle progression through JNK-Sp1 pathway, *Stem Cell Res 15*, 481-494.

22. Shin, J. Y., Wey, M., Umutesi, H. G., Sun, X., Simecka, J., and Heo, J. (2016) Thiopurine Prodrugs Mediate Immunosuppressive Effects by Interfering with Rac1 Protein Function, *J Biol Chem 291*, 13699-13714.

23. Heo, J., Thapar, R., and Campbell, S. L. (2005) Recognition and activation of Rho GTPases by Vav1 and Vav2 guanine nucleotide exchange factors, *Biochemistry 44*, 6573-6585.

24. Nakhaeizadeh, H., Amin, E., Nakhaei-Rad, S., Dvorsky, R., and Ahmadian, M. R. (2016) The RAS-Effector Interface: Isoform-Specific Differences in the Effector Binding Regions, *PLoS One 11*, e0167145.

25. Fritsch, R., de Krijger, I., Fritsch, K., George, R., Reason, B., Kumar, M. S., Diefenbacher, M., Stamp, G., and Downward, J. (2013) RAS and RHO families of GTPases directly regulate distinct phosphoinositide 3-kinase isoforms, *Cell 153*, 1050-1063.

26. Vanhaesebroeck, B., and Waterfield, M. D. (1999) Signaling by distinct classes of phosphoinositide 3-kinases, *Exp Cell Res 253*, 239-254.

27. Martini, M., De Santis, M. C., Braccini, L., Gulluni, F., and Hirsch, E. (2014) PI3K/AKT signaling pathway and cancer: an updated review, *Ann Med 46*, 372-383.

28. Tzenaki, N., Andreou, M., Stratigi, K., Vergetaki, A., Makrigiannakis, A., Vanhaesebroeck, B., and Papakonstanti, E. A. (2012) High levels of p110delta PI3K expression in solid tumor cells suppress PTEN activity, generating cellular sensitivity to p110delta inhibitors through PTEN activation, *FASEB J 26*, 2498-2508.

29. Tzenaki, N., and Papakonstanti, E. A. (2013) p110delta PI3 kinase pathway: emerging roles in cancer, *Front Oncol 3*, 40.

30. Rommel, C., Camps, M., and Ji, H. (2007) PI3K delta and PI3K gamma: partners in crime in inflammation in rheumatoid arthritis and beyond?, *Nat Rev Immunol 7*, 191-201.

31. Yu, M., and Grady, W. M. (2012) Therapeutic targeting of the phosphatidylinositol 3-kinase signaling pathway: novel targeted therapies and advances in the treatment of colorectal cancer, *Therap Adv Gastroenterol 5*, 319-337.

32. Juvin, V., Malek, M., Anderson, K. E., Dion, C., Chessa, T., Lecureuil, C., Ferguson, G. J., Cosulich, S., Hawkins, P. T., and Stephens, L. R. (2013) Signaling via class IA Phosphoinositide 3-kinases (PI3K) in human, breast-derived cell lines, *PLoS One 8*, e75045.

33. Khokhlatchev, A., Rabizadeh, S., Xavier, R., Nedwidek, M., Chen, T., Zhang, X. F., Seed, B., and Avruch, J. (2002) Identification of a novel Ras-regulated proapoptotic pathway, *Curr Biol 12*, 253-265.

34. Bee, C., Moshnikova, A., Mellor, C. D., Molloy, J. E., Koryakina, Y., Stieglitz, B., Khokhlatchev, A., and Herrmann, C. (2010) Growth and tumor suppressor NORE1A is a regulatory node between Ras signaling and microtubule nucleation, *J Biol Chem 285*, 16258-16266.

35. Stieglitz, B., Bee, C., Schwarz, D., Yildiz, O., Moshnikova, A., Khokhlatchev, A., and Herrmann, C. (2008) Novel type of Ras effector interaction established between tumour suppressor NORE1A and Ras switch II, *EMBO J 27*, 1995-2005.

36. Liao, T. J., Jang, H., Tsai, C. J., Fushman, D., and Nussinov, R. (2017) The dynamic mechanism of RASSF5 and MST kinase activation by Ras, *Phys Chem Chem Phys 19*, 6470-6480.

37. Xia, J., Zeng, M., Zhu, H., Chen, X., Weng, Z., and Li, S. (2017) Emerging role of Hippo signalling pathway in bladder cancer, *J Cell Mol Med*.

38. Cairns, L., Tran, T., and Kavran, J. M. (2017) Structural Insights into the Regulation of Hippo Signaling, *ACS Chem Biol 12*, 601-610.

39. Patel, S. H., Camargo, F. D., and Yimlamai, D. (2017) Hippo Signaling in the Liver Regulates Organ Size, Cell Fate, and Carcinogenesis, *Gastroenterology 152*, 533-545.

40. Nakatani, K., Maehama, T., Nishio, M., Goto, H., Kato, W., Omori, H., Miyachi, Y., Togashi, H., Shimono, Y., and Suzuki, A. (2017) Targeting the Hippo signalling pathway for cancer treatment, *J Biochem 161*, 237-244.

41. Harvey, K. F., Pfleger, C. M., and Hariharan, I. K. (2003) The Drosophila Mst ortholog, hippo, restricts growth and cell proliferation and promotes apoptosis, *Cell 114*, 457-467.

42. Barnoud, T., Donninger, H., and Clark, G. J. (2016) Ras Regulates Rb via NORE1A, *J Biol Chem 291*, 3114-3123.

43. Donninger, H., Calvisi, D. F., Barnoud, T., Clark, J., Schmidt, M. L., Vos, M. D., and Clark, G. J. (2015) NORE1A is a Ras senescence effector that controls the apoptotic/senescent balance of p53 via HIPK2, *J Cell Biol 208*, 777-789.

44. Hwang, E., Cheong, H. K., Ul Mushtaq, A., Kim, H. Y., Yeo, K. J., Kim, E., Lee, W. C., Hwang, K. Y., Cheong, C., and Jeon, Y. H. (2014) Structural basis of the

heterodimerization of the MST and RASSF SARAH domains in the Hippo signalling pathway, *Acta Crystallogr D Biol Crystallogr 70*, 1944-1953.

45. Hwang, E., Ryu, K. S., Paakkonen, K., Guntert, P., Cheong, H. K., Lim, D. S., Lee, J. O., Jeon, Y. H., and Cheong, C. (2007) Structural insight into dimeric interaction of the SARAH domains from Mst1 and RASSF family proteins in the apoptosis pathway, *Proc Natl Acad Sci U S A 104*, 9236-9241.

46. Sanchez-Sanz, G., Matallanas, D., Nguyen, L. K., Kholodenko, B. N., Rosta, E., Kolch, W., and Buchete, N. V. (2016) MST2-RASSF protein-protein interactions through SARAH domains, *Brief Bioinform 17*, 593-602.

47. Sanchez-Sanz, G., Tywoniuk, B., Matallanas, D., Romano, D., Nguyen, L. K., Kholodenko, B. N., Rosta, E., Kolch, W., and Buchete, N. V. (2016) SARAH Domain-Mediated MST2-RASSF Dimeric Interactions, *PLoS Comput Biol 12*, e1005051.

48. Densham, R. M., O'Neill, E., Munro, J., Konig, I., Anderson, K., Kolch, W., and Olson, M. F. (2009) MST kinases monitor actin cytoskeletal integrity and signal via c-Jun N-terminal kinase stress-activated kinase to regulate p21Waf1/Cip1 stability, *Mol Cell Biol 29*, 6380-6390.

49. Bi, W., Xiao, L., Jia, Y., Wu, J., Xie, Q., Ren, J., Ji, G., and Yuan, Z. (2010) c-Jun N-terminal kinase enhances MST1-mediated pro-apoptotic signaling through phosphorylation at serine 82, *J Biol Chem 285*, 6259-6264.

50. Ura, S., Masuyama, N., Graves, J. D., and Gotoh, Y. (2001) MST1-JNK promotes apoptosis via caspase-dependent and independent pathways, *Genes Cells 6*, 519-530.

51. Moya, I. M., and Halder, G. (2016) The Hippo pathway in cellular reprogramming and regeneration of different organs, *Curr Opin Cell Biol 43*, 62-68.

52. Zhao, Y., Fei, X., Guo, J., Zou, G., Pan, W., Zhang, J., Huang, Y., Liu, T., and Cheng, W. (2017) Induction of reprogramming of human amniotic epithelial cells into iPS cells by overexpression of Yap, Oct4, and Sox2 through the activation of the Hippo-Yap pathway, *Exp Ther Med 14*, 199-206.

53. Enomoto, M., Kizawa, D., Ohsawa, S., and Igaki, T. (2015) JNK signaling is converted from anti- to pro-tumor pathway by Ras-mediated switch of Warts activity, *Dev Biol 403*, 162-171.

54. Zhao, H. F., Wang, J., and Tony To, S. S. (2015) The phosphatidylinositol 3-kinase/Akt and c-Jun N-terminal kinase signaling in cancer: Alliance or contradiction? (Review), *Int J Oncol 47*, 429-436.

55. März, L., Altmann, F., Staudacher, E., and Kubelka, V. (1995) Chapter 10 Protein Glycosylation in Insects, *New Comprehensive Biochemistry 29*, 543-563.